

FINITE ELEMENT APPROXIMATION OF DIELECTROPHORETIC FORCE DRIVEN FLOW PROBLEMS

PHILIPP GERSTNER^{1,2,*} AND VINCENT HEUVELINE¹

Abstract. In this paper, we propose a full discretization scheme for the instationary thermal-electrohydrodynamic (TEHD) Boussinesq equations. These equations model the dynamics of a non-isothermal, dielectric fluid under the influence of a dielectrophoretic (DEP) force. Our scheme combines an H^1 -conformal finite element method for spatial discretization with a backward differentiation formula (BDF) for time stepping. The resulting scheme allows for a decoupled solution of the individual parts of this multi-physics system. Moreover, we derive *a priori* convergence rates that are of first and second order in time, depending on how the individual ingredients of the BDF scheme are chosen and of optimal order in space. In doing so, special care is taken of modeling the DEP force, since its original form is a cubic term. The obtained error estimates are verified by numerical experiments.

Mathematics Subject Classification. 65N12, 65N30, 76W05.

Received June 7, 2022. Accepted March 29, 2023.

1. INTRODUCTION

If a non-isothermal, dielectric fluid is exposed to an alternating, external electric field \mathbf{E} , then it experiences the so-called dielectrophoretic (DEP) force. The resulting state of the fluid, given by its velocity \mathbf{u} , pressure p , temperature θ and internal electric potential Φ , can be modeled by means of the thermal-electrohydrodynamic (TEHD) Boussinesq equations in the domain Ω [28],

$$\partial_t \mathbf{u} + (\mathbf{u} \cdot \nabla) \mathbf{u} - \nu \Delta \mathbf{u} + \nabla p = \alpha_e |\nabla \Phi|^2 \nabla \theta - \alpha_g \theta \mathbf{g} \quad (1.1)$$

$$\nabla \cdot \mathbf{u} = 0 \quad (1.2)$$

$$\partial_t \theta + (\mathbf{u} \cdot \nabla) \theta - \kappa \Delta \theta = 0 \quad (1.3)$$

$$-\nabla \cdot (\epsilon(\theta) \nabla \Phi) = 0, \quad (1.4)$$

with kinematic viscosity ν , thermal expansion coefficient α_g , thermal diffusion coefficient κ , gravitational field \mathbf{g} , constant in time, mixed Dirichlet–Neumann boundary conditions θ_D , Φ_D , and initial conditions \mathbf{u}_0 , θ_0 .

$$\mathbf{u} = 0 \quad \text{on } \partial\Omega = \Gamma_D \cup \Gamma_N, \quad \Gamma_D \cap \Gamma_N = \emptyset$$

Keywords and phrases. TEHD Boussinesq, finite element method, error estimation.

¹ Engineering Mathematics and Computing Lab, Heidelberg University, Im Neuenheimer Feld 205, 69120 Heidelberg, Germany.

² Heidelberg Institute for Theoretical Studies, Schloss-Wolfsbrunnengasse 35, 69118 Heidelberg, Germany.

*Corresponding author: philipp.gerstner@uni-heidelberg.de

$$\begin{aligned}
\theta &= \theta_D \text{ on } \Gamma_D, \quad \nabla\theta \cdot \mathbf{n} = 0 \text{ on } \Gamma_N \\
\Phi &= \Phi_D \text{ on } \Gamma_D, \quad \nabla\Phi \cdot \mathbf{n} = 0 \text{ on } \Gamma_N \\
\mathbf{u}(0) &= \mathbf{u}_0 \\
\theta(0) &= \theta_0.
\end{aligned} \tag{1.5}$$

System (1.1)–(1.5) is obtained by augmenting the standard Boussinesq equations with Gauss’ law (1.4) and with the DEP force $-\frac{1}{2}|\nabla\Phi|^2\nabla\epsilon$ and by linearizing the temperature dependent dielectric permittivity ϵ around a given reference temperature θ_r . The resulting DEP coefficient is then given by $\alpha_e = \frac{\epsilon_r\epsilon_0\gamma}{2\rho}$ with fluid density ρ , $\gamma = \partial_\theta\epsilon(\theta_r)$ and dielectric constant $\epsilon_r\epsilon_0$ [28].

In recent years, there has been growing interest in the investigation of DEP-driven flows, since the DEP force can be used to enhance the effectiveness of heat exchanging systems [7]. Moreover, the DEP force can be considered as artificial gravity and thereby allows to simulate Earth mantle convection in physical experiments [8]. While many works on this topic are of experimental nature [10, 23, 25, 27, 35], or address linear stability analysis [22, 24, 37, 38, 40, 45], there are also few contributions on the numerical solution of (1.1)–(1.5). For instance, in [19–21, 46] the use of finite volumes in combination with low order time stepping schemes is proposed. A spectral approach is presented in [42–44] and the finite element method (FEM) is used in [26, 35, 36].

However, to the best of the authors’ knowledge, there is a lack of publications that address the numerical analysis of any kind of discretization method applied to the TEHD Boussinesq equations. We thus propose a full discretization scheme, based on H^1 -conformal FEM and variants of the backward differentiation formula (BDF), and derive corresponding *a priori* error estimates in this work. The presented analysis is inspired by Tabata and Tagami [39], where error estimates for a FEM/backward Euler discretization of the standard Boussinesq equations with temperature dependent viscosity ν and thermal diffusion coefficient κ are derived. Further results on numerical analysis of FEM applied to the standard Boussinesq equations are derived in many works, see for instance [1, 2, 4, 5, 29–31, 33] and the references therein.

Compared to the natural convection case, the main difficulty that comes with system (1.1)–(1.5) is due to the DEP force term. For the typical $W^{1,2}$ -regularity of solutions θ and Φ of heat equation and Gauss’ law – involving non-smooth coefficients, Lipschitz domains and mixed boundary conditions – one cannot assume that $|\nabla\Phi|^2\nabla\theta$ is sufficiently regular to be an element of $\mathbf{H}^{-1}(\Omega)$. Therefore, we propose an approximate DEP force term, based on a cut-off operator, to obtain a well-defined variational formulation.

The error estimates are derived for this modified DEP term and convergence rates of the form $h^\alpha + k^\beta$ with mesh width h and time step k are obtained. As usual, the spatial order of convergence α depends on the assumed regularity of the exact solution and the approximation properties of the underlying finite element spaces. Concerning the temporal order of velocity, temperature and potential error, we obtain $\beta = 1$ or $\beta = 2$ for the one-step and two-step BDF scheme, respectively.

All presented error estimates only hold under a small data condition which originates from the DEP force and which is of the form

$$\alpha_e \max_{t \in [0, T], x \in \Omega} |\nabla\Phi(t, x)|^2 \leq c_\Omega \sqrt{\nu\kappa}, \tag{1.6}$$

with domain dependent constant c_Ω . Compared to small data conditions in other situations, see the ones for the stationary Boussinesq equations for instance [31], equation (1.6) is rather mild though and its validness can be shown in realistic scenarios, see Section 7 and [12].

The derived convergence rates are validated by numerical experiments and we further discuss in which sense the obtained results also apply to the original DEP term $|\nabla\Phi|^2\nabla\theta$.

The proposed time stepping schemes treat all nonlinear terms in a semi-implicit fashion, which allows for solving the incompressible flow equations, heat equation and Gauss’ law in a decoupled way. Moreover, the approximation of ∂_t and the extrapolation of \mathbf{u} in the arising convection terms are defined in a general manner. Thus, we are able to cover the aforementioned one- and two-step BDF schemes in a unified analysis.

The outline of this paper is as follows: First, the continuous variational formulation is stated in Section 2. In Section 3 we present the spatial and temporal discretization scheme and show well-posedness of the discrete

equations. Corresponding *a priori* error estimates are derived in Section 4. In Section 5 we address the modeling of the DEP force. Numerical experiments underlining the theoretical convergence rates are presented in Section 6. In Section 7 we discuss the relation between the original and modified DEP term. We conclude this work in Section 8.

Preliminaries

Throughout this work, let $\Omega \subset \mathbb{R}^d$, $d \in \{2, 3\}$ denote a bounded domain with Lipschitz boundary $\Gamma := \partial\Omega$, that is split into disjoint Dirichlet and Neumann parts, *i.e.* $\Gamma = \Gamma_D \cup \Gamma_N$, $\Gamma_D \cap \Gamma_N = \emptyset$. We suppose that Γ_D has positive $(d-1)$ -dimensional Hausdorff measure.

For $k \in \mathbb{N}_0$ and $p \in [1, \infty]$, let $W^{k,p}(\Omega)$ denote the common Sobolev spaces, where $W^{0,p}(\Omega) := L^p(\Omega)$. The associated norms and semi-norms are given by $\|\cdot\|_{k,p,\Omega}$ and $|\cdot|_{k,p,\Omega}$, respectively. If no potential ambiguity may arise, we skip the subscript Ω in the norm notation.

For $p = 2$ we use the abbreviations $\|\cdot\| := \|\cdot\|_{0,2,\Omega}$, $|\cdot|_1 := |\cdot|_{1,2,\Omega}$, $(u, v) := \int_{\Omega} uv$ and $H^k(\Omega) := W^{k,2}(\Omega)$.

Spaces of vanishing trace are given by the closures of $C_c^\infty(\Omega) := \{v \in C^\infty(\Omega) : \text{supp}(v) \subset\subset \Omega\}$ and $C_D^\infty(\Omega) := \{v|_{\Omega} : v \in C_c^\infty(\mathbb{R}^d), \text{supp}(v) \cap \Gamma_D = \emptyset\}$ in $H^1(\Omega)$ and denoted by $H_0^1(\Omega)$ and $H_D^1(\Omega)$, respectively. Friedrich's inequality, $\|u\|_{0,2} \leq c \|\nabla u\|_{0,2}$, is valid for these spaces with corresponding constants $c = c_0$ and $c = c_D$. We thus equip $H_0^1(\Omega)$ and $H_D^1(\Omega)$ with $|\cdot|_{1,2}$.

Moreover, $L_0^2(\Omega) := \{p \in L^2(\Omega) : \int_{\Omega} p = 0\}$ and spaces of vector-valued functions are indicated by boldface letters, *e.g.* $\mathbf{L}^p(\Omega)$. We write $H^{-1}(\Omega)$, $\mathbf{H}^{-1}(\Omega)$ for the dual spaces of $H_0^1(\Omega)$ and $\mathbf{H}_0^1(\Omega)$, respectively, and denote their corresponding norms by $\|\phi\|_{-1,2} = \sup_{\mathbf{u} \in \mathbf{H}_0^1(\Omega)} \frac{|\phi(\mathbf{u})|}{\|\mathbf{u}\|_{1,2}}$.

For $p \in [1, \infty]$ and a Banach space X let $L^p(X) := L^p(0, T; X)$ denote the space of Bochner-integrable, X -valued functions on the interval $(0, T)$. The associated norm is denoted by $\|\cdot\|_{p,X}$.

For integers $0 \leq m < M$ and $k \in (0, \infty)$ (time step), a space of Z -valued sequences is defined by $l^p(m, M; Z) := \{(z^n)_n : n = m, \dots, M, z^n \in Z\}$ and equipped with the norm $\|(z^n)_n\|_{l^p(m, M; Z), k}^p := k \sum_{n=m}^M \|z^n\|_Z^p$ if $p \in [1, \infty)$ and $\|(z^n)_n\|_{l^\infty(m, M; Z)} := \max\{\|z^n\|_Z : n = m, \dots, M\}$ if $p = \infty$. If no potential ambiguity may arise, we simply write $\|\cdot\|_{l^p(Z)}$ for $\|\cdot\|_{l^p(m, M; Z), k}$.

For a given equidistant partition $0 = t_0 < t_1 < \dots < t_N = T$ of $[0, T]$ with $k = t_i - t_{i-1}$, and a continuous function $z : [0, T] \rightarrow Z$ let $z^n := z(t_n)$ and $\|z\|_{l^p(Z)} := \|(z(t_n))_n\|_{l^p(Z)}$.

Furthermore, we write X^* for the dual space of a normed space X and $\langle \phi, x \rangle_{X^*} := \phi(x)$ for $\phi \in X^*$, $x \in X$. $X \hookrightarrow Y$ denotes the continuous injection of X into Y and $\mathcal{L}(X, Y)$ denotes the space of bounded linear operators between the normed spaces X, Y . For $r > 0$, $x \in X$, let $B_r(x, X) := \{y \in X : \|y - x\|_X < r\}$. Throughout this work, c denotes a generic constant that only depends on Ω , differentiability and integrability orders *via* embedding constants, but not on problem-dependent parameters, such as ν or κ , and discretization parameters h and k . Finally, $a \lesssim b$ for terms $a = a(h, k)$, $b = b(h, k)$, means that $a \leq Cb$ for some constant C that does not depend on h and k .

2. CONTINUOUS PROBLEM

In this section, we state a continuous variational formulation for the TEHD Boussinesq equations (1.1)–(1.5). As previously noted, a variational formulation of (1.1) which involves a DEP force of the form $|\nabla\Phi|^2 \nabla\theta$ would imply some problematic consequences. Using $W^{1,2}(\Omega) \hookrightarrow L^6(\Omega)$, the regularity conditions $\Phi \in W^{1,s}(\Omega)$, $\theta \in W^{1,t}(\Omega)$ with $1 = \frac{1}{t} + \frac{2}{s} + \frac{1}{6}$ (which is only possible to hold for $s \geq \frac{12}{5}$) are required to infer, by means of Hölder's inequality, that $\langle \mathbf{F}_{\text{dep}}(\theta, \Phi), \mathbf{v} \rangle_{\mathbf{H}^{-1}} := (|\nabla\Phi|^2 \nabla\theta, \mathbf{v})$ is well-defined. Similarly, a Lipschitz property of \mathbf{F}_{dep} (needed in the proposed error analysis) relies on the norms $\|\cdot\|_{1,s}$ and $\|\cdot\|_{1,t}$. However, the natural norm in this analysis for bounding θ , Φ is $\|\cdot\|_{1,2}$ and the conversion between these norms, *e.g.* by means of inverse estimates, would introduce negative powers of h , which could not be compensated. For this reason, we replace \mathbf{F}_{dep} by a general body force \mathbf{F} for now, which is supposed to model the DEP term \mathbf{F}_{dep} , and also incorporates additional terms such as gravitation and other source terms. Below, we impose conditions on \mathbf{F} that are sufficient

to perform the error analysis, see Assumption 3.13, and propose a suitable realization for \mathbf{F} as an approximation to the original DEP force \mathbf{F}_{dep} and possible additional terms, see Section 5. At this point, we only require the following assumption.

Assumption 2.1 (General body force). *Let a general body force $\mathbf{F}: \mathbf{H}^1(\Omega) \times \mathbf{H}^1(\Omega) \rightarrow \mathbf{H}^{-1}(\Omega)$ be given.*

Assumption 2.2 and 2.3 collect the remaining requirements imposed on the problem data.

Assumption 2.2 (Physical parameters). *Let $\nu, \kappa > 0$. The permittivity $\epsilon: \mathbb{R} \rightarrow [\epsilon_-, \epsilon_+]$ as a function of temperature is Lipschitz continuous with constant L_ϵ and $0 < \epsilon_- \leq \epsilon_+ < \infty$.*

Assumption 2.3 (Boundary and initial conditions). *The initial conditions and temporally constant Dirichlet boundary conditions θ_D, Φ_D posed on Γ_D satisfy the following conditions:*

- (i) $\mathbf{u}_0 \in \mathbf{H}_0^1(\Omega)$ with $\nabla \cdot \mathbf{u}_0 = 0$ and $\theta_0 \in \mathbf{H}_D^1(\Omega)$.
- (ii) There exists a boundary lifting $\Phi_b \in \mathbf{W}^{1,\infty}(\Omega)$ of Φ_D .
- (iii) There exists a boundary lifting $\theta_b \in \mathbf{W}^{1,\infty}(\Omega)$ of θ_D .

The variational formulation of (1.1)–(1.4) is based on the following function spaces. Velocity test and ansatz functions are taken from the spaces $\mathbf{U} := (\mathbf{H}_0^1(\Omega), |\cdot|_1)$ and the closure of $\mathcal{V}(\Omega) = \{\mathbf{u} \in C_c^\infty(\Omega)^d: \nabla \cdot \mathbf{u} = 0\}$ in $\mathbf{H}_0^1(\Omega)$ and $\mathbf{L}^2(\Omega)$, denoted by \mathbf{V} and \mathbf{H} , respectively. The spaces for pressure, temperature and potential are given by $M := (L_0^2(\Omega), \|\cdot\|)$, $\Theta := (\mathbf{H}_D^1(\Omega), |\cdot|_1)$ and $\Upsilon := (\mathbf{H}_D^1(\Omega), |\cdot|_1)$, respectively.

Moreover, we define the following set of bi- and trilinear forms for $\mathbf{u}, \mathbf{v}, \mathbf{w} \in \mathbf{H}^1(\Omega)$, $\theta, \tau, \Phi, \beta \in \mathbf{H}^1(\Omega)$ and $q \in L^2(\Omega)$:

$$\begin{aligned} a_{\mathbf{v}}(\mathbf{u}, \mathbf{v}) &:= \nu(\nabla \mathbf{u}, \nabla \mathbf{v}), & c_{\mathbf{v}}(\mathbf{u}, \mathbf{v}, \mathbf{w}) &:= (\mathbf{u} \cdot \nabla \mathbf{v}, \mathbf{w}), \\ a_\tau(\theta, \tau) &:= \kappa(\nabla \theta, \nabla \tau), & c_\tau(\mathbf{u}, \theta, \tau) &:= (\mathbf{u} \cdot \nabla \theta, \tau), \\ a_\beta(\theta, \Phi, \beta) &:= (\epsilon(\theta) \nabla \Phi, \nabla \beta), & b(\mathbf{u}, q) &:= (\nabla \cdot \mathbf{u}, q). \end{aligned} \tag{2.1}$$

We now state a definition of a continuous variational formulation and corresponding weak solutions of (1.1)–(1.5).

Problem 2.4 (Instationary TEHD equations). Let $T > 0$ and source terms $\mathbf{f}_{\mathbf{v}} \in C(0, T; \mathbf{U}^*)$, $f_\tau \in C(0, T; \Theta^*)$, $f_\beta \in C(0, T; \Upsilon^*)$ be given.

Find $\mathbf{u} \in L^2(0, T; \mathbf{V})$, $\theta \in L^2(0, T; \Theta)$, $p \in L^2(0, T; M)$ and $\Phi \in L^2(0, T; \Upsilon)$ with $\partial_t \mathbf{u} \in L^1(0, T; \mathbf{L}^2)$ and $\partial_t \theta \in L^1(0, T; L^2)$, such that for all $t \in [0, T]$ and $(\mathbf{v}, q, \tau, \beta) \in \mathbf{U} \times M \times \Theta \times \Upsilon$:

$$\begin{aligned} (\partial_t \mathbf{u}, \mathbf{v}) + a_{\mathbf{v}}(\mathbf{u}, \mathbf{v}) + c_{\mathbf{v}}(\mathbf{u}, \mathbf{u}, \mathbf{v}) - b(\mathbf{v}, p) &= \langle \mathbf{F}(\theta + \theta_b, \Phi + \Phi_b) + \mathbf{f}_{\mathbf{v}}, \mathbf{v} \rangle_{\mathbf{U}^*} \\ b(\mathbf{u}, q) &= 0 \\ (\partial_t \theta, \tau) + a_\tau(\theta + \theta_b, \tau) + c_\tau(\mathbf{u}, \theta + \theta_b, \tau) &= \langle f_\tau, \tau \rangle_{\Theta^*} \\ a_\beta(\theta + \theta_b, \Phi + \Phi_b, \beta) &= \langle f_\beta, \beta \rangle_{\Upsilon^*} \\ \mathbf{u}(0) &= \mathbf{u}_0 \\ \theta(0) &= \theta_0. \end{aligned}$$

Remark 2.5. To simplify presentation, we do not introduce additional notation for the temperature θ with homogenous boundary values in Problem 2.4. Thus, $\theta + \theta_b$ in Problem 2.4 and in the following corresponds to θ in the strong formulation (1.1)–(1.5). The potential Φ is treated analogously.

Remark 2.6. $\mathbf{f}_{\mathbf{v}}, f_\tau, f_\beta$ denote arbitrary source terms, that are independent of the unknown solution and boundary conditions. The strong formulation (1.1)–(1.5) corresponds to Problem 2.4 for $\mathbf{f}_{\mathbf{v}} = f_\tau = f_\beta = 0$.

Remark 2.7. If θ is additionally in H^2 and the boundary lifting is assumed to be in H^2 as well, then Green's formula can be applied in the usual way on the term $a_\tau(\theta + \theta_b, \tau)$; first with $\tau \in C_c^\infty(\Omega)$ to show that $\theta + \theta_b$ solves (1.3); second with $\tau \in C_D^\infty(\Omega)$ to obtain $\nabla(\theta + \theta_b) \cdot \mathbf{n} = 0$ on Γ_N . Analogous results hold for Φ, Φ_b .

Remark 2.8. In [12], existence and stability of solutions of the instationary TEHD equations in solenoidal form is shown. These solutions, however, are of lower temporal regularity, $\partial_t \mathbf{u} \in L^1(0, T; \mathbf{V}^*)$, $\partial_t \theta \in L^1(0, T; \Theta^*)$, and the instationary equations only hold in a distributional sense, *i.e.* in $C_c^\infty((0, T))^*$. Moreover, the underlying assumptions on \mathbf{F} in [12] differ from those imposed in Section 3. For this existence result it is assumed that weak convergence of sequences $(\theta_n, \Phi_n)_n \rightharpoonup (\theta, \Phi)$ in $H^1 \times H^1$ should imply pointwise convergence $\mathbf{F}(\theta_n, \Phi_n) \rightarrow \mathbf{F}(\theta, \Phi)$ in \mathbf{U}^* , which is not satisfied by the DEP model proposed for the numerical analysis in this work. Corresponding modelizations of \mathbf{F} are based on linearization w.r.t. Φ around a given reference potential. To the best of the authors' knowledge, this is the only work on well-posedness of the TEHD equations.

3. DISCRETE PROBLEM

In this section, we propose a full discretization of Problem 2.4, leading to the discrete Problem 3.12. Afterwards, unique existence and stability of discrete solutions is shown.

3.1. Spatial discretization

The spatial discretization is given by H^1 -conformal finite element spaces that satisfy the following conditions.

Assumption 3.1 (Finite element spaces). *For some $h_0 > 0$ and all $h \in (0, h_0]$ let finite element spaces $\mathbf{U}_h \subset \mathbf{U}$, $M_h \subset M$, $\Theta_h \subset \Theta$, $\Upsilon_h \subset \Upsilon$ with underlying triangulation \mathcal{T}_h of Ω be given that satisfy*

(i) *There is $\beta > 0$, independent of h , such that*

$$\inf_{q_h \in M_h} \sup_{\mathbf{v}_h \in \mathbf{U}_h} \frac{b(\mathbf{v}_h, q_h)}{\|\mathbf{v}_h\|_{1,2} \|q_h\|} \geq \beta.$$

(ii) *There are operators $\Pi_{\mathbf{U}} \in \mathcal{L}(\mathbf{H}^2(\Omega) \cap \mathbf{U}, \mathbf{U}_h)$, $\Pi_M \in \mathcal{L}(L^2(\Omega), M_h)$ and $\bar{m} \in \mathbb{N}$ such that for all integers $1 \leq s \leq \bar{m}$ and all $\mathbf{u} \in \mathbf{H}^{s+1}(\Omega) \cap \mathbf{U}$, $p \in H^s(\Omega) \cap M$*

$$\begin{aligned} \|\mathbf{u} - \Pi_{\mathbf{U}} \mathbf{u}\| + h \|\mathbf{u} - \Pi_{\mathbf{U}} \mathbf{u}\|_{1,2} &\leq ch^{s+1} \|\mathbf{u}\|_{s+1,2}, \\ \|p - \Pi_M p\| &\leq ch^s \|p\|_{s,2}. \end{aligned}$$

(iii) *There are operators $\Pi_X \in \mathcal{L}(H^2(\Omega) \cap X, X_h)$, $X \in \{\Theta, \Upsilon\}$ and $\bar{n} \in \mathbb{N}$ such that for all integers $1 \leq s \leq \bar{n}$ and all $\eta \in H^{s+1}(\Omega) \cap X$*

$$\|\eta - \Pi_X \eta\| + h \|\eta - \Pi_X \eta\|_{1,2} \leq ch^{s+1} \|\eta\|_{s+1,2}.$$

Moreover, the following stability estimate holds: there is $c_\Pi > 0$ such that for all $\eta \in H^2(\Omega) \cap X$ and $p \in \{2, 3\}$

$$\|\Pi_X \eta\|_{1,p} \leq c_\Pi \|\eta\|_{2,2}.$$

(iv) *For all $s, t \in \{0, 1\}$ with $0 \leq s \leq t \leq 1$ and $q, r \in [1, \infty]$ with $1 \leq q \leq r \leq \infty$ there holds for all $\mathbf{u}_h \in \mathbf{U}_h$, $\eta_h \in X_h$, $X \in \{\Theta, \Upsilon\}$,*

$$\begin{aligned} \|\mathbf{u}_h\|_{t,r} &\leq ch^{s-t+d(\frac{1}{r}-\frac{1}{q})} \|\mathbf{u}_h\|_{s,q}, \\ \|\eta_h\|_{t,r} &\leq ch^{s-t+d(\frac{1}{r}-\frac{1}{q})} \|\eta_h\|_{s,q}. \end{aligned}$$

Remark 3.2. The requirements of Assumption 3.1 can be met by choosing $\mathbf{U}_h \times M_h$ as the Taylor–Hood element $\mathbb{P}_2 \times \mathbb{P}_1$ and Θ_h, Υ_h as continuous Lagrange elements \mathbb{P}_k with $k \geq 1$ on a (shape-) regular, quasi-uniform family of triangulations \mathcal{T}_h of the polyhedral domain Ω , with all mesh cells being affine-equivalent simplices or hypercubes. In this case, Π_\cdot denotes the nodal interpolation operator. See Theorem A.127 in [12] and the references therein for (i), Theorem 4.4.20 and 4.5.11 in [6] for (ii), (iii) and (iv), respectively. The stability property in (iii) follows from Lemma A.2 and Section A.2 in [14], saying

$$\|\eta - \Pi_{\Theta}\eta\|_{1,4} \leq c|\eta|_{1,4} \quad \text{for all } \eta \in W^{1,4}(\Omega), \tag{3.1}$$

the triangle inequality and $L^4(\Omega) \hookrightarrow L^3(\Omega) \hookrightarrow L^2(\Omega), H^2(\Omega) \hookrightarrow W^{1,4}(\Omega)$.

In the upcoming error analysis, we make use of the well-known Stokes projection, *e.g.* [15], to bound the approximation error of velocity and pressure. In this way, some terms of the instationary error equation naturally cancel out.

Definition 3.3 (Stokes projection). For $(\mathbf{u}, p) \in \mathbf{U} \times M$ with $\nabla \cdot \mathbf{u} = 0$ let $(\mathbf{w}_h, r_h) \in \mathbf{U}_h \times M_h$ denote the unique solution of

$$\begin{aligned} a_{\mathbf{v}}(\mathbf{w}_h, \mathbf{v}_h) - b(\mathbf{v}_h, r_h) &= a_{\mathbf{v}}(\mathbf{u}, \mathbf{v}_h) - b(\mathbf{v}_h, p) & \text{for all } \mathbf{v}_h \in \mathbf{U}_h, \\ b(\mathbf{w}_h, q_h) &= 0 & \text{for all } q_h \in M_h. \end{aligned}$$

The *Stokes Projection* is defined as

$$\Pi_S: \mathbf{U} \times M \rightarrow \mathbf{U}_h \times M_h, (\mathbf{u}, p) \mapsto (\mathbf{w}_h, r_h).$$

Lemma 3.4 (Properties of stokes projection). *Let Assumption 3.1 (i) and (ii) hold. Then, Π_S is well-defined, linear and there holds for $(\mathbf{w}_h, r_h) = \Pi_S(\mathbf{u}, p)$,*

$$\|\nabla \mathbf{w}_h\| \leq \|\nabla \mathbf{u}\| + \nu^{-1}\|p\|.$$

Moreover, there is C_S , independent of h and ν , such that for all $(\mathbf{u}, p) \in (\mathbf{H}^{l+1}(\Omega) \cap \mathbf{U}) \times (H^l(\Omega) \cap M)$ with $1 \leq l \leq \bar{m}$ and \bar{m} defined by Assumption 3.1 (ii), there holds

$$\begin{aligned} \|\mathbf{u} - \mathbf{w}_h\|_{1,2} &\leq C_S h^l \left(\|\mathbf{u}\|_{l+1,2} + \nu^{-1}\|p\|_{l,2} \right), \\ \|p - r_h\| &\leq C_S h^l \left(\nu\|\mathbf{u}\|_{l+1,2} + \|p\|_{l,2} \right). \end{aligned}$$

If the Stokes problem is regular, *i.e.* the mapping $(\mathbf{u}, p) \mapsto -\nu\Delta\mathbf{u} + \nabla p$ is an isomorphism from $(\mathbf{H}^2(\Omega) \cap \mathbf{V}) \times (H^1(\Omega) \cap L_0^2(\Omega))$ onto $L^2(\Omega)$, then

$$\|\mathbf{u} - \mathbf{w}_h\| \leq C_{S,0} h^{l+1} \left(\|\mathbf{u}\|_{l+1,2} + \|p\|_{l,2} \right),$$

with $C_{S,0} > 0$, independent of h .

Proof. See Lemma 4.42 and 4.43 in [18] for the stability result and h^l convergence, and Theorem II.1.9 in [14] for the improved L^2 convergence rates. □

Remark 3.5. According to Theorem I.5.4 and Remark I.5.6 in [14], the Stokes problem is regular if $\Gamma \in C^2$ or if $d = 2$ and Ω is a convex polygon.

The full discretization scheme proposed in the next section will lead to a sequence of stationary, spatially discretized problems of the following form.

Problem 3.6 (Linearized stationary TEHD equations). Let $\delta > 0$, source terms $\mathbf{f}_v \in \mathbf{U}^*$, $f_\tau \in \Theta^*$, $f_\beta \in \Upsilon^*$ and functions $\bar{\mathbf{u}} \in \mathbf{U}$, $\bar{\theta}, \bar{\theta} \in \Theta$ be given.

Find $(\mathbf{u}_h, p_h, \theta_h, \Phi_h) \in \mathbf{U}_h \times M_h \times \Theta_h \times \Upsilon_h$ such that for all $(\mathbf{v}_h, q_h, \tau_h, \beta_h) \in \mathbf{U}_h \times M_h \times \Theta_h \times \Upsilon_h$:

$$\begin{aligned} \delta(\mathbf{u}_h, \mathbf{v}_h) + a_v(\mathbf{u}_h, \mathbf{v}_h) + \tilde{c}_v(\bar{\mathbf{u}}, \mathbf{u}_h, \mathbf{v}_h) - b(\mathbf{v}_h, p_h) \\ - \langle \mathbf{F}(\bar{\theta} + \theta_b, \Phi_h + \Phi_b), \mathbf{v}_h \rangle_{\mathbf{U}^*} = \langle \mathbf{f}_v, \mathbf{v}_h \rangle_{\mathbf{U}^*} \end{aligned} \quad (3.2)$$

$$b(\mathbf{u}_h, q_h) = 0 \quad (3.3)$$

$$\delta(\theta_h + \theta_b, \tau_h) + a_\tau(\theta_h + \theta_b, \tau_h) + \tilde{c}_\tau(\bar{\mathbf{u}}, \theta_h + \theta_b, \tau_h) = \langle f_\tau, \tau_h \rangle_{\Theta^*} \quad (3.4)$$

$$a_\beta(\bar{\theta} + \theta_b, \Phi_h + \Phi_b, \beta_h) = \langle f_\beta, \beta_h \rangle_{\Upsilon^*}. \quad (3.5)$$

In the spatially discretized equations (3.2) and (3.4), the respective convection terms are replaced by the skew-symmetrized trilinear forms [41]

$$\begin{aligned} \tilde{c}_v(\mathbf{u}, \mathbf{w}, \mathbf{v}) &:= \frac{1}{2}(c_v(\mathbf{u}, \mathbf{w}, \mathbf{v}) - c_v(\mathbf{u}, \mathbf{v}, \mathbf{w})), \\ \tilde{c}_\tau(\mathbf{u}, \theta, \tau) &:= \frac{1}{2}(c_v(\mathbf{u}, \theta, \tau) - c_v(\mathbf{u}, \tau, \theta)), \end{aligned}$$

to account for the fact that the discrete continuity equation (3.3), in general, does not imply $\nabla \cdot \mathbf{u}_h = 0$.

Remark 3.7. The functions $\bar{\mathbf{u}}, \bar{\theta}, \bar{\theta}$ stated in Problem 3.6 account for function values at previous time steps, resulting from an explicit time discretization of the nonlinear terms, see Problem 3.12.

Lemma 3.8 (Existence and uniqueness of stationary solutions). *Let Assumptions 2.1–3.1 hold. Then, Problem 3.6 is uniquely solvable.*

Proof. As $\delta(\cdot, \cdot) + a_\tau(\cdot, \cdot) + \tilde{c}_\tau(\bar{\mathbf{u}}, \cdot, \cdot)$ and $a_\beta(\bar{\theta} + \theta_b, \cdot, \cdot)$ are bounded, coercive bilinear forms on Θ_h and Υ_h , respectively, the unique existence of θ_h, Φ_h is a direct consequence of Lax–Milgram. Having these functions determined, equations (3.2) and (3.3) is just an Oseen system. Thus, unique existence of \mathbf{u}_h, p_h follows from the discrete inf-sup condition, Assumption 3.1 (i), and Lax–Milgram applied to the bounded, coercive bilinear form $\delta(\cdot, \cdot) + a_v(\cdot, \cdot) + \tilde{c}_v(\bar{\mathbf{u}}, \cdot, \cdot)$ on \mathbf{U}_h . \square

3.2. Full discretization

To set up the temporal discretization, let $0 = t_0 < t_1 < \dots < t_N = T$ denote an equidistant partition of the time interval $[0, T]$, i.e. $t_i = ik$ with $k := \frac{T}{N}$ and $N \in \mathbb{N}$. The approximation of ∂_t and the extrapolation in the nonlinear terms are described by multi-step difference operators.

Definition 3.9 (q -step difference operator). Let Z denote a vector space, $q \in \mathbb{N}$ and $\mathbf{c} \in \mathbb{R}^{q+1}$. The q -step difference operator $J_{\mathbf{c}}$, applied to a sequence $(z^n)_n \subset Z$, is defined as

$$J_{\mathbf{c}} z^n := \sum_{i=0}^q c_i z^{n-i}.$$

$J_{\mathbf{c}}$ is called *explicit*, if $c_0 = 0$, and $J_{\mathbf{1}}$ denotes the 1-step operator determined by $\mathbf{c} = (1, -1)$.

Assumption 3.10 (Difference operators). *Let q -step difference operators $J_{\mathbf{c}}, J_{\mathbf{d}}, J_{\mathbf{f}}, J_{\mathbf{g}}$ be given with*

- (i) $J_{\mathbf{c}}, J_{\mathbf{f}}, J_{\mathbf{g}}$ are explicit.
- (ii) $\sum_{i=1}^q f_i = \sum_{i=1}^q g_i = 1$.

(iii) *There exists a constant $\bar{o} \geq 0$ such that for each sequence $(z^n)_{n \geq 0} \subset Z$ with $Z \in \{\mathbf{L}^2(\Omega), \mathbf{L}^2(\Omega)\}$, there are sequences $(Z_n)_{n \geq q-1}, (\bar{Z}_n)_{n \geq q} \subset \mathbb{R}$ with*

$$(J_{\mathbf{d}} z^n, z^n)_Z \geq \bar{o} J_{\mathbf{1}} \left(\|z^n\|_Z^2 + Z_n^2 \right) + \bar{Z}_n^2 \quad \text{for all } n \geq q$$

and Z_n only depends on z^l for $l \leq n$.

The following lemma, see e.g. [9, 39], gives two possible choices, for which condition (iii) of Assumption 3.10 is satisfied.

Lemma 3.11 (Stability of difference operators).

(i) *If $\mathbf{d} = (1, -1)$, then Assumption 3.10 (iii) holds with*

$$\bar{o} = \frac{1}{2}, \quad Z_n = 0, \quad \bar{Z}_n = \frac{1}{\sqrt{2}} \|J_{\mathbf{d}} z^n\|_Z.$$

(ii) *If $\mathbf{d} = (\frac{3}{2}, -2, \frac{1}{2})$, then Assumption 3.10 (iii) holds with*

$$\bar{o} = \frac{1}{4}, \quad Z_n = \|2z^n - z^{n-1}\|_Z, \quad \bar{Z}_n = \frac{1}{2} \|z^{n+1} - 2z^n + z^{n-1}\|_Z.$$

The full discretization of Problem 2.4 is now given by the following sequence of stationary problems.

Problem 3.12 (Discretized instationary TEHD equations). Let $q \geq 1$ and initial conditions $\{(\mathbf{u}_h^i, \theta_h^i)\}_{i=0}^{q-1} \subset \mathbf{U}_h \times \Theta_h$ be given which are discretely divergence free, i.e.

$$b(\mathbf{u}_h^i, \mathbf{v}_h) = 0 \quad \text{for all } \mathbf{v}_h \in \mathbf{U}_h. \tag{3.6}$$

Assume that the q -step difference operators $J_{\mathbf{c}}, J_{\mathbf{d}}, J_{\mathbf{f}}, J_{\mathbf{g}}$ satisfy Assumption 3.10 and that the source terms are given by $\mathbf{f}_X^m := \mathbf{f}_X(t_m)$, where \mathbf{f}_X is defined as in Problem 2.4 for $X \in \{\mathbf{v}, \tau, \beta\}$.

For $m \in \{q, \dots, N\}$, find $(\mathbf{u}_h^m, p_h^m, \theta_h^m, \Phi_h^m) \in \mathbf{U}_h \times M_h \times \Theta_h \times \Upsilon_h$ such that for all $(\mathbf{v}_h, q_h, \tau_h, \beta_h) \in \mathbf{U}_h \times M_h \times \Theta_h \times \Upsilon_h$:

$$\begin{aligned} (k^{-1} J_{\mathbf{d}} \mathbf{u}_h^m, \mathbf{v}_h) + a_{\mathbf{v}}(\mathbf{u}_h^m, \mathbf{v}_h) + \tilde{c}_{\mathbf{v}}(J_{\mathbf{c}} \mathbf{u}_h^m, \mathbf{u}_h^m, \mathbf{v}_h) \\ - b(\mathbf{v}_h, p_h^m) - \langle \mathbf{F}(J_{\mathbf{f}} \theta_h^m + \theta_b, \Phi_h^m + \Phi_b), \mathbf{v}_h \rangle_{\mathbf{U}^*} = \langle \mathbf{f}_{\mathbf{v}}^m, \mathbf{v}_h \rangle_{\mathbf{U}^*} \end{aligned} \tag{3.7}$$

$$b(\mathbf{u}_h^m, q_h) = 0 \tag{3.8}$$

$$(k^{-1} J_{\mathbf{d}} \theta_h^m, \tau_h) + a_{\tau}(\theta_h^m + \theta_b, \tau_h) + \tilde{c}_{\tau}(J_{\mathbf{c}} \mathbf{u}_h^m, \theta_h^m + \theta_b, \tau_h) = \langle f_{\tau}^m, \tau_h \rangle_{\Theta^*} \tag{3.9}$$

$$a_{\beta}(J_{\mathbf{g}} \theta_h^m + \theta_b, \Phi_h^m + \Phi_b, \beta_h) = \langle f_{\beta}^m, \beta_h \rangle_{\Upsilon^*}. \tag{3.10}$$

Due to Assumption 3.10 (i), the nonlinear terms are treated semi-implicitly. In this way, the resulting system for each time step m is of the same form as Problem 3.6 and can be solved by solving a series of linear systems. Moreover, the corresponding proof of *a priori* error estimates does not require a time step restriction when applying Grönwall’s inequality, see Lemma A.1. Assumption 3.10 (ii) is a consistency condition, that implies $J_{\mathbf{f}} x_b = J_{\mathbf{g}} x_b = x_b$ for the (not time-dependent) boundary liftings $x_b \in \{\theta_b, \Phi_b\}$. The stability condition (iii) is used to obtain the L^2 -norm of the discretization error in the proof of Theorem 4.1. It remains to specify requirements on the general body force \mathbf{F} , that are sufficient for proving *a priori* error estimates. In particular, \mathbf{F} should satisfy a Lipschitz condition w.r.t. both arguments. Concerning the second argument Φ , local Lipschitz continuity is sufficient, since an $l^\infty(\mathbf{H}^1)$ bound on the discrete potential can be derived. For the same reason, the Lipschitz moduli w.r.t. the first argument θ may depend on $\|\Phi\|_{1,2}$.

Assumption 3.13 (Body force Lipschitz continuity). *Let $\mathbf{F}: \mathbf{H}^1(\Omega) \times \mathbf{H}^1(\Omega) \rightarrow \mathbf{U}^*$ satisfy:*

- (i) There are non-decreasing functions $L_{\mathbf{F}}^{(\theta, \mathbf{H}^1)}, L_{\mathbf{F}}^{(\theta, L_2)}: [0, \infty) \rightarrow [0, \infty)$ such that for all $\theta_1, \theta_2 \in \mathbf{H}^1(\Omega)$, $\Phi \in \mathbf{H}^1(\Omega)$, $\mathbf{v} \in \mathbf{U}$,

$$|\langle \mathbf{F}(\theta_1, \Phi) - \mathbf{F}(\theta_2, \Phi), \mathbf{v} \rangle_{\mathbf{U}^*}| \leq L_{\mathbf{F}}^{(\theta, \mathbf{H}^1)} \left(\|\Phi\|_{1,2} \right) \|\nabla(\theta_1 - \theta_2)\| \|\mathbf{v}\| + L_{\mathbf{F}}^{(\theta, L_2)} \left(\|\Phi\|_{1,2} \right) \|\theta_1 - \theta_2\| \|\mathbf{v}\|.$$

- (ii) For all $R > 0$ there is $L_{\mathbf{F}}^{(\Phi)} \geq 0$ such that for all $\Phi_1, \Phi_2 \in B_R(0, \mathbf{H}^1(\Omega))$, $\theta \in W^{1,3}(\Omega)$, $\mathbf{v} \in \mathbf{U}$,

$$|\langle \mathbf{F}(\theta, \Phi_1) - \mathbf{F}(\theta, \Phi_2), \mathbf{v} \rangle_{\mathbf{U}^*}| \leq L_{\mathbf{F}}^{(\Phi)} \|\theta\|_{1,3} \|\nabla(\Phi_1 - \Phi_2)\| \|\mathbf{v}\|_{0,6}.$$

- (iii) $\mathbf{F}(0, \Phi) = 0$ for all $\Phi \in \mathbf{H}^1(\Omega)$.

Well-posedness of the discrete Problem 3.12 is provided by Lemma 3.14.

Lemma 3.14 (Existence, uniqueness and stability of discrete solutions). *Let Assumptions 2.1–3.13 hold and assume that*

$$qc_0 |\mathbf{f}|_{\infty} L_{\mathbf{F}}^{(1)} < 2\sqrt{\nu\kappa} \quad (3.11)$$

with constants

$$G_{\Phi} := \frac{1}{\epsilon_-} \left(\epsilon_+ \|\nabla \Phi_b\| + \|f_{\beta}\|_{\infty; \Upsilon^*} \right) \quad (3.12)$$

$$G_{\Phi, \Phi_b} := \sqrt{1 + c_D^2} G_{\Phi} + \|\Phi_b\|_{1,2} \quad (3.13)$$

$$L_{\mathbf{F}}^{(1)} := L_{\mathbf{F}}^{(\theta, \mathbf{H}^1)}(G_{\Phi, \Phi_b}). \quad (3.14)$$

Here, c_0, c_D denote the constants of Friedrich's inequality w.r.t. $\mathbf{H}_0^1(\Omega)$ and $\mathbf{H}_D^1(\Omega)$, respectively. Further, \mathbf{f} is determined by $J_{\mathbf{f}}$. Moreover, suppose that the q starting values are chosen in such a way, that their respective norms can be bounded uniformly in h :

$$U_{q-1}^2 + T_{q-1}^2 + \sum_{i=0}^{q-1} \left\{ \|\mathbf{u}_h^i\|^2 + \|\nabla \mathbf{u}_h^i\|^2 + \|\theta_h^i\|^2 + \|\nabla \theta_h^i\|^2 \right\} \leq G_{\mathbf{u}, \theta, q}, \quad (3.15)$$

where U_{q-1}, T_{q-1} are obtained by plugging $(\mathbf{u}_h^n, \theta_h^n)_{n=0, \dots, q-1}$ into Assumption 3.10 (iii), respectively.

Then, there exists a unique sequence of solutions $\{(\mathbf{u}_h^m, p_h^m, \theta_h^m, \Phi_h^m)\}_{m=q}^N$ of Problem 3.12. Moreover, this sequence is stable in the following sense: there exist constants $\bar{\nu} \in (0, \nu)$, $\bar{\kappa} \in (0, \kappa)$ (independent of h, k , and the starting values) and $G_{\mathbf{u}, \theta}$ (independent of h, k), such that

$$\begin{aligned} \|(\mathbf{u}_h^m)_m\|_{l^\infty(0, N; \mathbf{L}^2)} &\leq G_{\mathbf{u}, \theta}, \\ \|(\theta_h^m)_m\|_{l^\infty(0, N; \mathbf{L}^2)} &\leq G_{\mathbf{u}, \theta}, \\ \|(\Phi_h^m)_m\|_{l^\infty(q, N; \mathbf{H}_D^1)} &\leq G_{\Phi}, \\ \bar{\nu} \|(\mathbf{u}_h^m)_m\|_{L^2(0, N; \mathbf{H}_0^1), k}^2 + \bar{\kappa} \|(\theta_h^m)_m\|_{L^2(0, N; \mathbf{H}_D^1), k}^2 &\leq G_{\mathbf{u}, \theta}. \end{aligned}$$

Proof. Unique existence of solutions is a direct consequence of Lemma 3.8 and the fact that $J_{\mathbf{c}}, J_{\mathbf{f}}, J_{\mathbf{g}}$ are explicit difference operators. It remains to show the existence of stability bounds that are independent of h and k . To this end, let $m \in \{q, \dots, N\}$ be arbitrary.

Setting $\beta_h = \Phi_h^m$ in (3.10) and using Assumption 2.2 yields

$$\|\nabla \Phi_h^m\| \leq \frac{1}{\epsilon_-} \left(\epsilon_+ \|\nabla \Phi_b\| + \|f_{\beta}\|_{\infty; \Upsilon^*} \right) = G_{\Phi},$$

and thus,

$$\|\Phi_h^m + \Phi_b\|_{1,2} \leq \sqrt{1 + c_D^2} G_\Phi + \|\Phi_b\|_{1,2} = G_{\Phi, \Phi_b}. \tag{3.16}$$

Setting $\mathbf{v}_h = \mathbf{u}_h^m$, $\tau_h = \theta_h^m$ in (3.7), (3.9) yields

$$\begin{aligned} L_1 &:= (J_{\mathbf{d}} \mathbf{u}_h^m, \mathbf{u}_h^m) + k\nu \|\nabla \mathbf{u}_h^m\|^2 \\ &= k \langle \mathbf{F}(J_{\mathbf{f}} \theta_h^m + \theta_b, \Phi_h^m + \Phi_b) + \mathbf{f}_{\mathbf{v}}^m, \mathbf{u}_h^m \rangle_{\mathbf{U}^*} =: R_1, \end{aligned} \tag{3.17}$$

$$\begin{aligned} L_2 &:= (J_{\mathbf{d}} \theta_h^m, \theta_h^m) + k\kappa \|\nabla \theta_h^m\|^2 \\ &= -k\kappa (\nabla \theta_b, \nabla \theta_h^m) - k\tilde{c}_\tau (J_{\mathbf{c}} \mathbf{u}_h^m, \theta_b, \theta_h^m) + k \langle f_\tau^m, \theta_h^m \rangle_{\Theta^*} =: R_2. \end{aligned} \tag{3.18}$$

The respective left-hand sides of (3.17) and (3.18) can be estimated from below by means of Assumption 3.10 (iii),

$$L_1 \geq \bar{o} J_1 \left(\|\mathbf{u}_h^m\|^2 + U_m^2 \right) + \bar{U}_m^2 + k\nu \|\nabla \mathbf{u}_h^m\|^2, \tag{3.19}$$

$$L_2 \geq \bar{o} J_1 \left(\|\theta_h^m\|^2 + T_m^2 \right) + \bar{T}_m^2 + k\kappa \|\nabla \theta_h^m\|^2, \tag{3.20}$$

for some real sequences $(U_m)_m, (\bar{U}_m)_m, (T_m)_m, (\bar{T}_m)_m$. Using Assumption 3.13 (iii) and (i) with the upper bound on $\|\Phi_h^m + \Phi_b\|_{1,2}$ (3.16), the right-hand side of (3.17) can be estimated from above by

$$\begin{aligned} R_1 &\leq k \left(\|\mathbf{f}_{\mathbf{v}}\|_{\infty; \mathbf{U}^*} + c_0 L_{\mathbf{F}}^{(\theta, H^1)} \|\nabla \theta_b\| + c_0 L_{\mathbf{F}}^{(\theta, L^2)} \|\theta_b\| \right) \|\nabla \mathbf{u}_h^m\| \\ &\quad + kc_0 \|\mathbf{f}\|_{\infty} \|\nabla \mathbf{u}_h^m\| \sum_{i=1}^q \left\{ L_{\mathbf{F}}^{(\theta, H^1)} \|\nabla \theta_h^{m-i}\| + L_{\mathbf{F}}^{(\theta, L^2)} \|\theta_h^{m-i}\| \right\} \\ &=: k \|\nabla \mathbf{u}_h^m\| \left(G_1 + G_* \sum_{i=1}^q \|\nabla \theta_h^{m-i}\| + G_2 \sum_{i=1}^q \|\theta_h^{m-i}\| \right), \end{aligned} \tag{3.21}$$

where $L_{\mathbf{F}}^{(\theta, H^1)} := L_{\mathbf{F}}^{(1)} = L_{\mathbf{F}}^{(\theta, H^1)}(G_{\Phi, \Phi_b})$ and $L_{\mathbf{F}}^{(\theta, L^2)} := L_{\mathbf{F}}^{(\theta, L^2)}(G_{\Phi, \Phi_b})$. Using the Sobolev interpolation estimate, R_2 can be estimated from above *via*

$$\begin{aligned} R_2 &\leq ck \|\nabla \theta_h^m\| \left(\kappa \|\nabla \theta_b\| + \|f_\tau\|_{\infty; \Theta^*} + \|\theta_b\|_{1,2} \|\mathbf{c}\|_{\infty} \sum_{i=1}^q \|\mathbf{u}_h^{m-i}\|^{\frac{1}{2}} \|\nabla \mathbf{u}_h^{m-i}\|^{\frac{1}{2}} \right) \\ &=: k \|\nabla \theta_h^m\| \left(G_3 + G_4 \sum_{i=1}^q \|\mathbf{u}_h^{m-i}\|^{\frac{1}{2}} \|\nabla \mathbf{u}_h^{m-i}\|^{\frac{1}{2}} \right). \end{aligned} \tag{3.22}$$

Combining (3.19) and (3.21) and using Young's inequality, as well as $(\sum_{i=1}^q a_i)^2 \leq q \sum_{i=1}^q a_i^2$ for $a_i \in [0, \infty)$, yields for arbitrary $\gamma \in (0, 2)$,

$$\begin{aligned} &\bar{o} \left(\|\mathbf{u}_h^m\|^2 - \|\mathbf{u}_h^{m-1}\|^2 + U_m^2 - U_{m-1}^2 \right) + \bar{U}_m^2 + k \frac{\nu}{4} (2 - \gamma) \|\nabla \mathbf{u}_h^m\|^2 \\ &\leq k \frac{2G_1^2}{\nu(2 - \gamma)} + k \frac{2G_2^2 q}{\nu(2 - \gamma)} \sum_{i=1}^q \|\theta_h^{m-i}\|^2 + k \frac{G_*^2 q}{2\gamma\nu} \sum_{i=1}^q \|\nabla \theta_h^{m-i}\|^2 \\ &=: kG_5 + k \sum_{i=1}^q \left\{ G_6 \|\theta_h^{m-i}\|^2 + \frac{1}{\gamma q} G_{**} \|\nabla \theta_h^{m-i}\|^2 \right\}. \end{aligned} \tag{3.23}$$

Analogously, combination of (3.20) and (3.22) yields for arbitrary $\epsilon \in (0, 1)$, $\sigma > 0$,

$$\bar{o} \left(\|\theta_h^m\|^2 - \|\theta_h^{m-1}\|^2 + T_m^2 - T_{m-1}^2 \right) + \bar{T}_m^2 + k\kappa(1 - \epsilon) \|\nabla \theta_h^m\|^2$$

$$\begin{aligned}
&\leq k \frac{G_3^2}{2\epsilon\kappa} + k \sum_{i=1}^q \left\{ \frac{\nu}{\sigma q} \|\nabla \mathbf{u}_h^{m-i}\|^2 + \frac{\sigma}{\epsilon^2} \frac{G_4^4 q^3}{16\kappa^2 \nu} \|\mathbf{u}_h^{m-i}\|^2 \right\} \\
&=: kG_7 + k \sum_{i=1}^q \left\{ \frac{\nu}{\sigma q} \|\nabla \mathbf{u}_h^{m-i}\|^2 + G_8 \|\mathbf{u}_h^{m-i}\|^2 \right\}, \tag{3.24}
\end{aligned}$$

Adding (3.23) and (3.24) and summation over $m = q, \dots, M$ for arbitrary $M \in \{q, \dots, N\}$ yields

$$\begin{aligned}
&\bar{o} \left(\|\mathbf{u}_h^M\|^2 + \|\theta_h^M\|^2 + U_M^2 + T_M^2 \right) + k \sum_{m=q}^M \left\{ \frac{1}{k} \bar{U}_m^2 + \frac{1}{k} \bar{T}_m^2 \right\} \\
&\quad + k \sum_{m=q}^M \left\{ \nu \left(\frac{1}{4}(2-\gamma) - \frac{1}{\sigma} \right) \|\nabla \mathbf{u}_h^m\|^2 + \left(\kappa(1-\epsilon) - \frac{1}{\gamma} G_{**} \right) \|\nabla \theta_h^m\|^2 \right\} \\
&\leq k \sum_{m=0}^{M-1} \left\{ G_8 q \|\mathbf{u}_h^m\|^2 + G_6 q \|\theta_h^m\|^2 \right\} + k \sum_{m=q}^M \{G_5 + G_7\} \\
&\quad + \bar{o} \left(\|\mathbf{u}_h^{q-1}\|^2 + \|\theta_h^{q-1}\|^2 + U_{q-1}^2 + T_{q-1}^2 \right) \\
&\quad + k \sum_{i=0}^{q-1} \left\{ \frac{\nu}{\sigma} \|\nabla \mathbf{u}_h^i\|^2 + \frac{G_{**}}{\gamma} \|\nabla \theta_h^i\|^2 \right\}. \tag{3.25}
\end{aligned}$$

If $G_{**} < 2\kappa$, which is equivalent to (3.11), then γ, ϵ, σ can be chosen such that

$$\begin{aligned}
\bar{\nu} &:= \nu(4^{-1}(2-\gamma) - \sigma^{-1}) > 0, \\
\bar{\kappa} &:= \kappa(1-\epsilon) - \gamma^{-1} G_{**} > 0.
\end{aligned}$$

Then, application of the discrete Grönwall's inequality, Lemma A.1, to (3.25) gives

$$\begin{aligned}
&\bar{o} \left(\|\mathbf{u}_h^M\|^2 + \|\theta_h^M\|^2 + U_M^2 + T_M^2 \right) + k \sum_{m=q}^M \left\{ \bar{\nu} \|\nabla \mathbf{u}_h^m\|^2 + \bar{\kappa} \|\nabla \theta_h^m\|^2 + \frac{1}{k} \bar{U}_m^2 + \frac{1}{k} \bar{T}_m^2 \right\} \\
&\leq \exp((T+k)q\sigma^{-1} \max\{G_6, G_8, 1\}) \\
&\quad \cdot \left[T(G_5 + G_7) + \bar{o} \left(\|\mathbf{u}_h^{q-1}\|^2 + \|\theta_h^{q-1}\|^2 + U_{q-1}^2 + T_{q-1}^2 \right) \right. \\
&\quad \left. + k \sum_{i=0}^{q-1} \left\{ \frac{\nu}{\sigma} \|\nabla \mathbf{u}_h^i\|^2 + \frac{G_{**}}{\gamma} \|\nabla \theta_h^i\|^2 \right\} \right]. \tag{3.26}
\end{aligned}$$

The stated estimates now follow from (3.16) and (3.26) in combination with (3.15). \square

Remark 3.15. Note that, if the difference operator $J_{\mathbf{d}}$ is given as stated in Lemma 3.11, then U_{q-1}, T_{q-1} do only depend on $(\mathbf{u}_h^i, \theta_h^i)$ for $i = 0, \dots, q-1$ and can be bounded in terms of $\sum_{i=0}^{q-1} \{ \|\mathbf{u}_h^i\| + \|\theta_h^i\| \}$.

Remark 3.16. The norm estimates appearing in Lemma 3.14 and its proof do still depend on the L^2 and H^1 norm of the discrete initial conditions $(\mathbf{u}_h^i, \theta_h^i)_{i=0, \dots, q-1}$. For $q = 1$, suitable discrete initial conditions can be obtained by applying the Stokes operator to $(\mathbf{u}_0, 0)$ and by applying an H^1 projection to $\theta_0 - \theta_b$. The appearing norms of $(\mathbf{u}_h^0, \theta_h^0)$ can then be bounded in terms of $(\mathbf{u}_0, \theta_0 - \theta_b)$ and uniformly in h .

For $q > 1$, suitable initial conditions $(\mathbf{u}_h^i, \theta_h^i)_{i=1, \dots, q-1}$ can be obtained by performing $q-1$ steps of a $(q=1)$ -time stepping scheme, followed by application of the norm estimates in Lemma 3.14 for $q = 1$ to uniformly bound $(\mathbf{u}_h^i, \theta_h^i)_{i=1, \dots, q-1}$.

Remark 3.17. The need for the small data condition (3.11) imposed by Lemma 3.14 stems from the occurrence of $\|\nabla\theta\|$ when bounding the \mathbf{U}^* -norm of the body force term \mathbf{F} , see (3.21). For this reason, the right-hand side in Assumption 3.13 (i) is split into H^1 and L^2 terms, where only the first one contributes to (3.11).

4. ERROR ESTIMATE

The main result of this work, Theorem 4.1, provides an *a priori* error estimate for the numerical scheme defined by Problem 3.12. The derived upper bounds depend on spatial approximation errors, which can be bounded in terms of h , errors induced by the initial conditions, and approximation properties of the temporal difference operators. At this point, no regularity on temporal derivatives of the exact solution is imposed and, consequently, no convergence rates w.r.t. k are derived. This is done as a separate step in form of Corollaries 4.7 and 4.8 in Section 4.2.

4.1. Main *a priori* estimate

Before stating Theorem 4.1, some notation has to be introduced. The exact solution at time t_n is denoted by $(\mathbf{u}^n, p^n, \theta^n, \Phi^n)$ and corresponding approximations in the underlying finite element spaces are obtained by using the Stokes projection Π_S and projections provided by Assumption 3.1,

$$(\mathbf{w}_h^n, r_h^n) := \Pi_S(\mathbf{u}^n, p^n), \quad \eta_h^n := \Pi_\Theta \theta^n, \quad \Psi_h^n := \Pi_\Upsilon \Phi^n. \tag{4.1}$$

The discretization errors between these projections and the discrete solution of Problem 3.12 are defined as

$$\mathbf{d}_{\mathbf{u},h}^n := \mathbf{w}_h^n - \mathbf{u}_h^n, \quad d_{p,h}^n := r_h^n - p_h^n, \quad d_{\theta,h}^n := \eta_h^n - \theta_h^n, \quad d_{\Phi,h}^n := \Psi_h^n - \Phi_h^n. \tag{4.2}$$

When applying the estimate stated in Assumption 3.10 (iii) for $z^m = \mathbf{d}_{\mathbf{u},h}^n$ and $z^m = d_{\theta,h}^n$, respectively, one further obtains real sequences $(U_n)_{n \geq q-1}$, $(T_n)_{n \geq q-1}$, $(\bar{U}_n)_{n \geq q}$, $(\bar{T}_n)_{n \geq q}$ such that the following estimates hold for all $n \geq q$,

$$(J_{\mathbf{d}} \mathbf{d}_{\mathbf{u},h}^n, \mathbf{d}_{\mathbf{u},h}^n)_Z \geq \bar{\sigma} J_1 \left(\|\mathbf{d}_{\mathbf{u},h}^n\|^2 + U_n^2 \right) + \bar{U}_n^2, \tag{4.3}$$

$$(J_{\mathbf{d}} d_{\theta,h}^n, d_{\theta,h}^n)_Z \geq \bar{\sigma} J_1 \left(\|d_{\theta,h}^n\|^2 + T_n^2 \right) + \bar{T}_n^2. \tag{4.4}$$

The error will be bounded in terms of the subsequent expressions. The first set of expressions measures the error contributions by the q initial conditions:

$$E_1(q)^2 := k \sum_{n=0}^{q-1} \left\{ \|\mathbf{u}^n - \mathbf{u}_h^n\|_{1,2}^2 + \|\theta^n - \theta_h^n\|_{1,2}^2 \right\} + \|\mathbf{u}^{q-1} - \mathbf{u}_h^{q-1}\|^2 + \|\theta^{q-1} - \theta_h^{q-1}\|^2 + U_{q-1}^2 + T_{q-1}^2, \tag{4.5}$$

$$E_2(q) := \max \left\{ \|\mathbf{u}^n - \mathbf{u}_h^n\|_{1,2} : n = 0, \dots, q-1 \right\}, \tag{4.6}$$

$$E_3(q) := \max \left\{ \|\theta^n - \theta_h^n\| : n = 0, \dots, q-1 \right\}. \tag{4.7}$$

Error contributions that are purely driven by the temporal discretization are given by

$$\begin{aligned} E(k)^2 := & k \sum_{n=q}^N \left\{ \|\partial_t \mathbf{u}^n - k^{-1} J_{\mathbf{d}} \mathbf{u}^n\|_{-1,2}^2 + \|\partial_t \theta^n - k^{-1} J_{\mathbf{d}} \theta^n\|_{-1,2}^2 \right\} \\ & + k \sum_{n=q}^N \left\{ \|\mathbf{u}^n - J_{\mathbf{c}} \mathbf{u}^n\|^2 + \|\theta^n - J_{\mathbf{f}} \theta^n\|_{1,2}^2 + \|\theta^n - J_{\mathbf{g}} \theta^n\|^2 \right\}. \end{aligned} \tag{4.8}$$

In Section 4.2, $E(k)$ is bounded in terms of k . Contributions by both temporal and spatial discretization are denoted by

$$E(h, k)^2 := h^{2(l+l^*)} k \sum_{n=q}^N \left\{ \|k^{-1} J_{\mathbf{d}} \mathbf{u}^n\|_{l+1,2}^2 + \|k^{-1} J_{\mathbf{d}} p^n\|_{l,2}^2 \right\} + h^{2l} k \sum_{n=q}^N \|k^{-1} J_{\mathbf{d}} \theta^n\|_{l+1,2}^2, \quad (4.9)$$

with constants l, l^* that depend on the spatial regularity of the exact solution and the approximation quality of the finite element spaces. Finally, the term

$$E_{\mathbf{d}}(h, k)^2 := k^{-1} \sum_{n=q}^N \|J_{\mathbf{d}} \mathbf{d}_{\mathbf{u},h}^n\|^2, \quad (4.10)$$

which involves the unknown velocity discretization error will be bounded by other terms and is used to bound the pressure discretization error. The actual error bounds are now composed by the previously defined terms:

$$\mathcal{E}_{\mathbf{u},\theta}(h, k, q) := h^l + E(k) + E(h, k) + E_1(q), \quad (4.11)$$

$$\mathcal{E}_{\Phi}(h, k, q) := \mathcal{E}_{\mathbf{u},\theta}(h, k, q) + E_3(q), \quad (4.12)$$

$$\mathcal{E}_p(h, k, q) := E(k) + E(h, k) + E_{\mathbf{d}}(k, h) + C_p(h, k, q) \mathcal{E}_{\mathbf{u},\theta}(h, k, q), \quad (4.13)$$

$$\mathcal{E}_{\mathbf{d}}(h, k, q) := k^{-\frac{1}{2}} (E(k) + E(h, k)) + C_p(h, k, q) \left(h^l + E_2(q) + k^{-\frac{1}{2}} \mathcal{E}_{\mathbf{u},\theta}(h, k, q) \right), \quad (4.14)$$

$$C_p(h, k, q) := 1 + h^l + \min \left\{ h^{-1}, k^{-\frac{1}{2}} \right\} \mathcal{E}_{\mathbf{u},\theta}(h, k, q) + E_2(q). \quad (4.15)$$

The following theorem states that the errors of velocity and temperature, contributed by the spatial discretization and measured in $L^2(\mathbf{H}^1)$, $l^\infty(L^2)$ -norm, converge with rate h^l for fixed time step size k . The analogous result in $L^2(\mathbf{H}^1)$ holds for the potential error. Concerning the pressure error, the factor $k^{-\frac{1}{2}}$ enters the corresponding upper bound \mathcal{E}_p through the term $E_{\mathbf{d}}(k, h)$, thus yielding a reduced temporal convergence rate compared to velocity, temperature and potential. Here, the term C_p denotes a bound on the $l^\infty(\mathbf{H}^1)$ -norm of discrete velocity (4.57) and one can show that it stays bounded for $h, k \rightarrow 0$, supposed that the exact solution is sufficiently regular and the initial conditions are chosen appropriately, see Corollaries 4.7, 4.8 and the subsequent remarks.

Theorem 4.1 (Error of numerical scheme). *In the framework of Problem 3.12, let a solution of Problem 2.4 be given that satisfies the following additional regularity requirements for some $l \geq 1$: $\mathbf{u} \in L^\infty(\mathbf{H}^{l+1})$, $p \in L^\infty(H^l)$, $\theta \in L^\infty(H^{l+1})$ and $\Phi \in L^\infty(H^{l+1}) \cap L^\infty(\mathbf{W}^{1,\infty})$. Moreover, the exact solution should be pointwise well-defined for all $t \in [0, T]$.*

Suppose that Assumption 3.1 holds with $\bar{m} = \bar{n} = l$. Moreover, let $l^ = 1$ if the underlying Stokes problem is regular and $l^* = 0$, otherwise. Let further the assumptions of Lemma 3.14 hold; in particular, assume that \mathbf{F} satisfies Assumption 3.13 and the small data conditions*

$$c_0 \sqrt{q} |\mathbf{f}|_2 L_{\mathbf{F}}^{(2)} < \sqrt{2\tilde{\nu}\tilde{\kappa}} \quad (4.16)$$

with $\tilde{\nu} := \nu \frac{1}{2(1+c_D^2)}$, $\tilde{\kappa} := \kappa \frac{1}{2(1+c_D^2)}$ and c_0, c_D denoting the respective constants from Friedrich's inequality w.r.t. \mathbf{H}_0^1 and \mathbf{H}_D^1 . Moreover,

$$L_{\mathbf{F}}^{(2)} := L_{\mathbf{F}}^{(\theta, \mathbf{H}^1)} \left(\max \left\{ \|\Phi\|_{\infty; \mathbf{H}^1}, c_{\Pi} \|\Phi\|_{\infty; \mathbf{H}^2}, \sqrt{1 + c_D^2} G_{\Phi} \right\} + \|\Phi_b\|_{1,2} \right),$$

with c_{Π} given by Assumption 3.1 and G_{Φ} given by Lemma 3.14. Then,

$$\|(\mathbf{u}^n - \mathbf{u}_h^n)_n\|_{l^\infty(q, N; \mathbf{L}_2)} + \|(\theta^n - \theta_h^n)_n\|_{l^\infty(q, N; L_2)} \lesssim \mathcal{E}_{\mathbf{u},\theta}(h, k, q),$$

$$\begin{aligned} \|(\mathbf{u}^n - \mathbf{u}_h^n)_n\|_{L^2(q,N;\mathbf{H}^1),k} + \|(\theta^n - \theta_h^n)_n\|_{L^2(q,N;\mathbf{H}^1),k} &\lesssim \mathcal{E}_{\mathbf{u},\theta}(h, k, q), \\ \|(\Phi^n - \Phi_h^n)_n\|_{L^2(q,N;\mathbf{H}^1),k} &\lesssim \mathcal{E}_\Phi(h, k, q), \\ \|(p^n - p_h^n)_n\|_{L^2(q,N;L_2),k} &\lesssim \mathcal{E}_p(h, k, q), \\ E_{\mathbf{d}}(h, k) &\lesssim \mathcal{E}_{\mathbf{d}}(h, k, q). \end{aligned}$$

The underlying principle of the corresponding proof is inspired by comparable results on the error of fully discretized flow problems, see *e.g.* [39] for the Boussinesq problem with temperature-dependent coefficients.

Proof. The error of the respective variables is decomposed into approximation and discretization contributions:

$$\begin{aligned} e_{\mathbf{u},h}^n &:= \mathbf{u}^n - \mathbf{u}_h^n = \mathbf{u}^n - \mathbf{w}_h^n + \mathbf{w}_h^n - \mathbf{u}_h^n =: \mathbf{z}_{\mathbf{u},h}^n + \mathbf{d}_{\mathbf{u},h}^n, \\ e_{p,h}^n &:= p^n - p_h^n = p^n - r_h^n + r_h^n - p_h^n =: z_{p,h}^n + d_{p,h}^n, \\ e_{\theta,h}^n &:= \theta^n - \theta_h^n = \theta^n - \eta_h^n + \eta_h^n - \theta_h^n =: z_{\theta,h}^n + d_{\theta,h}^n, \\ e_{\Phi,h}^n &:= \Phi^n - \Phi_h^n = \Phi^n - \Psi_h^n + \Psi_h^n - \Phi_h^n =: z_{\Phi,h}^n + d_{\Phi,h}^n. \end{aligned}$$

Error equation

Subtracting the discrete equations, Problem 3.12, from the continuous ones, Problem 2.4, at each time t_n , $n \in \{q, \dots, N\}$ yields the following error equation for all $(\mathbf{v}_h, q_h, \tau_h, \beta_h) \in \mathbf{U}_h \times M_h \times \Theta_h \times \Upsilon_h$:

$$k^{-1}(J_{\mathbf{d}}\mathbf{d}_{\mathbf{u},h}^n, \mathbf{v}_h) + a_{\mathbf{v}}(\mathbf{d}_{\mathbf{u},h}^n, \mathbf{v}_h) - b(\mathbf{v}_h, d_{p,h}^n) = \sum_{i=1}^4 \langle R_i^n, \mathbf{v}_h \rangle, \tag{4.17}$$

$$b(\mathbf{d}_{\mathbf{u},h}^n, q_h) = \langle R_5^n, q_h \rangle, \tag{4.18}$$

$$k^{-1}(J_{\mathbf{d}}d_{\theta,h}^n, \tau_h) + a_{\tau}(d_{\theta,h}^n, \tau_h) = \sum_{i=6}^8 \langle R_i^n, \tau_h \rangle, \tag{4.19}$$

$$a_{\beta}(\theta^n + \theta_b, \Phi^n + \Phi_b, \beta_h) - a_{\beta}(J_{\mathbf{g}}\theta_h^n + \theta_b, \Phi_h^n + \Phi_b, \beta_h) = 0, \tag{4.20}$$

with residuals

$$\begin{aligned} \langle R_1^n, \mathbf{v}_h \rangle &= -(\partial_t \mathbf{u}^n - k^{-1}J_{\mathbf{d}}\mathbf{w}_h^n, \mathbf{v}_h), \\ \langle R_2^n, \mathbf{v}_h \rangle &= -(a_{\mathbf{v}}(\mathbf{z}_{\mathbf{u},h}^n, \mathbf{v}_h) - b(\mathbf{v}_h, z_{p,h}^n)), \\ \langle R_3^n, \mathbf{v}_h \rangle &= -(\tilde{c}_{\mathbf{v}}(\mathbf{u}^n, \mathbf{u}^n, \mathbf{v}_h) - \tilde{c}_{\mathbf{v}}(J_{\mathbf{c}}\mathbf{u}_h^n, \mathbf{u}_h^n, \mathbf{v}_h)), \\ \langle R_4^n, \mathbf{v}_h \rangle &= \langle \mathbf{F}(\theta^n + \theta_b, \Phi^n + \Phi_b) - \mathbf{F}(J_{\mathbf{f}}\theta_h^n + \theta_b, \Phi_h^n + \Phi_b), \mathbf{v}_h \rangle, \\ \langle R_5^n, q_h \rangle &= -b(\mathbf{z}_{\mathbf{u},h}^n, q_h), \\ \langle R_6^n, \tau_h \rangle &= -(\partial_t \theta^n - k^{-1}J_{\mathbf{d}}\eta_h^n, \tau_h), \\ \langle R_7^n, \tau_h \rangle &= -a_{\tau}(z_{\theta,h}^n, \tau_h), \\ \langle R_8^n, \tau_h \rangle &= -(\tilde{c}_{\tau}(\mathbf{u}^n, \theta^n + \theta_b, \tau_h) - \tilde{c}_{\tau}(J_{\mathbf{c}}\mathbf{u}_h^n, \theta_h^n + \theta_b, \tau_h)). \end{aligned}$$

By definition of (\mathbf{w}_h^n, r_h^n) and the Stokes projection, there holds $\langle R_2^n, \mathbf{v}_h \rangle = 0$ and $\langle R_5^n, q_h \rangle = 0$ and for residual R_7 one obtains

$$|\langle R_7, d_{\theta,h}^n \rangle| \leq \kappa \|z_{\theta,h}^n\|_{1,2} \|d_{\theta,h}^n\|_{1,2}. \tag{4.21}$$

In the following, the introduced constants $\{C_{i,j}\}$ do not depend on the discrete solution, the discretization parameters h, k and the diffusion constants ν, κ . However, they may include norms of the exact solution.

Estimation of potential error

Setting $\beta_h = d_{\Phi,h}^n$ in Gauss' law in (4.20) gives

$$\begin{aligned} 0 &= a_\beta(\theta^n + \theta_b, \Phi^n + \Phi_b, d_{\Phi,h}^n) - a_\beta(J_{\mathbf{g}}\theta^n + \theta_b, \Phi^n + \Phi_b, d_{\Phi,h}^n) \\ &\quad + a_\beta(J_{\mathbf{g}}\theta^n + \theta_b, \Phi^n + \Phi_b, d_{\Phi,h}^n) - a_\beta(J_{\mathbf{g}}\theta_h^n + \theta_b, \Phi^n + \Phi_b, d_{\Phi,h}^n) \\ &\quad + a_\beta(J_{\mathbf{g}}\theta_h^n + \theta_b, \Phi^n + \Phi_b, d_{\Phi,h}^n) - a_\beta(J_{\mathbf{g}}\theta_h^n + \theta_b, \Psi_h^n + \Phi_b, d_{\Phi,h}^n) \\ &\quad + a_\beta(J_{\mathbf{g}}\theta_h^n + \theta_b, \Psi_h^n + \Phi_b, d_{\Phi,h}^n) - a_\beta(J_{\mathbf{g}}\theta_h^n + \theta_b, \Phi_h^n + \Phi_b, d_{\Phi,h}^n) \\ &=: J_1 + J_2 + J_3 + J_4. \end{aligned}$$

Using Hölder's inequality and Assumption 2.2 on ϵ gives

$$\begin{aligned} |J_1| &= |((\epsilon(\theta^n + \theta_b) - \epsilon(J_{\mathbf{g}}\theta^n + \theta_b))\nabla(\Phi^n + \Phi_b), \nabla d_{\Phi,h}^n)| \\ &\leq L_\epsilon \|\theta^n - J_{\mathbf{g}}\theta^n\| \|\Phi^n + \Phi_b\|_{1,\infty} \|\nabla d_{\Phi,h}^n\| \\ |J_2| &= |((\epsilon(J_{\mathbf{g}}\theta^n + \theta_b) - \epsilon(J_{\mathbf{g}}\theta_h^n + \theta_b))\nabla(\Phi^n + \Phi_b), \nabla d_{\Phi,h}^n)| \\ &\leq L_\epsilon \|J_{\mathbf{g}}(\theta^n - \theta_h^n)\| \|\Phi^n + \Phi_b\|_{1,\infty} \|\nabla d_{\Phi,h}^n\| \\ |J_3| &= |(\epsilon(J_{\mathbf{g}}\theta_h^n + \theta_b)\nabla(\Phi^n - \Psi_h^n), \nabla d_{\Phi,h}^n)| \\ &\leq \epsilon_+ \|z_{\Phi,h}^n\|_{1,2} \|\nabla d_{\Phi,h}^n\| \\ J_4 &= (\epsilon(J_{\mathbf{g}}\theta_h^n + \theta_b)\nabla(\Psi_h^n - \Phi_h^n), \nabla d_{\Phi,h}^n) \\ &\geq \epsilon_- \|\nabla d_{\Phi,h}^n\|^2. \end{aligned}$$

Combining these estimates yields

$$\|\nabla d_{\Phi,h}^n\| \leq C_{0,1} (\|\theta^n - J_{\mathbf{g}}\theta^n\| + \|J_{\mathbf{g}}z_{\theta,h}^n\| + \|J_{\mathbf{g}}d_{\theta,h}^n\|) + C_{0,2} \|z_{\Phi,h}^n\|_{1,2}. \quad (4.22)$$

According to Lemma 3.14 and Assumption 3.1 (iii),

$$\|\Phi^n\|_{1,2} \leq \sqrt{1 + c_D^2} G_\Phi, \quad (4.23)$$

$$\|\Phi_h^n\|_{1,2} \leq \sqrt{1 + c_D^2} G_\Phi, \quad (4.24)$$

$$\|\eta_h^n\|_{1,2} \leq c_\Pi \|\theta^n\|_{2,2} \leq c_\Pi \|\theta\|_{\infty;H^2}, \quad (4.25)$$

$$\|\eta_h^n\|_{1,3} \leq c_\Pi \|\theta^n\|_{2,2} \leq c_\Pi \|\theta\|_{\infty;H^2}, \quad (4.26)$$

$$\|\Psi_h^n\|_{1,2} \leq c_\Pi \|\Phi^n\|_{2,2} \leq c_\Pi \|\Phi\|_{\infty;H^2}. \quad (4.27)$$

Estimation of body force residual

$$\begin{aligned} \langle R_4^n, \mathbf{v}_h \rangle &= \langle \mathbf{F}(\theta^n + \theta_b, \Phi^n + \Phi_b) - \mathbf{F}(J_{\mathbf{f}}\theta^n + \theta_b, \Phi^n + \Phi_b), \mathbf{v}_h \rangle, \\ &\quad + \langle \mathbf{F}(J_{\mathbf{f}}\theta^n + \theta_b, \Phi^n + \Phi_b) - \mathbf{F}(J_{\mathbf{f}}\theta^n + \theta_b, \Psi_h^n + \Phi_b), \mathbf{v}_h \rangle \\ &\quad + \langle \mathbf{F}(J_{\mathbf{f}}\theta^n + \theta_b, \Psi_h^n + \Phi_b) - \mathbf{F}(J_{\mathbf{f}}\eta_h^n + \theta_b, \Psi_h^n + \Phi_b), \mathbf{v}_h \rangle \\ &\quad + \langle \mathbf{F}(J_{\mathbf{f}}\eta_h^n + \theta_b, \Psi_h^n + \Phi_b) - \mathbf{F}(J_{\mathbf{f}}\eta_h^n + \theta_b, \Phi_h^n + \Phi_b), \mathbf{v}_h \rangle \\ &\quad + \langle \mathbf{F}(J_{\mathbf{f}}\eta_h^n + \theta_b, \Phi_h^n + \Phi_b) - \mathbf{F}(J_{\mathbf{f}}\theta_h^n + \theta_b, \Phi_h^n + \Phi_b), \mathbf{v}_h \rangle \\ &=: \sum_{i=1}^5 \langle L_i, \mathbf{v}_h \rangle. \end{aligned}$$

Then, by using the Lipschitz continuity of \mathbf{F} as given by Assumption 3.13,

$$\begin{aligned}
 |\langle L_1, \mathbf{v}_h \rangle| &\leq c_0 \left(L_{\mathbf{F}}^{(\theta, H^1)} \|\nabla(\theta^n - J_{\mathbf{f}}\theta^n)\| + L_{\mathbf{F}}^{(\theta, L^2)} \|\theta^n - J_{\mathbf{f}}\theta^n\| \right) \|\mathbf{v}_h\|_{1,2}, \\
 |\langle L_2, \mathbf{v}_h \rangle| &\leq L_{\mathbf{F}}^{(\Phi)} \|J_{\mathbf{f}}\theta^n + \theta_b\|_{1,3} \|\nabla z_{\Phi,h}^n\| \|\mathbf{v}_h\|_{0,6} \\
 &\leq cL_{\mathbf{F}}^{(\Phi)} \left(c|\mathbf{f}|_1 \|\theta\|_{\infty; H^2} + \|\theta_b\|_{1,3} \right) \|\nabla z_{\Phi,h}^n\| \|\mathbf{v}_h\|_{1,2}, \\
 &\quad (\text{by (4.27), } H^2(\Omega) \hookrightarrow W^{1,3}(\Omega) \text{ and } H^1(\Omega) \hookrightarrow L^6(\Omega)) \\
 |\langle L_3, \mathbf{v}_h \rangle| &\leq c_0 L_{\mathbf{F}}^{(\theta, H^1)} \|\nabla J_{\mathbf{f}}z_{\theta,h}^n\| \|\mathbf{v}_h\|_{1,2} + c_0 L_{\mathbf{F}}^{(\theta, L^2)} \|J_{\mathbf{f}}z_{\theta,h}^n\| \|\mathbf{v}_h\|_{1,2}, \\
 |\langle L_4, \mathbf{v}_h \rangle| &\leq L_{\mathbf{F}}^{(\Phi)} \|J_{\mathbf{f}}\eta_h^n + \theta_b\|_{1,3} \|\nabla d_{\Phi,h}^n\| \|\mathbf{v}_h\|_{0,6} \\
 &\leq cL_{\mathbf{F}}^{(\Phi)} \left(c|\mathbf{f}|_1 \|\theta\|_{\infty; H^2} + \|\theta_b\|_{1,3} \right) \|\nabla d_{\Phi,h}^n\| \|\mathbf{v}_h\|_{1,2}, \\
 &\quad (\text{by (4.24, 4.27, 4.26), and } H^1(\Omega) \hookrightarrow L^6(\Omega)) \\
 |\langle L_5, \mathbf{v}_h \rangle| &\leq c_0 L_{\mathbf{F}}^{(\theta, H^1)} \|\nabla J_{\mathbf{f}}d_{\theta,h}^n\| \|\mathbf{v}_h\|_{1,2} + c_0 L_{\mathbf{F}}^{(\theta, L^2)} \|J_{\mathbf{f}}d_{\theta,h}^n\| \|\mathbf{v}_h\|_{1,2}.
 \end{aligned}$$

In the previous estimates, we used the uniform boundedness of $(\|\eta_h^n\|_{1,2})_n$, $(\|\Phi^n\|_{1,2})_n$, $(\|\Phi_h^n\|_{1,2})_n$, $(\|\Psi_h^n\|_{1,2})_n$ (4.23)–(4.27), to infer maximal values of the Lipschitz moduli of \mathbf{F} w.r.t. θ , *i.e.*

$$L_{\mathbf{F}}^{(\theta, X)} := L_{\mathbf{F}}^{(\theta, X)} \left(\max \left\{ \|\Phi\|_{\infty; H^1}, c_{\Pi} \|\Phi\|_{\infty; H^2}, \sqrt{1 + c_D^2} G_{\Phi} \right\} + \|\Phi_b\|_{1,2} \right),$$

for $X \in \{H^1, L^2\}$ and and, similarly, w.r.t. Φ .

Using (4.22) to substitute $\|\nabla d_{\Phi,h}^n\|$, the force residual norm can be estimated from above *via*

$$\begin{aligned}
 \frac{|\langle R_4^n, \mathbf{v}_h \rangle|}{\|\mathbf{v}_h\|_{1,2}} &\leq C_{4,1} \|\theta^n - J_{\mathbf{f}}\theta^n\|_{1,2} + C_{4,2} \left(\|J_{\mathbf{f}}z_{\theta,h}^n\|_{1,2} + \|z_{\Phi,h}^n\|_{1,2} \right) \\
 &\quad + C_{4,3} (C_{0,1} (\|\theta^n - J_{\mathbf{g}}\theta^n\| + \|J_{\mathbf{g}}z_{\theta,h}^n\| + \|J_{\mathbf{g}}d_{\theta,h}^n\|)) \\
 &\quad + C_{4,3} C_{0,2} \|z_{\Phi,h}^n\|_{1,2} + C_{4,i} \|J_{\mathbf{f}}d_{\theta,h}^n\| + C_{4,ii} \|J_{\mathbf{f}}d_{\theta,h}^n\|_{1,2},
 \end{aligned} \tag{4.28}$$

with $C_{4,i} = c_0 L_{\mathbf{F}}^{(\theta, L^2)}$, $C_{4,ii} = c_0 L_{\mathbf{F}}^{(\theta, H^1)}$.

Estimation of convection residual

$$\begin{aligned}
 |\langle R_3, \mathbf{d}_{\mathbf{u},h}^n \rangle| &= |\tilde{c}_{\mathbf{v}}(\mathbf{u}^n, \mathbf{u}^n, \mathbf{d}_{\mathbf{u},h}^n) - \tilde{c}_{\mathbf{v}}(J_{\mathbf{c}}\mathbf{u}_h^n, \mathbf{u}_h^n, \mathbf{d}_{\mathbf{u},h}^n)| \\
 &\leq |\tilde{c}_{\mathbf{v}}(\mathbf{u}^n - J_{\mathbf{c}}\mathbf{u}^n, \mathbf{u}^n, \mathbf{d}_{\mathbf{u},h}^n)| + |\tilde{c}_{\mathbf{v}}(J_{\mathbf{c}}\mathbf{z}_{\mathbf{u},h}^n, \mathbf{u}^n, \mathbf{d}_{\mathbf{u},h}^n)| \\
 &\quad + |\tilde{c}_{\mathbf{v}}(J_{\mathbf{c}}\mathbf{d}_{\mathbf{u},h}^n, \mathbf{u}^n, \mathbf{d}_{\mathbf{u},h}^n)| + |\tilde{c}_{\mathbf{v}}(J_{\mathbf{c}}\mathbf{u}_h^n, \mathbf{z}_{\mathbf{u},h}^n, \mathbf{d}_{\mathbf{u},h}^n)|,
 \end{aligned} \tag{4.29}$$

$$\begin{aligned}
 |\langle R_8, d_{\theta,h}^n \rangle| &= |\tilde{c}_{\tau}(\mathbf{u}^n, \theta^n + \theta_b, d_{\theta,h}^n) - \tilde{c}_{\tau}(J_{\mathbf{c}}\mathbf{u}_h^n, \theta_h^n + \theta_b, d_{\theta,h}^n)| \\
 &\leq |\tilde{c}_{\tau}(\mathbf{u}^n - J_{\mathbf{c}}\mathbf{u}^n, \theta^n + \theta_b, d_{\theta,h}^n)| + |\tilde{c}_{\tau}(J_{\mathbf{c}}\mathbf{z}_{\mathbf{u},h}^n, \theta^n + \theta_b, d_{\theta,h}^n)| \\
 &\quad + |\tilde{c}_{\tau}(J_{\mathbf{c}}\mathbf{d}_{\mathbf{u},h}^n, \theta^n + \theta_b, d_{\theta,h}^n)| + |\tilde{c}_{\tau}(J_{\mathbf{c}}\mathbf{u}_h^n, z_{\theta,h}^n, d_{\theta,h}^n)|.
 \end{aligned} \tag{4.30}$$

Further, by standard estimates for $\tilde{c}_{\mathbf{v}}$, \tilde{c}_{τ} [39] and $H^2(\Omega) \hookrightarrow C^0(\overline{\Omega})$, $H^2(\Omega) \hookrightarrow W^{1,3}(\Omega)$, $H^1(\Omega) \hookrightarrow L^6(\Omega)$ as well as the Sobolev interpolation estimates and $\theta_b \in W^{1,\infty}(\Omega)$,

$$\frac{|\langle R_3, \mathbf{d}_{\mathbf{u},h}^n \rangle|}{\|\mathbf{d}_{\mathbf{u},h}^n\|_{1,2}} \leq C_{3,1} \left(\|\mathbf{u}^n - J_{\mathbf{c}}\mathbf{u}^n\| + \|J_{\mathbf{c}}\mathbf{z}_{\mathbf{u},h}^n\|_{1,2} + \|J_{\mathbf{c}}\mathbf{d}_{\mathbf{u},h}^n\|^{\frac{1}{2}} \|J_{\mathbf{c}}\mathbf{d}_{\mathbf{u},h}^n\|^{\frac{1}{2}} \right) + C_{3,2} \|J_{\mathbf{c}}\mathbf{u}_h^n\|_{1,2} \|\mathbf{z}_{\mathbf{u},h}^n\|_{1,2}, \quad (4.31)$$

$$\frac{|\langle R_8, d_{\theta,h}^n \rangle|}{\|d_{\theta,h}^n\|_{1,2}} \leq C_{8,1} \left(\|\mathbf{u}^n - J_{\mathbf{c}}\mathbf{u}^n\| + \|J_{\mathbf{c}}\mathbf{z}_{\mathbf{u},h}^n\|_{1,2} + \|J_{\mathbf{c}}\mathbf{d}_{\mathbf{u},h}^n\|^{\frac{1}{2}} \|J_{\mathbf{c}}\mathbf{d}_{\mathbf{u},h}^n\|^{\frac{1}{2}} \right) + C_{8,2} \|J_{\mathbf{c}}\mathbf{u}_h^n\|_{1,2} \|z_{\theta,h}^n\|_{1,2}. \quad (4.32)$$

Estimation of difference quotient residual

$$\frac{|\langle R_1, \mathbf{v}_h \rangle|}{\|\mathbf{v}_h\|_{1,2}} \leq \|\partial_t \mathbf{u}^n - k^{-1} J_{\mathbf{d}} \mathbf{u}^n\|_{-1,2} + k^{-1} \|J_{\mathbf{d}} \mathbf{z}_{\mathbf{u},h}^n\|_{-1,2}, \quad (4.33)$$

$$\frac{|\langle R_6, \tau_h \rangle|}{\|\tau_h\|_{1,2}} \leq \|\partial_t \theta^n - k^{-1} J_{\mathbf{d}} \theta^n\|_{-1,2} + k^{-1} \|J_{\mathbf{d}} z_{\theta,h}^n\|_{-1,2}. \quad (4.34)$$

Left-hand sides

By using Assumption 3.10 (iii) and the definition of \mathbf{w}_h^n by means of the Stokes projection, the left-hand sides of (4.17), (4.19) can be estimated from below,

$$k^{-1} (J_{\mathbf{d}} \mathbf{d}_{\mathbf{u},h}^n, \mathbf{d}_{\mathbf{u},h}^n) + a_{\mathbf{v}}(\mathbf{d}_{\mathbf{u},h}^n, \mathbf{d}_{\mathbf{u},h}^n) - b(\mathbf{d}_{\mathbf{u},h}^n, d_{p,h}^n) \geq \bar{\sigma} k^{-1} J_1 \left(\|\mathbf{d}_{\mathbf{u},h}^n\|^2 + U_n^2 \right) + k^{-1} \bar{U}_n^2 + (1 + c_0^2)^{-1} \nu \|\mathbf{d}_{\mathbf{u},h}^n\|_{1,2}^2, \quad (4.35)$$

$$k^{-1} (J_{\mathbf{d}} d_{\theta,h}^n, d_{\theta,h}^n) + a_{\tau}(d_{\theta,h}^n, d_{\theta,h}^n) \geq \bar{\sigma} k^{-1} J_1 \left(\|d_{\theta,h}^n\|^2 + T_n^2 \right) + k^{-1} \bar{T}_n^2 + (1 + c_D^2)^{-1} \kappa \|d_{\theta,h}^n\|_{1,2}^2. \quad (4.36)$$

Application of discrete Grönwall inequality

Combining the error equations (4.17)–(4.20) and inequalities (4.21), (4.28)–(4.36) with $\mathbf{v}_h = \mathbf{d}_{\mathbf{u},h}^n$ and $\tau_h = d_{\theta,h}^n$, yields for $n \geq q$:

$$\omega_l \leq c(\omega_r^{\mathbf{v}} + \omega_r^{\tau}) \quad (4.37)$$

with c depending only on constants obtained by application of Young's inequality $ab \leq \frac{1}{2\epsilon} a^2 + \frac{\epsilon}{2} b^2$ for all $a, b \in \mathbb{R}$, $\epsilon > 0$ and of $(\sum_{i=1}^m a_i)^2 \leq m \sum_{i=1}^m a_i^2$. Here,

$$\begin{aligned} \omega_r^{\mathbf{v}} &:= \frac{1}{\epsilon_1} \left(\|\partial_t \mathbf{u}^n - k^{-1} J_{\mathbf{d}} \mathbf{u}^n\|_{-1,2}^2 + k^{-2} \|J_{\mathbf{d}} \mathbf{z}_{\mathbf{u},h}^n\|_{-1,2}^2 \right) \\ &+ \frac{1}{\epsilon_{3,1}} \left(C_{3,1}^2 \|\mathbf{u}^n - J_{\mathbf{c}} \mathbf{u}^n\|^2 + C_{3,1}^2 \|J_{\mathbf{c}} \mathbf{z}_{\mathbf{u},h}^n\|_{1,2}^2 + C_{3,2}^2 \|J_{\mathbf{c}} \mathbf{u}_h^n\|_{1,2}^2 \| \mathbf{z}_{\mathbf{u},h}^n \|_{1,2}^2 \right) + \frac{1}{\epsilon_{3,1}^2 \epsilon_{3,2}} C_{3,1}^4 \|J_{\mathbf{c}} \mathbf{d}_{\mathbf{u},h}^n\|^2 \\ &+ \frac{1}{\epsilon_4} \left(C_{4,1}^2 \|\theta^n - J_{\mathbf{f}} \theta^n\|_{1,2}^2 + C_{4,2}^2 \left(\|J_{\mathbf{f}} z_{\theta,h}^n\|_{1,2}^2 + \|z_{\Phi,h}^n\|_{1,2}^2 \right) \right) \\ &+ \frac{1}{\epsilon_4} C_{4,3}^2 \left(C_{0,1}^2 \left(\|\theta^n - J_{\mathbf{g}} \theta^n\|^2 + \|J_{\mathbf{g}} z_{\theta,h}^n\|^2 + \|J_{\mathbf{g}} d_{\theta,h}^n\|^2 \right) + C_{0,2}^2 \|z_{\Phi,h}^n\|_{1,2}^2 \right) + \frac{1}{\epsilon_{4,i}} C_{4,i}^2 \|J_{\mathbf{f}} d_{\theta,h}^n\|^2, \\ \omega_r^{\tau} &:= \frac{1}{\epsilon_6} \left(\|\partial_t \theta^n - k^{-1} J_{\mathbf{d}} \theta^n\|_{-1,2}^2 + k^{-2} \|J_{\mathbf{d}} z_{\theta,h}^n\|_{-1,2}^2 \right) + \frac{\kappa}{\epsilon_7} \|z_{\theta,h}^n\|_{1,2}^2 \\ &+ \frac{1}{\epsilon_{8,1}} \left(C_{8,1}^2 \|\mathbf{u}^n - J_{\mathbf{c}} \mathbf{u}^n\|^2 + C_{8,1}^2 \|J_{\mathbf{c}} \mathbf{z}_{\mathbf{u},h}^n\|_{1,2}^2 + C_{8,2}^2 \|J_{\mathbf{c}} \mathbf{u}_h^n\|_{1,2}^2 \|z_{\theta,h}^n\|_{1,2}^2 \right) + \frac{1}{\epsilon_{8,1}^2 \epsilon_{8,2}} C_{8,1}^4 \|J_{\mathbf{c}} \mathbf{d}_{\mathbf{u},h}^n\|^2 \end{aligned}$$

and

$$\begin{aligned} \omega_l := & \bar{\delta}k^{-1}J_1\left(\|\mathbf{d}_{\mathbf{u},h}^n\|^2 + \|d_{\theta,h}^n\|^2 + U_n^2 + T_n^2\right) + k^{-1}\left(\bar{U}_n^2 + \bar{T}_n^2\right) \\ & + (2\tilde{\nu} - 2^{-1}(\epsilon_1 + \epsilon_{3,1} + \epsilon_4 + \epsilon_{4,i} + \epsilon_{4,ii}))\|\mathbf{d}_{\mathbf{u},h}^n\|_{1,2}^2 - 2^{-1}(\epsilon_{3,2} + \epsilon_{8,2})\|J_{\mathbf{c}}\mathbf{d}_{\mathbf{u},h}^n\|_{1,2}^2 \\ & + (2\tilde{\kappa} - 2^{-1}(\epsilon_6 + \epsilon_{7\kappa} + \epsilon_{8,1}))\|d_{\theta,h}^n\|_{1,2}^2 - 2^{-1}C_{4,ii}^2\epsilon_{4,ii}^{-1}\|J_{\mathbf{f}}d_{\theta,h}^n\|_{1,2}^2. \end{aligned}$$

If $q|\mathbf{f}|_2^2 C_{4,ii}^2 < 2\tilde{\nu}\tilde{\kappa}$ holds, which is equivalent to the small data condition (4.16), then there exists $\epsilon_{4,ii} \in (0, 2\tilde{\nu})$ such that $C_{4,ii}^2\epsilon_{4,ii}^{-1} < \frac{\tilde{\kappa}}{q|\mathbf{f}|_2^2}$. Thus, the last term in ω_l can be bounded from below,

$$-2^{-1}C_{4,ii}^2\epsilon_{4,ii}^{-1}\|J_{\mathbf{f}}d_{\theta,h}^n\|_{1,2}^2 \geq -2^{-1}\tilde{\kappa}q^{-1}\sum_{i=1}^q\|d_{\theta,h}^{n-i}\|_{1,2}^2. \tag{4.38}$$

Choosing the remaining factors ϵ . appropriately, one obtains from (4.37), (4.38)

$$\begin{aligned} & \bar{\delta}k^{-1}J_1\left(\|\mathbf{d}_{\mathbf{u},h}^n\|^2 + \|d_{\theta,h}^n\|^2 + U_n^2 + T_n^2\right) + k^{-1}\left(\bar{U}_n^2 + \bar{T}_n^2\right) \\ & + \tilde{\nu}\|\mathbf{d}_{\mathbf{u},h}^n\|_{1,2}^2 + \tilde{\kappa}\|d_{\theta,h}^n\|_{1,2}^2 - \frac{\tilde{\nu}}{2q}\sum_{i=1}^q\|\mathbf{d}_{\mathbf{u},h}^{n-i}\|_{1,2}^2 - \frac{\tilde{\kappa}}{2q}\sum_{i=1}^q\|d_{\theta,h}^{n-i}\|_{1,2}^2 \\ & \leq \sum_{i=1}^q\left\{\alpha_{\mathbf{u}}\|\mathbf{d}_{\mathbf{u},h}^{n-i}\|^2 + \alpha_{\theta}\|d_{\theta,h}^{n-i}\|^2\right\} + \alpha^n + \beta^n + \gamma^n + \delta^n, \end{aligned} \tag{4.39}$$

with factors

$$\alpha_{\mathbf{u}} := c(\nu^{-3}C_{3,1}^4 + \kappa^{-2}\nu^{-1}C_{8,1}^4)|\mathbf{c}|_{\infty}^2, \tag{4.40}$$

$$\alpha_{\theta} := c\nu^{-1}C_{4,i}^2|\mathbf{f}|_{\infty}^2 + c\nu^{-1}C_{4,3}^2C_{0,1}^2|\mathbf{g}|_{\infty}^2 \tag{4.41}$$

and sequences $\{(\alpha^n, \beta^n, \gamma^n, \delta^n)\}_{n \geq q}$ that satisfy

$$\begin{aligned} \frac{\alpha^n}{c} & \leq \nu^{-1}\|\partial_t \mathbf{u}^n - k^{-1}J_{\mathbf{d}}\mathbf{u}^n\|_{-1,2}^2 + (\nu^{-1}C_{3,1}^2 + \kappa^{-1}C_{8,1}^2)\|\mathbf{u}^n - J_{\mathbf{c}}\mathbf{u}^n\|^2 \\ & \quad + \kappa^{-1}\|\partial_t \theta^n - k^{-1}J_{\mathbf{d}}\theta^n\|_{-1,2}^2 + \nu^{-1}C_{4,1}^2\|\theta^n - J_{\mathbf{f}}\theta^n\|_{1,2}^2 + \nu^{-1}C_{4,3}^2C_{0,1}^2\|\theta^n - J_{\mathbf{g}}\theta^n\|^2, \\ \frac{\beta^n}{c} & \leq (\nu^{-1}C_{3,1}^2 + \kappa^{-1}C_{8,1}^2)\|J_{\mathbf{c}}\mathbf{z}_{\mathbf{u},h}^n\|_{1,2}^2 + \nu^{-1}C_{4,2}^2\|J_{\mathbf{f}}z_{\theta,h}^n\|_{1,2}^2 + \kappa\|z_{\theta,h}^n\|_{1,2}^2 \\ & \quad + (\nu^{-1}C_{4,2}^2 + \nu^{-1}C_{4,3}^2C_{0,2}^2)\|z_{\Phi,h}^n\|_{1,2}^2 + \nu^{-1}C_{4,3}^2C_{0,1}^2\|J_{\mathbf{g}}z_{\theta,h}^n\|^2, \\ \frac{\gamma^n}{c} & \leq \nu^{-1}k^{-2}\|J_{\mathbf{d}}\mathbf{z}_{\mathbf{u},h}^n\|_{-1,2}^2 + \kappa^{-1}k^{-2}\|J_{\mathbf{d}}z_{\theta,h}^n\|_{-1,2}^2, \\ \frac{\delta^n}{c} & \leq \|J_{\mathbf{c}}\mathbf{u}_h^n\|_{1,2}^2\left(\nu^{-1}C_{3,2}^2\|\mathbf{z}_{\mathbf{u},h}^n\|_{1,2}^2 + \kappa^{-1}C_{8,2}^2\|z_{\theta,h}^n\|_{1,2}^2\right). \end{aligned}$$

Multiplication of (4.39) by $k\bar{\delta}^{-1}$ and summation over $n = q, \dots, M$ for arbitrary $M \in \{q, \dots, N\}$ gives

$$\begin{aligned} & \|\mathbf{d}_{\mathbf{u},h}^M\|^2 + \|d_{\theta,h}^M\|^2 + U_M^2 + T_M^2 + k\sum_{n=q}^M\frac{1}{\bar{\delta}}\left\{k^{-1}\left(\bar{U}_n^2 + \bar{T}_n^2\right) + \frac{\tilde{\nu}}{2}\|\mathbf{d}_{\mathbf{u},h}^n\|_{1,2}^2 + \frac{\tilde{\kappa}}{2}\|d_{\theta,h}^n\|_{1,2}^2\right\} \\ & \leq k\sum_{n=0}^{M-1}\frac{q}{\bar{\delta}}\left\{\alpha_{\mathbf{u}}\|\mathbf{d}_{\mathbf{u},h}^n\|^2 + \alpha_{\theta}\|d_{\theta,h}^n\|^2\right\} + k\sum_{n=q}^M\frac{1}{\bar{\delta}}\{\alpha^n + \beta^n + \gamma^n + \delta^n\} \end{aligned}$$

$$+ k \sum_{i=0}^{q-1} \frac{1}{\bar{\omega}} \left\{ \frac{\tilde{\nu}}{2} \|\mathbf{d}_{\mathbf{u},h}^i\|_{1,2}^2 + \frac{\tilde{\kappa}}{2} \|d_{\theta,h}^i\|_{1,2}^2 \right\} + \|\mathbf{d}_{\mathbf{u},h}^{q-1}\|^2 + \|d_{\theta,h}^{q-1}\|^2 + U_{q-1}^2 + T_{q-1}^2. \quad (4.42)$$

Application of the discrete Grönwall's inequality, Lemma A.1, finally yields

$$\begin{aligned} & \|\mathbf{d}_{\mathbf{u},h}^M\|^2 + \|d_{\theta,h}^M\|^2 + U_M^2 + T_M^2 + k \sum_{n=q}^M \frac{1}{\bar{\omega}} \left\{ k^{-1} (\bar{U}_n^2 + \bar{T}_n^2) + \frac{\tilde{\nu}}{2} \|\mathbf{d}_{\mathbf{u},h}^n\|_{1,2}^2 + \frac{\tilde{\kappa}}{2} \|d_{\theta,h}^n\|_{1,2}^2 \right\} \\ & \leq \exp(Tq\omega^{-1} \max\{\alpha_{\mathbf{u}}, \alpha_{\theta}\}) \cdot \left(k \sum_{n=q}^N \frac{1}{\bar{\omega}} \{\alpha^n + \beta^n + \gamma^n + \delta^n\} + \bar{C}_{q-1}^2 \right), \end{aligned} \quad (4.43)$$

with \bar{C}_{q-1}^2 denoting those terms in (4.42) that correspond to time steps $i \leq q-1$ only, *i.e.* the last two rows in (4.42).

Finite element approximation error

The finite element approximation errors can be bounded by means of Assumption 3.1, Lemma 3.4, and the imposed regularity of the exact solution:

$$\|\mathbf{z}_{\mathbf{u},h}^n\|_{1,2} \leq C_S h^l \left(\|\mathbf{u}\|_{\infty; \mathbf{H}^{l+1}} + \nu^{-1} \|p\|_{\infty; H^l} \right), \quad (4.44)$$

$$\|z_{p,h}^n\| \leq C_S h^l \left(\nu \|\mathbf{u}\|_{\infty; \mathbf{H}^{l+1}} + \|p\|_{\infty; H^l} \right), \quad (4.45)$$

$$\|z_{\theta,h}^n\|_{1,2} \leq ch^l \|\theta\|_{\infty; H^{l+1}}, \quad (4.46)$$

$$\|z_{\Phi,h}^n\|_{1,2} \leq ch^l \|\Phi\|_{\infty; H^{l+1}}. \quad (4.47)$$

By using the linearity of Π_S , Π_{Θ} , Π_{Υ} , Assumption 3.1 and Lemma 3.4, one obtains for an arbitrary q -step difference operator $J_{\mathbf{h}}$,

$$\|J_{\mathbf{h}} \mathbf{z}_{\mathbf{u},h}^n\|_{j,2} = \|J_{\mathbf{h}} \mathbf{u}^n - \Pi_S(J_{\mathbf{h}} \mathbf{u}^n, J_{\mathbf{h}} p^n)\|_{j,2} \leq C^* h^{l+l^*} \left(\|J_{\mathbf{h}} \mathbf{u}^n\|_{l+1,2} + \nu^{-1} \|J_{\mathbf{h}} p^n\|_{l,2} \right), \quad (4.48)$$

$$\|J_{\mathbf{h}} z_{x,h}^n\|_{j,2} = \|J_{\mathbf{h}} x^n - \Pi_X J_{\mathbf{h}} x^n\|_{j,2} \leq ch^l \|J_{\mathbf{h}} x^n\|_{l+1,2}, \quad (4.49)$$

for $x \in \{\theta, \Phi\}$, $X \in \{\Theta, \Upsilon\}$ and $j \in \{0, 1\}$. Here, $l^* = 1$, $C^* = C_{S,0}$ if the underlying Stokes problem is regular and $j = 0$. Otherwise, $l^* = 0$, $C^* = C_S$.

Final error estimation for velocity, temperature and potential

Using (4.44)–(4.49) with $\mathbf{h} = \mathbf{d}$ and the discrete stability result, Lemma 3.14, the following estimate follows:

$$\frac{k}{\bar{\omega}} \sum_{n=q}^N \{\alpha^n + \beta^n + \gamma^n + \delta^n\} \lesssim E(k)^2 + h^{2l} + E(h, k)^2. \quad (4.50)$$

Squaring and multiplying (4.22) by k , summing over $n = q, \dots, N$ and using (4.46), (4.47) gives

$$\begin{aligned} k \sum_{n=q}^N \|\nabla d_{\Phi,h}^n\|^2 & \lesssim k \sum_{n=q}^N \|\theta^n - J_{\mathbf{g}} \theta^n\|^2 + k \sum_{n=0}^N \|d_{\theta,h}^n\|^2 + h^{2l} \\ & \lesssim E(k)^2 + E_3(q)^2 + k \sum_{n=q}^N \|d_{\theta,h}^n\|^2 + h^{2l}. \end{aligned} \quad (4.51)$$

Using (4.50), the right-hand side in (4.43) is equal to $\mathcal{E}_{\mathbf{u},\theta}(h,k,q)^2$, up to a multiplicative constant that is independent of h and k . In this way, the estimates

$$\left\| (\mathbf{d}_{\mathbf{u},h}^n)_n \right\|_{L^2(\mathbf{H}^1)} + \left\| (d_{\theta,h}^n)_n \right\|_{L^2(\mathbf{H}^1)} \lesssim \mathcal{E}_{\mathbf{u},\theta}(h,k,q), \tag{4.52}$$

$$\left\| (\mathbf{d}_{\mathbf{u},h}^n)_n \right\|_{l^\infty(\mathbf{L}^2)} + \left\| (d_{\theta,h}^n)_n \right\|_{l^\infty(\mathbf{L}^2)} \lesssim \mathcal{E}_{\mathbf{u},\theta}(h,k,q), \tag{4.53}$$

$$\| (U_n)_n \|_{l^\infty(\mathbb{R})} + \| (T_n)_n \|_{l^\infty(\mathbb{R})} \lesssim \mathcal{E}_{\mathbf{u},\theta}(h,k,q), \tag{4.54}$$

$$\| (\bar{U}_n)_n \|_{L^2(\mathbb{R})} + \| (\bar{T}_n)_n \|_{L^2(\mathbb{R})} \lesssim \mathcal{E}_{\mathbf{u},\theta}(h,k,q)k^{\frac{1}{2}} \tag{4.55}$$

follow. Similarly, the square root of the right-hand side in (4.51) can be estimated from above by $\mathcal{E}_\Phi(h,k,q)$ (under the use of (4.52)). Thus,

$$\left\| (d_{\Phi,h}^n)_n \right\|_{L^2(\mathbf{H}^1)} \lesssim \mathcal{E}_\Phi(h,k,q) \tag{4.56}$$

is obtained. The stated assertions on the complete error of velocity, temperature and potential now follow by the decomposition $e_{\cdot,h}^n = z_{\cdot,h}^n + d_{\cdot,h}^n$, (4.52), (4.53), (4.56), estimation (4.44)–(4.47) for $z_{\cdot,h}^n$ and the triangle inequality.

Pressure error estimation

As next step, the pressure error $d_{p,h}^n$ is considered, following the approach proposed in [39]. To this end, note that there holds

$$\begin{aligned} \| \mathbf{d}_{\mathbf{u},h}^n \|_{1,2} &\leq \min \left\{ ch^{-1} \| \mathbf{d}_{\mathbf{u},h}^n \|, \| \mathbf{d}_{\mathbf{u},h}^n \|_{1,2} \right\} \\ &\leq \min \left\{ ch^{-1} \left\| (\mathbf{d}_{\mathbf{u},h}^n)_n \right\|_{l^\infty(q,N;\mathbf{L}^2),k}, k^{-\frac{1}{2}} \left\| (\mathbf{d}_{\mathbf{u},h}^n)_n \right\|_{L^2(q,N;\mathbf{H}^1),k} \right\} \\ &\lesssim \min \left\{ h^{-1}, k^{-\frac{1}{2}} \right\} \mathcal{E}_{\mathbf{u},\theta}(h,k,q) \\ &=: \tilde{D}(h,k,q) \end{aligned}$$

by the inverse estimate, Assumption 3.1 (iv), and (4.52), (4.53). Thus,

$$\begin{aligned} \left\| (\mathbf{d}_{\mathbf{u},h}^n)_n \right\|_{l^\infty(0,N;\mathbf{H}^1)} &\lesssim \max \left\{ \tilde{D}(h,k,q), \| \mathbf{d}_{\mathbf{u},h}^n \|_{1,2} : n = 0, \dots, q-1 \right\} \\ &=: D(h,k,q). \end{aligned}$$

leading to

$$\begin{aligned} \| \mathbf{u}_h^n \|_{1,2} &\leq \| \mathbf{u}^n \|_{1,2} + \| \mathbf{z}_{\mathbf{u},h}^n \|_{1,2} + \| \mathbf{d}_{\mathbf{u},h}^n \|_{1,2} \\ &\lesssim \| \mathbf{u} \|_{\infty;\mathbf{H}^1} + C_S h^l \left(\| \mathbf{u} \|_{\infty;\mathbf{H}^{l+1}} + \nu^{-1} \| p \|_{\infty;H^l} \right) + D(h,k,q) \\ &\lesssim 1 + h^l + \min \left\{ h^{-1}, k^{-\frac{1}{2}} \right\} \mathcal{E}_{\mathbf{u},\theta}(h,k,q) + \max \left\{ \| \mathbf{u}^n - \mathbf{u}_h^n \|_{1,2} : n = 0, \dots, q-1 \right\} \\ &= C_p(h,k,q). \end{aligned} \tag{4.57}$$

Now, by the discrete inf-sup condition, Assumption 3.1 (i), and the error equation (4.17),

$$\begin{aligned} \beta \| d_{p,h}^n \| &\leq \sup_{\mathbf{v}_h \in \mathbf{U}_h} \frac{b(\mathbf{v}_h, d_{p,h}^n)}{\| \mathbf{v}_h \|_{1,2}} \\ &\leq k^{-1} \| J_{\mathbf{d}} \mathbf{d}_{\mathbf{u},h}^n \| + \nu \| \mathbf{d}_{\mathbf{u},h}^n \|_{1,2} + \| R_1^n \|_{\mathbf{U}_h^*} + \| R_3^n \|_{\mathbf{U}_h^*} + \| R_4^n \|_{\mathbf{U}_h^*}. \end{aligned} \tag{4.58}$$

$\|R_1^n\|_{\mathbf{U}_h^*}$ and $\|R_4^n\|_{\mathbf{U}_h^*}$ can be estimated from above by (4.33) and (4.28) respectively,

$$\|R_1^n\|_{\mathbf{U}_h^*} \leq \|\partial_t \mathbf{u}^n - k^{-1} J_{\mathbf{d}} \mathbf{u}^n\|_{-1,2} + k^{-1} \|J_{\mathbf{d}} \mathbf{z}_{\mathbf{u},h}^n\|_{-1,2}, \quad (4.59)$$

$$\begin{aligned} \|R_4^n\|_{\mathbf{U}_h^*} &\lesssim \|\theta^n - J_{\mathbf{f}} \theta^n\|_{1,2} + \|\theta^n - J_{\mathbf{g}} \theta^n\| + \|J_{\mathbf{g}} z_{\theta,h}^n\| + \|J_{\mathbf{f}} z_{\theta,h}^n\|_{1,2} + \|z_{\Phi,h}^n\|_{1,2} + \|J_{\mathbf{f}} d_{\theta,h}^n\| \\ &\quad + \|J_{\mathbf{f}} d_{\theta,h}^n\|_{1,2} + \|J_{\mathbf{g}} d_{\theta,h}^n\|. \end{aligned} \quad (4.60)$$

To estimate $\|R_3^n\|_{\mathbf{U}_h^*}$, use $H^2(\Omega) \hookrightarrow C^0(\bar{\Omega})$, $H^2(\Omega) \hookrightarrow W^{1,3}(\Omega)$ and the bound (4.57) to obtain

$$\begin{aligned} \|R_3^n\|_{\mathbf{U}_h^*} &= \sup_{\mathbf{v}_h \in \mathbf{U}_h} \frac{|\langle R_3^n, \mathbf{v}_h \rangle|}{\|\mathbf{v}_h\|_{1,2}} \\ &\leq \sup_{\mathbf{v}_h \in \mathbf{U}_h} \frac{1}{\|\mathbf{v}_h\|_{1,2}} (|\tilde{c}_{\mathbf{v}}(\mathbf{u}^n - J_{\mathbf{c}} \mathbf{u}^n, \mathbf{u}^n, \mathbf{v}_h)| + |\tilde{c}_{\mathbf{v}}(J_{\mathbf{c}}(\mathbf{u}^n - \mathbf{u}_h^n), \mathbf{u}^n, \mathbf{v}_h)| + |\tilde{c}_{\mathbf{v}}(J_{\mathbf{c}} \mathbf{u}_h^n, \mathbf{u}^n - \mathbf{u}_h^n, \mathbf{v}_h)|) \\ &\lesssim \|\mathbf{u}^n - J_{\mathbf{c}} \mathbf{u}^n\| + \sum_{i=1}^q \left\{ \left\| \mathbf{z}_{\mathbf{u},h}^{n-i} \right\|_{1,2} + \left\| \mathbf{d}_{\mathbf{u},h}^{n-i} \right\|_{1,2} \right\} + C_p(h, k, q) \left(\left\| \mathbf{z}_{\mathbf{u},h}^n \right\|_{1,2} + \left\| \mathbf{d}_{\mathbf{u},h}^n \right\|_{1,2} \right). \end{aligned} \quad (4.61)$$

Squaring and multiplication by k of (4.58), summing over $n = q, \dots, N$, using the estimates on the residual norms (4.59)–(4.61), the estimate of the approximation errors (4.44)–(4.49) and the estimates of the discretization errors (4.52), (4.53) yields

$$\begin{aligned} k \sum_{n=q}^N \|d_{p,h}^n\|^2 &\lesssim E(k)^2 + E(h, k)^2 + E_{\mathbf{d}}(h, k)^2 + C_p(h, k, q)^2 (h^{2l} + E_1(q)^2 + \mathcal{E}_{\mathbf{u},\theta}(h, k, q)^2) \\ &\lesssim \mathcal{E}_p(h, k, q)^2. \end{aligned} \quad (4.62)$$

The stated assertion on $e_{p,h}^n$ now follows from (4.62) and the triangle inequality.

Bound on temporal variation of estimation error

It remains to derive an upper bound for $E_{\mathbf{d}}(h, k)$. Setting $\mathbf{v}_h = J_{\mathbf{d}} \mathbf{d}_{\mathbf{u},h}^n$ in (4.17), using $b(\mathbf{w}_h^n, \mathbf{v}_h) = b(\mathbf{u}_h^n, \mathbf{v}_h) = 0$ for all \mathbf{v}_h , $n \geq 0$, and using Young's inequality yields

$$k^{-1} \|J_{\mathbf{d}} \mathbf{d}_{\mathbf{u},h}^n\|^2 \leq \frac{\nu}{2} \sum_{i=0}^q |d_i| \left\{ \|\nabla \mathbf{d}_{\mathbf{u},h}^n\|^2 + \|\nabla \mathbf{d}_{\mathbf{u},h}^{n-i}\|^2 \right\} + c \left(\|R_1^n\|_{\mathbf{U}_h^*}^2 + \|R_3^n\|_{\mathbf{U}_h^*}^2 + \|R_4^n\|_{\mathbf{U}_h^*}^2 \right).$$

Summing this inequality from $n = q, \dots, N$ and using the previously derived bounds on $\|R_1^n\|_{\mathbf{U}_h^*}$, $\|R_3^n\|_{\mathbf{U}_h^*}$, $\|R_4^n\|_{\mathbf{U}_h^*}$, (4.59)–(4.61), the approximation estimates (4.44)–(4.49) and the error estimates for velocity and temperature, (4.52), (4.53), yields

$$\begin{aligned} E_{\mathbf{d}}(h, k)^2 &= k^{-1} \sum_{n=q}^N \|J_{\mathbf{d}} \mathbf{d}_{\mathbf{u},h}^n\|^2 \\ &\lesssim C_p(h, k, q)^2 (k^{-1} \mathcal{E}_{\mathbf{u},\theta}(h, k, q)^2 + h^{2l} + E_2(q)^2) + k^{-1} E^2(h, k) + k^{-1} E^2(k) \\ &\lesssim \mathcal{E}_{\mathbf{d}}(h, k, q)^2 \end{aligned} \quad (4.63)$$

□

Remark 4.2. We required that $C_{4,ii}^2 < 2\tilde{\nu}\tilde{\kappa}|\mathbf{f}|_2^{-2}q^{-1}$. However, this assumption could be relaxed to $C_{4,ii}^2 < 4\tilde{\nu}\tilde{\kappa}|\mathbf{f}|_2^{-2}q^{-1}$, to the expense of a slightly more technical presentation.

Remark 4.3. The small data conditions (3.11) of Lemma 3.14 and (4.16) of Theorem 4.1 are of similar structure:

$$L_{\mathbf{F}}^{(1)} < \frac{2}{q|\mathbf{f}|_{\infty}} \frac{1}{c_0} \sqrt{\nu\kappa} \tag{4.64}$$

$$L_{\mathbf{F}}^{(2)} < \frac{1}{\sqrt{2(1+c_0^2)(1+c_D^2)}q|\mathbf{f}|_2} \frac{1}{c_0} \sqrt{\nu\kappa}. \tag{4.65}$$

In particular, they depend on the typically small physical constants ν, κ in the same way and on the diameter of the domain by virtue of Friedrich’s inequality. The DEP model presented in the next section is globally Lipschitz continuous w.r.t. θ with a constant independent of Φ . In this case, $L_{\mathbf{F}}^{(1)} = L_{\mathbf{F}}^{(2)}$.

Remark 4.4. A time step size restriction when applying Grönwall’s inequality could be avoided, since the right-hand side in (4.42) only contains terms $\|\mathbf{d}_{\mathbf{u},h}^n\|, \|d_{\theta,h}^n\|$ for $n < M$. For this reason, it is assumed that $J_{\mathbf{c}}, J_{\mathbf{f}}, J_{\mathbf{g}}$ are explicit difference operators.

One drawback of the presented proof lies in the exponential factor that arises due to the application of Grönwall’s inequality. This exponent is proportional to negative powers of viscosity and thermal diffusion and may thus take very large values for typical fluids. Strictly speaking, one obtains an exponent C_{exp} with

$$C_{\text{exp}} \propto T \max\{\alpha_{\mathbf{u}}, \alpha_{\theta}\} \propto T(\nu^{-3} + \kappa^{-2}\nu^{-1} + \nu^{-1}). \tag{4.66}$$

The term $\nu^{-3} + \kappa^{-2}\nu^{-1}$ comes from the estimation of the convection terms $\tilde{c}_{\mathbf{v}}, \tilde{c}_{\tau}$, see (4.40), (4.31) and (4.32). In [34], an approach is shown that avoids the explicit occurrence of ν in the exponential factor when deriving error estimates for the instationary incompressible Navier–Stokes equations. This is achieved by the use of $\mathbf{H}(\text{div})$ -conforming elements that yield exactly divergence free discrete velocities in combination with $\nabla \mathbf{u} \in L^1(0, T; L^\infty)$ and a $W^{1,\infty}$ -stability assumption on the Stokes projection. Conditions for this stability are given in [15], for instance.

The remaining factor ν^{-1} arises due to the body force and is multiplied by the constant

$$C_{4,i}^2 + C_{4,3}^2 C_{0,1}^2 \propto \left(c_0 L_{\mathbf{F}}^{(\theta, L^2)}\right)^2 + \left(\frac{L_{\epsilon} L_{\mathbf{F}}^{(\Phi)}}{\epsilon_{-}} \left(\|\theta\|_{\infty; \text{H}^2} + \|\theta_b\|_{1,3}\right) \|\Phi + \Phi_b\|_{\infty; W^{1,\infty}}\right)^2.$$

Thus, large values of ν^{-1} could be compensated if the domain has a small diameter, *i.e.* small c_0 , and if the spatial variations of temperature and potential are rather low.

4.2. Temporal convergence rates

We now consider two concrete realizations of the temporal discretization by setting the difference operators introduced in Problem 3.12. The resulting schemes are given by a 1-step BDF (similar to semi-implicit Euler) and a 2-step BDF method.

Definition 4.5 (BDF1 scheme). The 1-step BDF scheme is given by $\mathbf{d} := (1, -1), \mathbf{c} = \mathbf{f} = \mathbf{g} := (0, 1)$.

Definition 4.6 (BDF2 scheme). The 2-step BDF scheme is given by $\mathbf{d} := (\frac{3}{2}, -2, \frac{1}{2}), \mathbf{c} = \mathbf{f} = \mathbf{g} := (0, 2, -1)$.

Both schemes are widely used for discretizing viscous flow problems, see *e.g.* [39] for the use of BDF1 for the Boussinesq equations and [9, 13] for the use of BDF2 for the incompressible Navier–Stokes equations.

It is easy to verify that difference operators given by Definition 4.5 and 4.6 satisfy Assumption 3.10 (i) and (ii). The stability condition (iii) is stated by Lemma 3.11.

For both schemes, the k -dependent error contributions in Theorem 4.1, $E(k), E(h, k)$ and $E_{\mathbf{d}}(h, k)$, are bounded from above in order to derive convergence rates w.r.t. k by employing Taylor series, see Corollaries 4.7 and 4.8. In doing so, one has to impose temporal regularity conditions on the solution which imply

non-local compatibility conditions on the initial data which may be uncheckable in practice [16]. Among others, these critical conditions include the finiteness of the following quantities [16]: $\|\mathbf{u}\|_{\infty;\mathbf{H}^3}$, $\|\partial_t \mathbf{u}\|_{\infty;\mathbf{H}^1}$, $\|\partial_t \mathbf{u}\|_{2;\mathbf{H}^2}$, $\|\partial_{tt} \mathbf{u}\|_{2;\mathbf{L}^2}$. In this work, however, we do not address this issue and impose temporal regularity that is sufficient to obtain optimal convergence rates. We refer to [12] for a more detailed consideration on this topic, where reduced convergence rates for weaker regularity conditions are derived.

Corollary 4.7 (Convergence rates of BDF1 scheme). *Let the assumptions of Theorem 4.1 hold and suppose that the exact solution satisfies the following, additional regularity conditions:*

$$\begin{aligned}\partial_t \mathbf{u} &\in L^2(\mathbf{H}^{l+1}), \quad \partial_{tt} \mathbf{u} \in L^2(\mathbf{H}^{-1}), \\ \partial_t p &\in L^2(H^l), \\ \partial_t \theta &\in L^2(H^{l+1}), \quad \partial_{tt} \theta \in L^2(H_D^{-1}).\end{aligned}$$

Let the difference operators in Problem 3.12 be given according to Definition 4.5 and $h, k < 1$. Then,

$$\begin{aligned}\mathcal{E}_{\mathbf{u},\theta}(h, k, q) &\lesssim h^l + k + E_1(q), \\ \mathcal{E}_{\Phi}(h, k, q) &\lesssim h^l + k + E_1(q) + E_3(q), \\ \mathcal{E}_p(h, k, q) &\lesssim h^l k^{-\frac{1}{2}} + k^{\frac{1}{2}} + k^{-\frac{1}{2}} E_1(q) + C_p(h, k, q)(k + h^l + E_1(q)), \\ C_p(h, k, q) &\lesssim 1 + E_2(q) + \min\{h^{-1}, k^{-\frac{1}{2}}\} E_1(q).\end{aligned}$$

Proof. Application of Lemma A.2 (i), (iii), with $\beta = 0$, yields

$$E(k)^2 \lesssim k^2 \left(\|\partial_{tt} \mathbf{u}\|_{2;\mathbf{H}^{-1}}^2 + \|\partial_{tt} \theta\|_{2;H_D^{-1}}^2 \right) + k^2 \left(\|\partial_t \mathbf{u}\|_{2;\mathbf{L}^2}^2 + \|\partial_t \theta\|_{2;\mathbf{H}^1}^2 + \|\partial_t \theta\|_{2;\mathbf{L}^2}^2 \right).$$

Moreover, by Lemma A.2 (i) with $\beta = 0$,

$$E(h, k)^2 \lesssim h^{2l+2l^*} \left(\|\partial_t \mathbf{u}\|_{2;\mathbf{H}^{l+1}}^2 + \|\partial_t p\|_{2;H^l}^2 \right) + h^{2l} \|\partial_t \theta\|_{2;H^{l+1}}^2.$$

Thus,

$$\mathcal{E}_{\mathbf{u},\theta}(h, k, q) \lesssim h^l + k + h^{l+l^*} + E_1(q).$$

Further, by Lemma 3.11 (i) and (4.55),

$$E_{\mathbf{d}}(h, k)^2 = k^{-1} \sum_{n=1}^N \|J_{\mathbf{d}} \mathbf{d}_{\mathbf{u},h}^n\|^2 = 2k^{-1} \sum_{n=1}^N \bar{U}_n^2 = 2k^{-2} \|(\bar{U}_n)_n\|_{L^2(1,N;\mathbb{R})}^2 \lesssim k^{-1} \mathcal{E}_{\mathbf{u},\theta}(h, k, q)^2$$

and

$$\begin{aligned}\mathcal{E}_p(h, k, q) &\lesssim k + h^l + (k^{-\frac{1}{2}} + C_p(h, k, q))(h^l + k + E_1(q)) \\ C_p(h, k, q) &\lesssim 1 + \min\{h^{-1}, k^{-\frac{1}{2}}\} (h^l + k + E_1(q)) + E_2(q).\end{aligned}$$

□

Corollary 4.8 (Convergence rates of BDF2 scheme). *Let the assumptions of Theorem 4.1 hold and suppose that the exact solution satisfies the following, additional regularity conditions:*

$$\begin{aligned}\partial_t \mathbf{u} &\in L^2(\mathbf{H}^{l+1}), \quad \partial_{tt} \mathbf{u} \in L^2(\mathbf{L}^2) \cap L^1(\mathbf{H}^{l+1}), \\ t\partial_{tt} \mathbf{u} &\in L^2(\mathbf{H}^{l+1}), \quad \partial_{ttt} \mathbf{u} \in L^2(\mathbf{H}^{-1}),\end{aligned}$$

$$\begin{aligned} \partial_t p &\in L^2(H^l), & \partial_{tt} p &\in L^1(H^l), & t\partial_{tt} p &\in L^2(H^l), \\ \partial_t \theta &\in L^2(H^{l+1}), & \partial_{tt} \theta &\in L^2(H^1) \cap L^1(H^{l+1}), \\ t\partial_{tt} \theta &\in L^2(H^{l+1}), & \partial_{ttt} \theta &\in L^2(H_D^{-1}). \end{aligned}$$

Let the difference operators in Problem 3.12 be given according to Definition 4.6 and $h, k < 1$. Then,

$$\begin{aligned} \mathcal{E}_{\mathbf{u},\theta}(h, k, q) &\lesssim k^2 + h^l + E_1(q), \\ \mathcal{E}_{\Phi}(h, k, q) &\lesssim k^2 + h^l + E_1(q) + E_3(q), \\ \mathcal{E}_p(h, k, q) &\lesssim C_p(h, k, q) \left(k^{\frac{3}{2}} + k^{-\frac{1}{2}} h^l + k^{-\frac{1}{2}} E_1(q) + E_2(q) \right), \\ C_p(h, k, q) &\lesssim 1 + E_2(q) + \min\left\{ h^{-1}, k^{-\frac{1}{2}} \right\} E_1(q). \end{aligned}$$

Proof. Application of Lemma A.2 (ii), (iv) with $\beta = 0$ yields

$$E(k)^2 \lesssim k^4 \left(\|\partial_{ttt} \mathbf{u}\|_{2;\mathbf{H}^{-1}}^2 + \|\partial_{ttt} \theta\|_{2;H_D^{-1}}^2 \right) + k^4 \left(\|\partial_{tt} \mathbf{u}\|_{2;\mathbf{L}^2}^2 + \|\partial_{tt} \theta\|_{2;H^1}^2 + \|\partial_{tt} \theta\|_{2;\mathbf{L}^2}^2 \right)$$

and by Lemma A.2 (v) with $\beta = 0, \gamma = 1$,

$$E(h, k)^2 \lesssim h^{2l+2l^*} \left(\|\partial_t \mathbf{u}\|_{2;\mathbf{H}^{l+1}}^2 + \|\partial_t p\|_{2;H^l}^2 + \|t\partial_{tt} \mathbf{u}\|_{2;\mathbf{H}^{l+1}}^2 + \|t\partial_{tt} p\|_{2;H^l}^2 \right) + h^{2l} \left(\|\partial_t \theta\|_{2;H^{l+1}}^2 + \|t\partial_{tt} \theta\|_{2;H^{l+1}}^2 \right).$$

Plugging these estimates into the definitions of the individual error terms yields

$$\begin{aligned} \mathcal{E}_{\mathbf{u},\theta}(h, k, q) &\lesssim h^l + k^2 + h^{l+l^*} + E_1(q), \\ \mathcal{E}_{\mathbf{d}}(h, k, q) &\lesssim k^{-1} (k^4 + h^{2l}) + C_p(h, k, q)^2 (h^{2l} + E_2(q)^2 + k^{-1} (k^4 + h^{2l} + E_1(q)^2)), \\ \mathcal{E}_p(h, k, q) &\lesssim k^2 + h^l + k^{\frac{3}{2}} + k^{-\frac{1}{2}} h^l + C_p(h, k, q) \left(h^l + E_2(q) + k^{-\frac{1}{2}} (k^2 + h^l + E_1(q)) \right) \\ &\quad + C_p(h, k, q) \left(h^l + k^2 + h^{l+l^*} + E_1(q) \right). \end{aligned}$$

□

Remark 4.9. For the BDF1 scheme, there holds $Z_n = 0$ according to Lemma 3.11. Thus, the terms U_{q-1}, T_{q-1} in the error bound $E_1(q)$ vanish. In the BDF2 case, we have $Z_n = \|2z^n - z^{n-1}\|_Z$ and therefore

$$\begin{aligned} |U_{q-1}| &\lesssim \left\| \mathbf{d}_{\mathbf{u},h}^{q-1} \right\| + \left\| \mathbf{d}_{\mathbf{u},h}^{q-2} \right\| \\ &\lesssim \left\| \mathbf{u}^{q-1} - \mathbf{u}_h^{q-1} \right\| + \left\| \mathbf{u}^{q-2} - \mathbf{u}_h^{q-2} \right\| + h^l, \end{aligned}$$

with an analogous estimate holding for $|T_{q-1}|$. In summary, if the initial conditions $(\mathbf{u}_h^i, \theta_h^i)_{i=0}^q$ are chosen appropriately, for instance by applying the projection operators of Assumption 3.1 to the continuous initial conditions (\mathbf{u}^0, θ^0) and by computing $(\mathbf{u}_h^i, \theta_h^i)_{i=1}^q$ by means of BDF1 with time step size k^2 , then the corresponding error contributions $E_j(q)$ are of order $\mathcal{O}(h^l)$ (BDF1) and $\mathcal{O}(h^l + k^2)$ (BDF2).

Remark 4.10. Under the assumptions imposed by Corollaries 4.7, 4.8 and under the use of Remark 4.9, there holds $C(h, k, q) \lesssim 1$.

Corollaries 4.7, 4.8 and Remarks 4.9, 4.10 show that the proposed BDF1 and BDF2 methods are indeed of first and second order w.r.t. the temporal discretization. To be precise, the error of velocity, temperature and potential, as defined by Theorem 4.1, is of order $\mathcal{O}(h^l + k^\beta)$ with $\beta = 1$ for BDF1 and $\beta = 2$ for BDF2. Regarding the pressure error, a factor $k^{\frac{1}{2}}$ is lost, similar to the estimates derived in [39].

5. MODELING OF DEP FORCE

We now propose a modification of the standard DEP and buoyancy force term

$$\mathbf{F}_s(\theta, \Phi) = \alpha_e |\nabla \Phi|^2 \nabla \theta - \alpha_g \theta \mathbf{g}, \quad (5.1)$$

that satisfies Assumption 3.13. The critical term $\mathbf{F}_{\text{dep}} = |\nabla \Phi|^2 \nabla \theta$ contains the squared magnitude of the electric field $|\nabla \Phi|^2$ which is only in $L^1(\Omega)$, since the natural space for the solution Φ of Gauss' law is $H^1(\Omega)$. In order to increase the integrability of this term, we thus replace it by $|\mathbf{m}_K \circ \nabla \Phi|^2$, where \mathbf{m}_K denotes a suitable cut-off function. In this way, $L^\infty(\Omega)$ integrability is obtained and Assumption 3.13 is satisfied, as shown in the subsequent Definition 5.1 and Lemma 5.2.

Definition 5.1 (Cut-off DEP force). For $K > 0$ let $\mathbf{m}_K \in \mathbf{L}^\infty(\mathbb{R}^d)$ denote a Lipschitz continuous function with Lipschitz constant L_K and $\|\mathbf{m}_K\|_{0,\infty} \leq K$. Define

$$\begin{aligned} \mathbf{F}_K: H^1(\Omega) \times H^1(\Omega) &\rightarrow \mathbf{U}^* \\ (\theta, \Phi) &\mapsto \alpha_e (|\mathbf{m}_K \circ \nabla \Phi|^2 \nabla \theta, \cdot) - \alpha_g (\theta \mathbf{g}, \cdot). \end{aligned}$$

Lemma 5.2 (Properties of cut-off DEP force term). *The force term \mathbf{F}_K satisfies Assumption 3.13 with $L_{\mathbf{F}}^{(\theta, H^1)} = \alpha_e K^2$, $L_{\mathbf{F}}^{(\theta, L^2)} = \alpha_g \|\mathbf{g}\|_{0,\infty}$ and $L_{\mathbf{F}}^{(\Phi)} = 2\alpha_e K L_K$.*

Proof. Let $\theta_1, \theta_2, \Phi \in H^1(\Omega)$ and $\mathbf{v} \in \mathbf{U}$. Then, (i) follows from

$$\begin{aligned} |\langle \mathbf{F}_K(\theta_1, \Phi) - \mathbf{F}_K(\theta_2, \Phi), \mathbf{v} \rangle_{\mathbf{U}^*}| &\leq \alpha_e \left\| |\mathbf{m}_K \circ \nabla \Phi|^2 \right\|_{0,\infty} \|\nabla(\theta_1 - \theta_2)\| \|\mathbf{v}\| + \alpha_g \|\mathbf{g}\|_{0,\infty} \|\theta_1 - \theta_2\| \|\mathbf{v}\| \\ &\leq \alpha_e K^2 \|\nabla(\theta_1 - \theta_2)\| \|\mathbf{v}\| + \alpha_g \|\mathbf{g}\|_{0,\infty} \|\theta_1 - \theta_2\| \|\mathbf{v}\|. \end{aligned}$$

Moreover, for $\theta \in W^{1,3}(\Omega)$, $\Phi_1, \Phi_2 \in H^1(\Omega)$ there holds

$$\begin{aligned} |\langle \mathbf{F}_K(\theta, \Phi_1) - \mathbf{F}_K(\theta, \Phi_2), \mathbf{v} \rangle_{\mathbf{U}^*}| &\leq \alpha_e \|\mathbf{m}_K \circ \nabla \Phi_1 + \mathbf{m}_K \circ \nabla \Phi_2\|_{0,\infty} \cdot \|\mathbf{m}_K \circ \nabla \Phi_1 - \mathbf{m}_K \circ \nabla \Phi_2\| \\ &\quad \cdot \|\nabla \theta\|_{0,3} \|\mathbf{v}\|_{0,6} \\ &\leq \alpha_e 2K L_K \|\nabla(\Phi_1 - \Phi_2)\| \|\nabla \theta\|_{0,3} \|\mathbf{v}\|_{0,6}. \end{aligned}$$

Thus, (ii) is satisfied and (iii) follows trivially. \square

An example of a suitable cut-off function \mathbf{m}_K is given by the metric projection of a vector $\mathbf{w} \in \mathbb{R}^d$ onto the ball $\{\mathbf{x} \in \mathbb{R}^d: |\mathbf{x}| \leq K\}$.

Definition 5.3 (Metric projection). For $K > 0$ the *metric projection* is defined by

$$\mathbf{m}_K: \mathbb{R}^d \rightarrow \mathbb{R}^d, \quad \mathbf{w} \mapsto \begin{cases} \mathbf{w}, & |\mathbf{w}| \leq K \\ K |\mathbf{w}|^{-1} \mathbf{w}, & |\mathbf{w}| > K. \end{cases}$$

The following Lemma 5.4 states that the previously defined cut-off function satisfies the required properties as stated in Definition 5.1.

Lemma 5.4 (Properties of cut-off function). *Let \mathbf{m}_K be given by Definition 5.3. Then, $\|\mathbf{m}_K\|_{0,\infty} = K$ and \mathbf{m}_K is Lipschitz continuous with constant $L_K = 1$.*

Proof. The stated assertion $\|\mathbf{m}_K\|_{0,\infty} = K$ is clear and the Lipschitz continuity follows from the fact, that \mathbf{m}_K can be written as $\mathbf{m}_K(\mathbf{w}) = \mathbf{w}_0$ where \mathbf{w}_0 is the unique solution of the minimization $\min_{\mathbf{r} \in B} |\mathbf{w} - \mathbf{r}|$, with the compact and convex set $B = \{\mathbf{x} \in \mathbb{R}^d: |\mathbf{x}| \leq K\}$, see e.g. [3]. \square

Concerning the choice of K , note that Lemma 3.14 and Theorem 4.1 require a small data condition of the form

$$L_{\mathbf{F}}^{(\theta, \mathbf{H}^1)} \leq c_{\Omega} \sqrt{\nu \kappa}, \quad (5.2)$$

with domain-dependent constant c_{Ω} , see (4.64), (4.65). Following Lemma 5.2, there holds $L_{\mathbf{F}}^{(\theta, \mathbf{H}^1)} = \alpha_e K^2$ which yields an upper bound on K , given by

$$K^2 \leq \frac{c_{\Omega}}{\alpha_e} \sqrt{\nu \kappa}. \quad (5.3)$$

6. NUMERICAL EXPERIMENTS

In this section we consider a 2D test case to underline the theoretically derived error estimates of Section 4.2 by numerical experiments. To this end, let $T = 1$, $\Omega = (0, 1)^2$ with Dirichlet boundary $\Gamma_D := \{0, 1\} \times [0, 1]$ and Neumann boundary $\Gamma_N := [0, 1] \times \{0, 1\}$. The Dirichlet boundary conditions for temperature and potential are given by $\theta_b(x, y) = 1 - x$ and $\Phi_b(x, y) = (1 - x)V$, $V > 0$, respectively. All physical parameters are listed in Figure 1. We further assume that the permittivity depends linearly on the temperature [28] and set for $\bar{\theta} = 10^2$, $\gamma \in (0, \bar{\theta}^{-1})$

$$\epsilon: \mathbb{R} \rightarrow [1 - \gamma\bar{\theta}, 1 + \gamma\bar{\theta}], \quad \epsilon(s) = \epsilon_r \cdot \begin{cases} 1 + \gamma\bar{\theta}, & s \leq -\bar{\theta} \\ 1 - \gamma s, & s \in (-\bar{\theta}, \bar{\theta}), \\ 1 - \gamma\bar{\theta}, & s \geq \bar{\theta} \end{cases} \quad (6.1)$$

to meet the requirements of Assumption 2.2.

The right-hand side terms \mathbf{f}_v , f_{τ} , f_{β} are chosen such that

$$\begin{aligned} \mathbf{u}_{*,x}(t, x, y) &= \sin(\pi x)^2 \sin(2\pi y) g^{(1)}(t) \\ \mathbf{u}_{*,y}(t, x, y) &= -\sin(2\pi x) \sin(\pi y)^2 g^{(1)}(t) \\ p_*(t, x, y) &= -\sin(\pi x) \sin(\pi y) g^{(1)}(t) \\ \theta_*(t, x, y) &= 1 - x + (1 - 4(x - 0.5)^2) g^{(2)}(t) \\ \Phi_*(t, x, y) &= (1 - x)V + V \sin(\pi x) g^{(2)}(t), \end{aligned} \quad (6.2)$$

solves the TEHD Boussinesq equations in strong form (1.1) to (1.5) with those source terms added. The temporal factors $g^{(1)}$, $g^{(2)}$ are either chosen as $g_{\text{per}}^{(1)}(t) := \sin(2\pi t)$, $g_{\text{per}}^{(2)}(t) := \cos(2\pi t) + 1$ or as $g_{\text{alg}}^{(1)}(t) = g_{\text{alg}}^{(2)}(t) := g_{\text{alg}}(t) = t^{1.51}$ to cover different temporal regularities of the exact solution. In particular, $g_{\text{per}}^{(i)} \in C^{\infty}([0, T])$ and

$$g_{\text{alg}}, g'_{\text{alg}} \in L^{\infty}(0, T; \mathbb{R}), \quad g''_{\text{alg}}, tg''_{\text{alg}} \in L^2(0, T; \mathbb{R}), \quad g'''_{\text{alg}} \notin L^2(0, T; \mathbb{R}). \quad (6.3)$$

Thus, for $g = g_{\text{per}}$ the exact solution satisfies the regularity conditions for both, BDF1 and BDF2, assumed by Corollaries 4.7 and 4.8, respectively. On the other hand, for $g = g_{\text{alg}}$ the regularity conditions for BDF1 are still satisfied, whereas the conditions for BDF2 do not hold.

The initial condition is set to the exact solution at $t = 0$ and for BDF2, the approximate solution for the first time step is set to the exact solution at $t = k$. Thus, errors induced by the initial conditions, given by $E_j(q)$, can be neglected.

The spatial discretization is based on a mesh consisting of quadrilaterals with finite element spaces given by Taylor–Hood elements for velocity and pressure ($\mathbb{Q}_2/\mathbb{Q}_1$), and continuous quadratic Lagrange elements for temperature and potential (\mathbb{Q}_2). The arising linear systems are solved by a preconditioned GMRES method [32]. We use a block Jacobi method as preconditioner whereat the inverse of each diagonal block is approximated by an incomplete LU factorization. The implementation is based on the open-source, general purpose FEM package *HiFlow*³ [11].

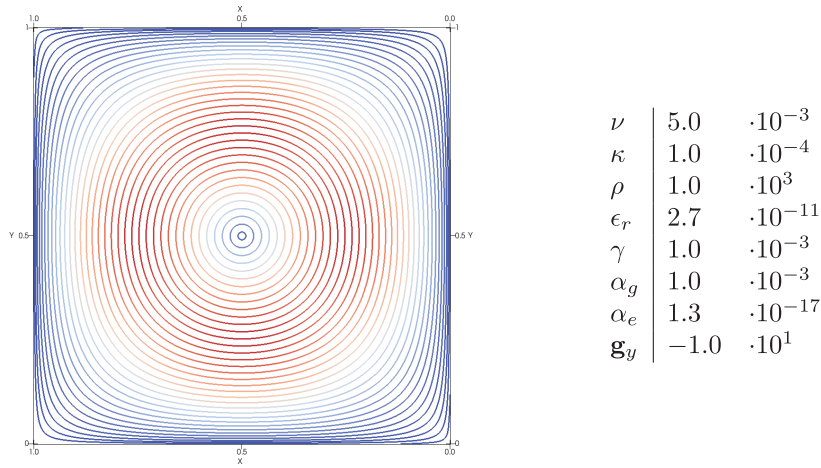


FIGURE 1. *Left:* streamlines of exact flow field with colors indicating the velocity magnitude. *Right:* physical parameters.

Concerning the modified DEP force \mathbf{F}_K , the cut-off threshold K should be small enough such that the requirements imposed by Lemma 3.14 and Theorem 4.1 are satisfied. As pointed out in Section 5, these conditions are of the form

$$\alpha_e K^2 \leq c_\Omega \sqrt{\nu \kappa}, \quad (6.4)$$

with domain dependent constant

$$c_\Omega = c_0^{-1} \min \left\{ (2q(1+c_0^2)(1+c_D^2))^{-\frac{1}{2}} |\mathbf{f}|_2^{-1}, 2q^{-1} |\mathbf{f}|_\infty^{-1} \right\}. \quad (6.5)$$

As c_0, c_D denote the respective constants in Friedrich's inequalities for H_0^1, H_D^1 on a square domain, they can be bounded as $c_0 \leq 1$ and $c_D \leq 1$, see [12] for instance. Concerning the time stepping contributions, we have

$$\begin{aligned} \text{BDF1: } q &= 1, |\mathbf{f}|_2 = 1, \quad |\mathbf{f}|_\infty = 1 \\ \text{BDF2: } q &= 2, |\mathbf{f}|_2 = \sqrt{5}, \quad |\mathbf{f}|_\infty = 2. \end{aligned} \quad (6.6)$$

In summary, equations (6.5), (6.6) and $\alpha_e = \frac{\epsilon_0 \epsilon_r \gamma}{2\rho}$ imply that $K \leq K_*$ with

$$K_* := \left(4\sqrt{5}\alpha_e \right)^{-\frac{1}{2}} (\nu \kappa)^{\frac{1}{4}} = 5.5 \times 10^6 \quad (6.7)$$

is sufficient for (6.4) to hold. On the other hand, the exact potential solution is chosen such that

$$\|\nabla \Phi_*(t)\|_{0,\infty} = V(1+\pi) |g^{(2)}(t)|. \quad (6.8)$$

Using $\max_{t \in [0,1]} |g^{(2)}(t)| \leq 2$, there holds $M_\Phi := \max_{t \in [0,1]} \|\nabla \Phi_*(t)\|_{0,\infty} \leq 10V$. Setting $K \geq 10V$ thus implies that the modified DEP force reduces to the original version for the exact potential. Therefore, as long as $V \leq 5.5 \times 10^5$, it is possible to define K such that both $\mathbf{F}_s(\theta_*, \Phi_*) = \mathbf{F}_K(\theta_*, \Phi_*)$ and $K < K_*$ do hold.

For the first test series we set $V = K = 10^3 \ll K_*$, *i.e.* the small data condition is satisfied and $\mathbf{F}_s(\theta_*, \Phi_*) \neq \mathbf{F}_K(\theta_*, \Phi_*)$. Tables 1 (BDF1) and 2 (BDF2) list the corresponding errors and convergence rates

$$\beta(k) = \log \left(\frac{\text{error}(k_0)}{\text{error}(k)} \right) \log \left(\frac{k_0}{k} \right)^{-1}, \quad k_0 = 0.05. \quad (6.9)$$

TABLE 1. BDF1, $g = g_{\text{per}}$, $V = K = 10^3$, $h = 1.25k$.

k	$\ e_{\mathbf{u}}\ _{L^2(\mathbf{H}^1)}$		$\ e_p\ _{L^2(L^2)}$		$\ e_\theta\ _{L^2(\mathbf{H}^1)}$		$\ e_\Phi\ _{L^2(\mathbf{H}^1)}$	
	Error	β	Error	β	Error	β	Error	β
5.00×10^{-2}	7.9×10^{-1}	0.0	5.5×10^1	0.0	7.6×10^{-1}	0.0	3.9×10^0	0.0
2.50×10^{-2}	4.0×10^{-1}	1.0	2.8×10^1	1.0	3.9×10^{-1}	0.9	9.8×10^{-1}	2.0
1.25×10^{-2}	2.0×10^{-1}	1.0	1.4×10^1	1.0	2.0×10^{-1}	1.0	2.5×10^{-1}	2.0
6.25×10^{-3}	9.9×10^{-2}	1.0	7.0×10^0	1.0	1.0×10^{-1}	1.0	6.6×10^{-2}	2.0
3.13×10^{-3}	5.0×10^{-2}	1.0	3.5×10^0	1.0	5.2×10^{-2}	1.0	2.0×10^{-2}	1.9

TABLE 2. BDF2, $g = g_{\text{per}}$, $V = K = 10^3$, $h = 1.25k$.

k	$\ e_{\mathbf{u}}\ _{L^2(\mathbf{H}^1)}$		$\ e_p\ _{L^2(L^2)}$		$\ e_\theta\ _{L^2(\mathbf{H}^1)}$		$\ e_\Phi\ _{L^2(\mathbf{H}^1)}$	
	Error	β	Error	β	Error	β	Error	β
5.00×10^{-2}	1.1×10^{-1}	0.0	6.3×10^0	0.0	1.6×10^{-1}	0.0	3.9×10^0	0.0
2.50×10^{-2}	2.7×10^{-2}	2.0	1.5×10^0	2.0	4.6×10^{-2}	1.8	9.8×10^{-1}	2.0
1.25×10^{-2}	6.7×10^{-3}	2.0	3.8×10^{-1}	2.0	1.1×10^{-2}	2.0	2.4×10^{-1}	2.0
6.25×10^{-3}	1.7×10^{-3}	2.0	9.3×10^{-2}	2.0	2.3×10^{-3}	2.0	6.1×10^{-2}	2.0
3.13×10^{-3}	4.2×10^{-4}	2.0	2.3×10^{-2}	2.0	5.5×10^{-4}	2.0	1.5×10^{-2}	2.0

for decreasing k and $h \propto k$ in case of full temporal regularity of the exact solution. Since $h \propto k$, the h^l terms in the error estimates given by Corollaries 4.7, 4.8 are transformed to k^l . We obtain $l = 2$ due to the spatial regularity of the exact solution and due to the polynomial order of the underlying finite element space. Thus, the temporal contributions in the derived error estimates dominate the spatial contributions $h^l \propto k^l$ and the observed errors should resemble the temporal convergence order. This is indeed the case for velocity, temperature and potential whose corresponding error rates are inline with Corollaries 4.7, 4.8, see Tables 1 and 2.

Tables 3 and 4 illustrate the errors for $g = g_{\text{alg}}$. As pointed out by (6.3), the exact solution does not satisfy the regularity requirements of Corollary 4.8 any more, whereas the weaker assumptions supposed by Corollary 4.7 do still hold. In practice, one can observe $\beta = 1$ for the BDF1 scheme, in accordance with Corollary 4.7 and $\beta = 1.6$ for the velocity error when BDF2 is employed. Thus, the regularity condition that is supposed for second order convergence appears not only sufficient, but also necessary. Since the condition $\partial_{ttt}\mathbf{u}_* \in L^2(0, T; \mathbf{H}^{-1})$ in Corollary 4.8 is violated, but not $\partial_t\mathbf{u}_* \in L^2(0, T; \mathbf{H}^{l+1})$, we conclude that the overall convergence is reduced due to the purely temporal contributions $E(k)$, but not due to the mixed contributions $E(h, k)$.

Next, we consider the case when all conditions imposed by Theorem 4.1 and Corollaries 4.7, 4.8 are satisfied, except of the small data condition. To this end, we set $V = 10^7$ and $K = 10^{12}$. With this choice, equation (6.4) is violated since $K \gg K_*$. Moreover, the modified DEP force \mathbf{F}_K reduces to the original version \mathbf{F}_s , because the Euclidean norm of the potential gradients of the exact and discrete solution (both are of order $\mathcal{O}(10V)$) are way below K . Tables 5 and 6 list the corresponding errors. Apparently, the respective convergence orders are almost identical to those obtained for $V = K = 10^3$. These results indicate that the small data condition imposed by Theorem 4.1 might not be a necessary condition for the stated error estimates to hold.

In all considered cases, the pressure error converges faster than predicted by the theory. In fact, it converges with the same order as the velocity error in the high temporal regularity case $g = g_{\text{per}}$. In the low regularity case $g = g_{\text{alg}}$ the pressure convergence rate is slightly higher (BDF1) and lower (BDF2) than its velocity counterpart. Overall, one cannot observe a rate that is reduced by $\frac{1}{2}$. In the proof of Theorem 4.1, the factor $k^{-\frac{1}{2}}$ stems from estimating the term $E_d(h, k)$, (4.63), which basically measures the temporal variation of the discretization error $(\mathbf{d}_{\mathbf{u},h}^n)_n$. The similar quantity $E(h, k)$, which measures the temporal variation of the exact solution $(\mathbf{u}^n)_n$, does

TABLE 3. BDF1, $g = g_{\text{alg}}$, $V = K = 10^3$, $h = 1.25k$.

k	$\ e_{\mathbf{u}}\ _{L^2(\mathbf{H}^1)}$		$\ e_p\ _{L^2(L^2)}$		$\ e_{\theta}\ _{L^2(\mathbf{H}^1)}$		$\ e_{\Phi}\ _{L^2(\mathbf{H}^1)}$	
	Error	β	Error	β	Error	β	Error	β
5.00×10^{-2}	9.7×10^{-2}	0.0	2.4×10^0	0.0	9.5×10^{-2}	0.0	1.7×10^0	0.0
2.50×10^{-2}	4.9×10^{-2}	1.0	1.0×10^0	1.3	4.1×10^{-2}	1.2	4.1×10^{-1}	2.0
1.25×10^{-2}	2.5×10^{-2}	1.0	4.5×10^{-1}	1.2	1.9×10^{-2}	1.2	1.0×10^{-1}	2.0
6.25×10^{-3}	1.3×10^{-2}	1.0	2.1×10^{-1}	1.2	9.3×10^{-3}	1.1	2.5×10^{-2}	2.0
3.13×10^{-3}	6.4×10^{-3}	1.0	9.7×10^{-2}	1.2	4.6×10^{-3}	1.1	6.4×10^{-3}	2.0

TABLE 4. BDF2, $g = g_{\text{alg}}$, $V = K = 10^3$, $h = 1.25k$.

k	$\ e_{\mathbf{u}}\ _{L^2(\mathbf{H}^1)}$		$\ e_p\ _{L^2(L^2)}$		$\ e_{\theta}\ _{L^2(\mathbf{H}^1)}$		$\ e_{\Phi}\ _{L^2(\mathbf{H}^1)}$	
	Error	β	Error	β	Error	β	Error	β
5.00×10^{-2}	1.8×10^{-2}	0.0	1.0×10^0	0.0	5.9×10^{-2}	0.0	1.7×10^0	0.0
2.50×10^{-2}	5.1×10^{-3}	1.8	3.4×10^{-1}	1.6	1.8×10^{-2}	1.7	4.1×10^{-1}	2.0
1.25×10^{-2}	1.6×10^{-3}	1.7	1.1×10^{-1}	1.6	3.9×10^{-3}	2.0	1.0×10^{-2}	2.0
6.25×10^{-3}	5.6×10^{-4}	1.7	3.8×10^{-2}	1.6	7.3×10^{-4}	2.1	2.5×10^{-2}	2.0
3.13×10^{-3}	2.0×10^{-4}	1.6	1.3×10^{-2}	1.6	1.9×10^{-4}	2.1	6.2×10^{-3}	2.0

TABLE 5. BDF1, $g = g_{\text{per}}$, $V = 10^7$, $K = 10^{12}$, $h = 1.25k$.

k	$\ e_{\mathbf{u}}\ _{L^2(\mathbf{H}^1)}$		$\ e_p\ _{L^2(L^2)}$		$\ e_{\theta}\ _{L^2(\mathbf{H}^1)}$		$\ e_{\Phi}\ _{L^2(\mathbf{H}^1)}$	
	Error	β	Error	β	Error	β	Error	β
5.00×10^{-2}	7.9×10^{-1}	0.0	5.5×10^1	0.0	7.5×10^{-1}	0.0	3.9×10^4	0.0
2.50×10^{-2}	4.0×10^{-1}	1.0	2.8×10^1	1.0	3.9×10^{-1}	0.9	9.8×10^3	2.0
1.25×10^{-2}	2.0×10^{-1}	1.0	1.4×10^1	1.0	2.0×10^{-1}	1.0	2.5×10^3	2.0
6.25×10^{-3}	9.9×10^{-2}	1.0	7.0×10^0	1.0	1.0×10^{-1}	1.0	6.6×10^2	2.0
3.13×10^{-3}	5.0×10^{-2}	1.0	3.5×10^0	1.0	5.1×10^{-2}	1.0	2.0×10^2	1.9

TABLE 6. BDF2, $g = g_{\text{per}}$, $V = 10^7$, $K = 10^{12}$, $h = 1.25k$.

k	$\ e_{\mathbf{u}}\ _{L^2(\mathbf{H}^1)}$		$\ e_p\ _{L^2(L^2)}$		$\ e_{\theta}\ _{L^2(\mathbf{H}^1)}$		$\ e_{\Phi}\ _{L^2(\mathbf{H}^1)}$	
	Error	β	Error	β	Error	β	Error	β
5.00×10^{-2}	1.1×10^{-1}	0.0	6.2×10^0	0.0	1.6×10^{-1}	0.0	3.9×10^4	0.0
2.50×10^{-2}	2.7×10^{-2}	2.0	1.5×10^0	2.0	4.6×10^{-2}	1.8	9.8×10^3	2.0
1.25×10^{-2}	6.7×10^{-3}	2.0	3.7×10^{-1}	2.0	1.1×10^{-2}	2.0	2.4×10^3	2.0
6.25×10^{-3}	1.7×10^{-3}	2.0	9.3×10^{-2}	2.0	2.3×10^{-3}	2.0	6.1×10^2	2.0
3.13×10^{-3}	4.2×10^{-4}	2.0	2.3×10^{-2}	2.0	5.5×10^{-4}	2.0	1.5×10^2	2.0

not cause the occurrence of $k^{-\frac{1}{2}}$, since the temporal regularity of \mathbf{u} could be exploited. From a theoretical point of view, this temporal regularity could not be derived for $(\mathbf{d}_{\mathbf{u},h}^n)_n$. In the underlying test problem, however, this discretization error might have a similar temporal smoothness as the exact solution, resulting in comparable k -convergence rates for pressure and velocity.

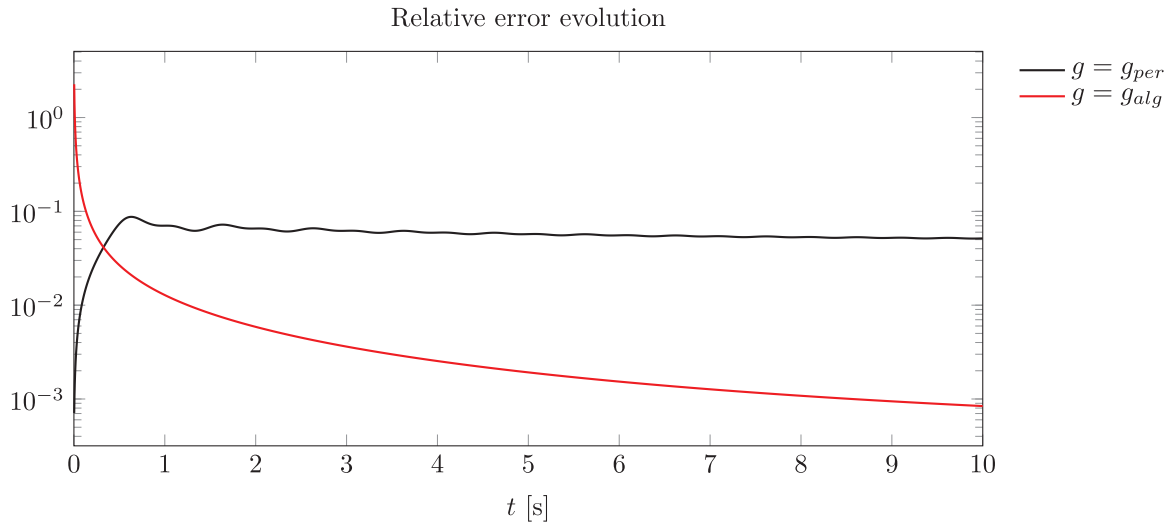


FIGURE 2. Relative velocity error $E(t)$ over time for BDF1, $V = K = 10^3$, $h = 1.25k$.

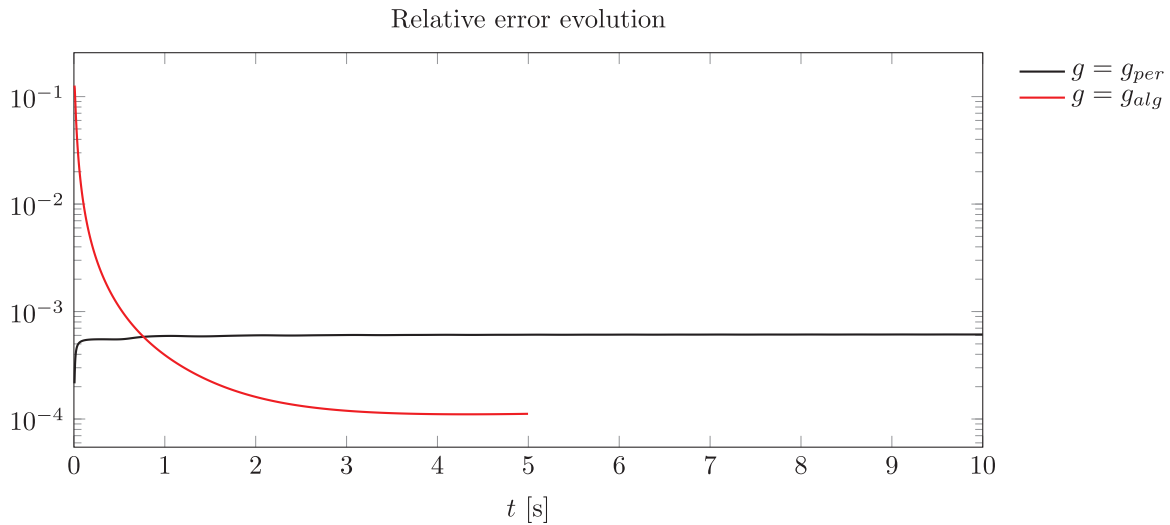


FIGURE 3. Velocity error $E(t)$ over time for BDF2, $V = K = 10^3$, $h = 1.25k$. For $t \geq 5$ the employed algebraic solver failed to converge for $g = g_{alg}$.

Finally, Figures 2 and 3 visualize the long-term error evolution for the BDF1 and BDF2 scheme, respectively. To this end, the normalized velocity error

$$E(t) := \left(\frac{k \sum_{n=1}^{\lfloor \frac{t}{k} \rfloor} |e_{\mathbf{u}_1}^n|^2}{\int_0^t |g^{(1)}(s)|^2 ds} \right)^{\frac{1}{2}} \tag{6.10}$$

is plotted over time for the different temporal functions $g = g_{per}$ (black curve) and $g = g_{alg}$ (red curve). Note that $g^{(1)}$ is just the temporal factor in the exact solution. Thus, $E(t)$ equals the relative velocity error, up to

a time-independent constant. Apparently, the actual error does not exhibit the exponential growth that enters the estimates by means of Gröwall's inequality, see (4.43). Instead, $E(t)$ stabilizes on a fairly constant level. However, the lack of temporal regularity of g_{alg} at $t = 0$ can be observed through high relative errors in the beginning of the simulation.

7. DISCUSSION ON THE CONSTRUCTED DEP FORCE

Summing up the previous sections, we derived a discrete well-posedness result and error estimates for the TEHD Boussinesq equations, provided a DEP force \mathbf{F} satisfying Assumption 3.13. Since these conditions are not fulfilled by the original force \mathbf{F}_s , we constructed a family of modified forces $\{\mathbf{F}_K, K > 0\}$, based on a cut-off function applied to the gradient of the potential, see Section 5. With this choice, the theoretical results of Section 3 and 4 do hold for $\mathbf{F} = \mathbf{F}_K$, as long the cut-off threshold K satisfies

$$K \leq \left(\frac{c_\Omega}{\alpha_e}\right)^{\frac{1}{2}} (\nu\kappa)^{\frac{1}{4}} =: \bar{K}. \quad (7.1)$$

Note that (7.1) implies both previously used small data conditions, (3.11) and (4.16), when c_Ω is defined as in (6.5).

The domain-dependent constant c_Ω depends on the constants in Friedrich's inequality and time-stepping parameters and can be explicitly computed or estimated. This is done in Section 6 for an hypercube and below for a vertical annulus that is commonly used in physical experiments. In these cases, the upper bound \bar{K} can be calculated and one can draw the following conclusions on the error between the discrete solution obtained for $\mathbf{F} = \mathbf{F}_K$ and the exact solution for $\mathbf{F} = \mathbf{F}_s$ if the initially stated small data condition (1.6) does hold:

Corollary 7.1 (Convergence rates for $\mathbf{F} = \mathbf{F}_s$). *Suppose that the exact solution of Problem 2.4 with $\mathbf{F} = \mathbf{F}_s$, denoted by $(\mathbf{u}_*, p_*, \theta_*, \Phi_*)$, satisfies the regularity conditions stated by Theorem 4.1 and Corollary 4.7 (case I) or Corollary 4.8 (case II). In addition, assume that*

$$\|\nabla\Phi_*\|_{\infty; \mathbf{L}^\infty} < \bar{K}. \quad (7.2)$$

Further suppose that the physical parameters and discretization fulfill Assumptions 2.2–3.10 and that the q starting values are chosen to fulfill condition (3.15). Let the discrete solution $(\mathbf{u}_h^n, p_h^n, \theta_h^n, \Phi_h^n)$ be obtained by solving Problem 3.12 with cut-off DEP force $\mathbf{F} = \mathbf{F}_{\bar{K}}$.

Then, the error estimates stated by Corollary 4.7 (case I) and Corollary 4.8 (case II) remain valid for $(\mathbf{u}, p, \theta, \Phi) = (\mathbf{u}_, p_*, \theta_*, \Phi_*)$.*

Proof. Since (7.2) implies $|\nabla\Phi_*(t, x)| < \bar{K}$ for almost all (t, x) , we conclude that $\mathbf{m}_{\bar{K}} \circ \nabla\Phi_* = \nabla\Phi_*$ a.e. by the definition of the metric projection $\mathbf{m}_{\bar{K}}$, see Definition 5.3. Thus, $\mathbf{F}_{\bar{K}}(\theta_*, \Phi_*) = \mathbf{F}_s(\theta_*, \Phi_*)$, which implies that $(\mathbf{u}_*, p_*, \theta_*, \Phi_*)$ solves Problem 2.4 with $\mathbf{F} = \mathbf{F}_{\bar{K}}$.

The stated assertion now follows by the fact that $\mathbf{F}_{\bar{K}}$ satisfies Assumption 3.13 and the validness of the small data conditions supposed by Lemma 3.14 and Theorem 4.1 through the definition of \bar{K} and c_Ω , see (6.5). \square

Corollary 7.1 creates the link between the original DEP formulation and the modified version, under the assumption that the exact electric field $\mathbf{E} = -\nabla\Phi$ satisfies (7.2).

Summing up, condition (3.11) and (4.16) have their origin in the fact that there is a force term in the momentum equation, that is an element of \mathbf{U}^* and depends on $\nabla\theta$. Bounding this term from above yields the product $\|\nabla\theta\|_{1,2}\|\nabla\mathbf{u}\|_{1,2}$ before applying Young's inequality. After this step, the small data conditions are needed to ensure positive factors when collecting all $\|\nabla\theta\|_{1,2}^2, \|\nabla\mathbf{u}\|_{1,2}^2$ terms on the left-hand side. Thus, (3.11) and (4.16) are induced by the applied proof technique. On the other hand, condition (7.2) stems from the fact that \mathbf{F}_s also depends on $|\nabla\Phi|^2$, which cannot be handled properly if Φ is only in H^1 . We introduced the cut-off based modification \mathbf{F}_K to circumvent this issue. With the chosen construction, equations (3.11) and (4.16) are

ν	5.0	$\cdot 10^{-6}$	$\left[\begin{array}{c} \text{m}^2 \text{ s}^{-1} \\ \text{m}^2 \text{ s}^{-1} \\ \text{kg m}^{-3} \\ \text{kg m}^{-3} \\ \text{K}^{-1} \\ \text{K}^{-1} \\ \text{A s m}^2 (\text{kg K V})^{-1} \\ \text{[K]} \end{array} \right]$	$\delta\theta$	7		$\left[\begin{array}{c} \text{[K]} \\ \text{[V]} \\ \text{[m s}^{-2} \\ \text{[m s}^{-2} \\ \text{[m s}^{-2} \end{array} \right]$
κ	7.74	$\cdot 10^{-8}$		$\delta\Phi \in$	[0.7, 7]	$\cdot 10^3$	
ρ	9.23	$\cdot 10^2$		\mathbf{g}_x	0		
ϵ_r	2.391	$\cdot 10^{-11}$		\mathbf{g}_y	0		
γ	1.065	$\cdot 10^{-3}$		\mathbf{g}_z	-9.81		
α_g	1.08	$\cdot 10^{-3}$		r_i	5.0	$\cdot 10^{-3}$	$\left[\begin{array}{c} \text{[m]} \\ \text{[m]} \\ \text{[m]} \end{array} \right]$
α_e	1.379	$\cdot 10^{-17}$		r_o	1.0	$\cdot 10^{-2}$	
θ_r	2.9815	$\cdot 10^2$		H	1.0	$\cdot 10^{-1}$	

FIGURE 4. Experiment parameters.

summarized by condition (7.1) which can actually always be met (if K is made sufficiently small). Also by the way \mathbf{F}_K is constructed, the additional condition (7.2) onto the exact potential implies that the modified force term reduces to the original one. The higher the critical value \bar{K} , the more likely it is that we find a K that satisfies (7.1) and $\mathbf{F}_K(\theta, \Phi) = \mathbf{F}_s(\theta, \Phi)$ for the exact solution; thus solving the original, unmodified equations.

We now present experiments for a realistic scenario, for which (7.2) is indeed fulfilled (for the numerical solution). To this end, we consider the DEP-driven flow inside the vertical annulus $\Omega := \{(x_1, x_2, x_3) : r_i < x_1^2 + x_2^2 < r_o, x_3 \in (0, H)\}$ of height H and inner / outer radii $0 < r_i < r_o$. The top and bottom endplates $\Gamma_b = \partial\Omega \cap \{x_3 = 0\}$, $\Gamma_t = \partial\Omega \cap \{x_3 = H\}$ are supposed to be thermally and electrically insulating, *i.e.* there holds $\nabla\theta \cdot \mathbf{n} = \nabla\Phi \cdot \mathbf{n} = 0$ with \mathbf{n} denoting the unit outward normal. We further apply a temperature and potential difference between the inner and outer wall $\Gamma_i = \partial\Omega \cap \{x_1^2 + x_2^2 = r_i\}$, $\Gamma_o = \partial\Omega \cap \{x_1^2 + x_2^2 = r_o\}$ by imposing Dirichlet boundary conditions

$$\theta_D(x) = \begin{cases} \theta_r - \frac{1}{2}\delta\theta, & x \in r_i \\ \theta_r + \frac{1}{2}\delta\theta, & x \in r_o \end{cases}, \quad \Phi_D(x) = \begin{cases} 0, & x \in r_i \\ \delta\Phi, & x \in r_o \end{cases}$$

for some temperature difference $\delta\theta \geq 0$ and potential difference $\delta\Phi \geq 0$.

Suitable boundary liftings θ_b, Φ_b can easily be obtained by using cylinder coordinates and linear interpolation in the radius e_r direction. Here, we will vary the potential difference $\delta\Phi$ in the interval [700 V, 7000 V] and the initial conditions are given by \mathbf{u}_0, θ_0 as stationary solution of the TEHD equations with $\alpha_e = 0$ (*i.e.* the standard Boussinesq equations for natural convection) and Φ_0 is defined as solution of (1.4) with $\theta(x) = \theta_r = \text{const}$ (*i.e.* the standard Gauss' law with constant permittivity, evaluated at room temperature). The considered fluid is the silicone oil AK5 with properties listed in Table 4.

The simulations are performed for $\mathbf{F} = \mathbf{F}_{K_*}$, $K_* = 2.4 \times 10^6$, $k = 0.05s$ and on a rectangular grid of $60 \times 16 \times 100$ cells in ϕ, r, z direction, respectively, as discretization for $\Omega = [0, 2\pi] \times [r_i, r_o] \times [0, H]$ (using cylinder coordinates).

The proposed scenario is often used in physical experiments to investigate the influence of DEP force onto heat transfer enhancement between inner and outer wall, see [35] and the references therein, for instance. Corresponding experiments are conducted under laboratory conditions (with standard gravitational acceleration \mathbf{g}), as well as under microgravity conditions obtained during parabolic flights ($\mathbf{g} \approx 0$), see *e.g.* [27].

Here, we present numerical experiments for the laboratory case as done in chapter 6.3 of the first author's Ph.D. thesis [12]. In this scenario, the fluid flow undergoes a rapid change from the initial unicellular, natural convection-like, pattern to a final, stationary state which is made up by multiple, axially aligned vortices. See Figure 5 for a prototypical flow evolution.

The flow behaviour can be best understood by looking at the strength of axial vorticity plotted over time for different values of $\delta\Phi$, see Figure 6. The previously described transition from unicellular pattern to multiple vortices manifests itself in an exponential increase of axial vorticity from 0 to a certain, fixed final value. Both, exponential growth rate and final value, are monotonically increasing w.r.t. $\delta\Phi$. However, one can also observe

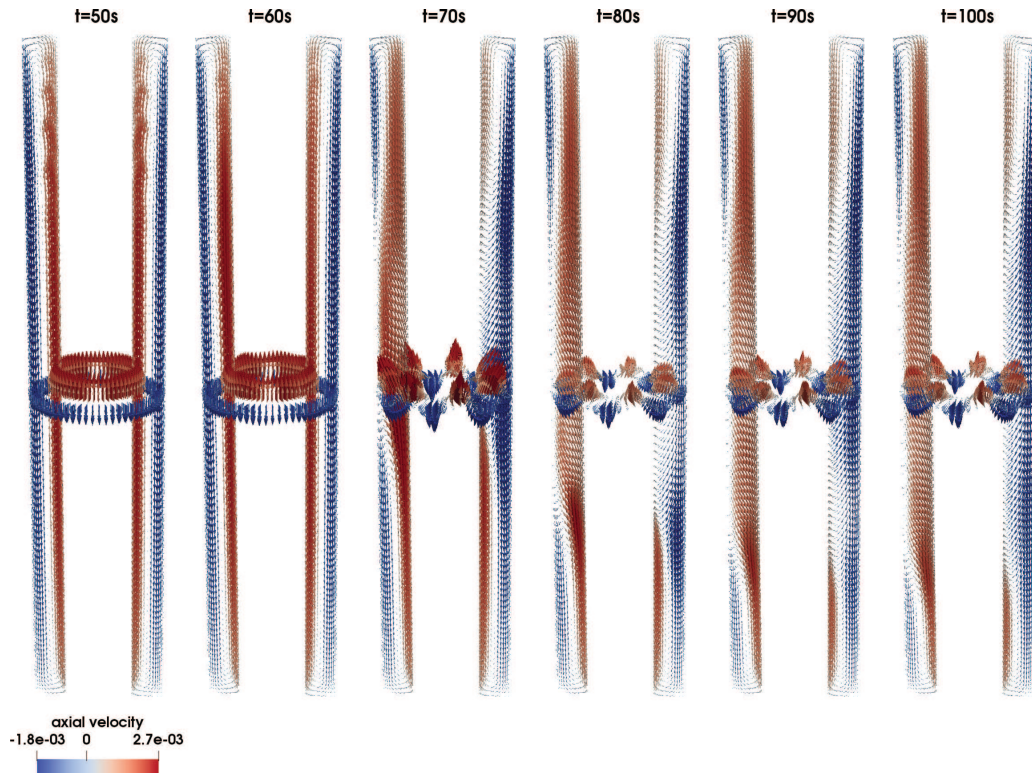


FIGURE 5. Velocity field for $\delta\theta = 7$ K, $\delta\Phi = 7000$ V at multiple time instances on a vertical and horizontal cut plane through the domain. The color map indicates axial velocity with red/blue denoting rising/falling fluid.

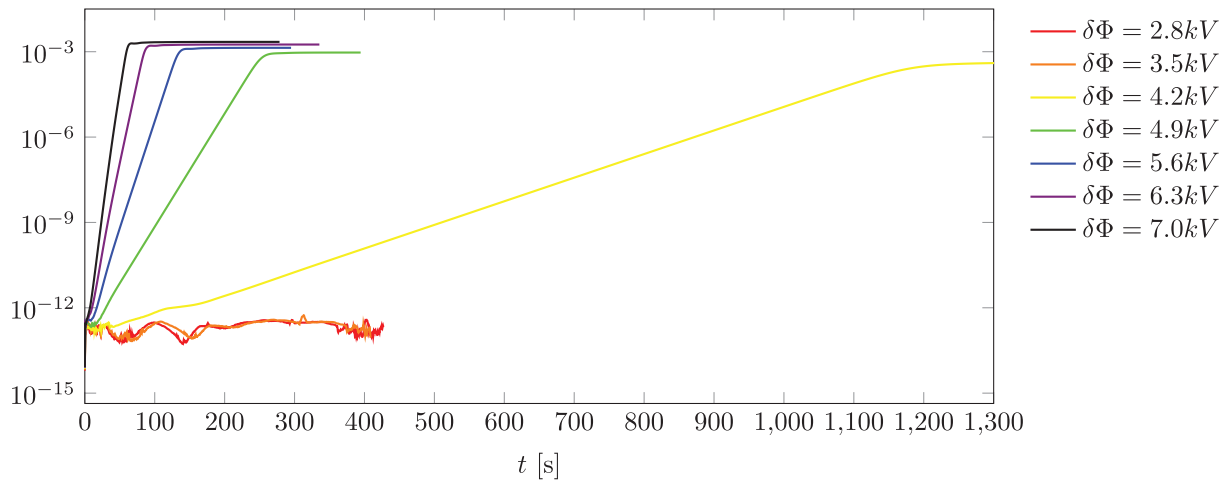


FIGURE 6. Temporal evolution of discrete axial vorticity $\|(\nabla \times \mathbf{u}_h^n)_z\|_{0,2}$ for different potential differences.

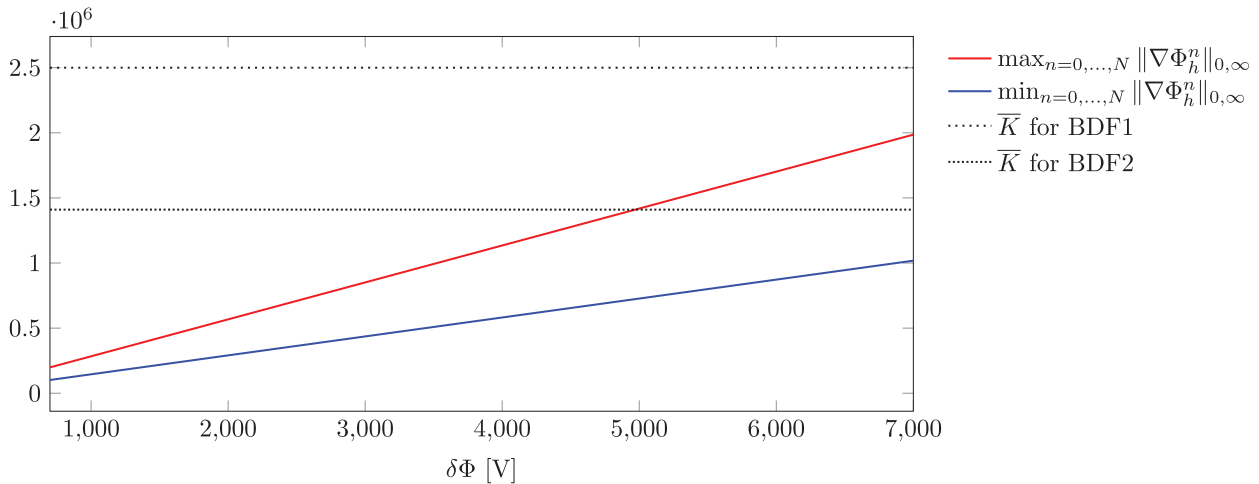


FIGURE 7. Norm of discrete potential gradient for different potential differences.

that for values of $\delta\Phi$ below some critical threshold (here for $\delta\Phi \in \{2800 \text{ V}, 3500 \text{ V}\}$), axial vorticity stays around 0 and the flow pattern does not significantly deviate from the natural convection base state. This behaviour can also be observed experimentally [35] and can be explained by linear stability analysis [45].

Coming back to the small data condition, we note that the corresponding domain dependent constant c_Ω can be calculated in a similar way as in Section 6, where the constants of Friedrich’s inequality for the annular shaped cylinder can be estimated from above by $c_0, c_D \leq c_*$ with

$$c_* = \left(\frac{1}{2} (\ln(r_o) - \ln(r_i)) (r_o^2 - r_i^2) \right)^{\frac{1}{2}}, \tag{7.3}$$

see Lemma A.107 in [12]. Using (6.5), (7.1), (7.3) the critical value can now be calculated:

$$\bar{K} = \begin{cases} 2.5 \times 10^6 & \text{for BDF1} \\ 1.41 \times 10^6 & \text{for BDF2.} \end{cases} \tag{7.4}$$

In Figure 7 we plot minimal and maximal values of the discrete electrical field magnitude $|\nabla\Phi_h^n|$ over different applied potential differences $\delta\Phi$. The critical values \bar{K} are marked as dotted lines for both time stepping schemes. Apparently, the discrete potential satisfies (7.2) in case of BDF1 for all considered potential differences, whereas (7.2) is satisfied for BDF2 as long as $\delta\Phi < \approx 5000 \text{ V}$.

We thus showed that our crucial small data assumption (7.2) is fulfilled by the numerically obtained solution in an application relevant scenario over a parameter range of physical interest (note that the previously described transition of flow pattern can be observed for $\delta\Phi \geq 4200 \text{ V}$).

We finally provide some data that underlines the derived discrete energy estimates of Lemma 3.14. Figures 8 and 9 plot kinetic energy and energy dissipation over time for BDF1 and BDF2 and different time step sizes. The spatial resolution is kept fixed and $\delta\Phi = 7000 \text{ V}$. Except of the case BDF2, $k = 0.1$, only small differences between the different energy courses can be observed during the transition phase from unicellular to multi vortex flow pattern. In particular, the respective final states hardly differ and k -independent energy bounds are observed, as predicted by Lemma 3.14. Only in case of BDF2, a time step size of $k = 0.1$ appears to be too coarse to obtain an accurate solution, while the energy still stays within reasonable bounds.

Recall that we set $\mathbf{F} = \mathbf{F}_{K_*}$, with $K_* = 2.4 \times 10^6 < \bar{K}(\text{BDF1})$ for the presented simulation data, *i.e.* this choice for \mathbf{F} fulfills the small data conditions (3.11) and (4.16) which are imposed by the stability and error

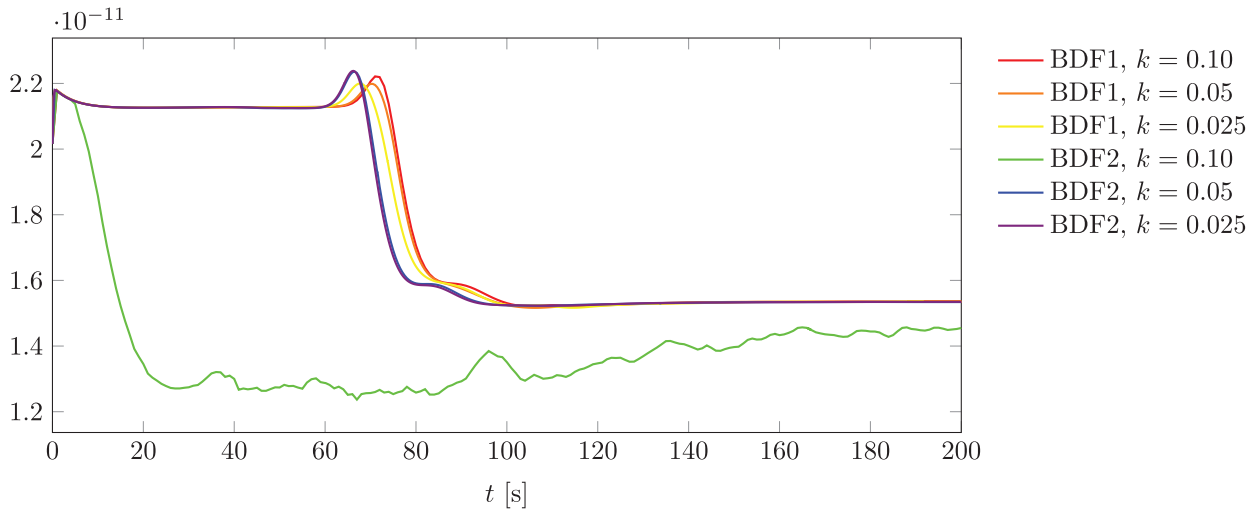


FIGURE 8. Temporal evolution of discrete kinetic energy $\frac{1}{2}\|\mathbf{u}_h^n\|_{0,2}^2$ for different time step sizes and schemes for $\delta\Phi = 7.0$ kV.

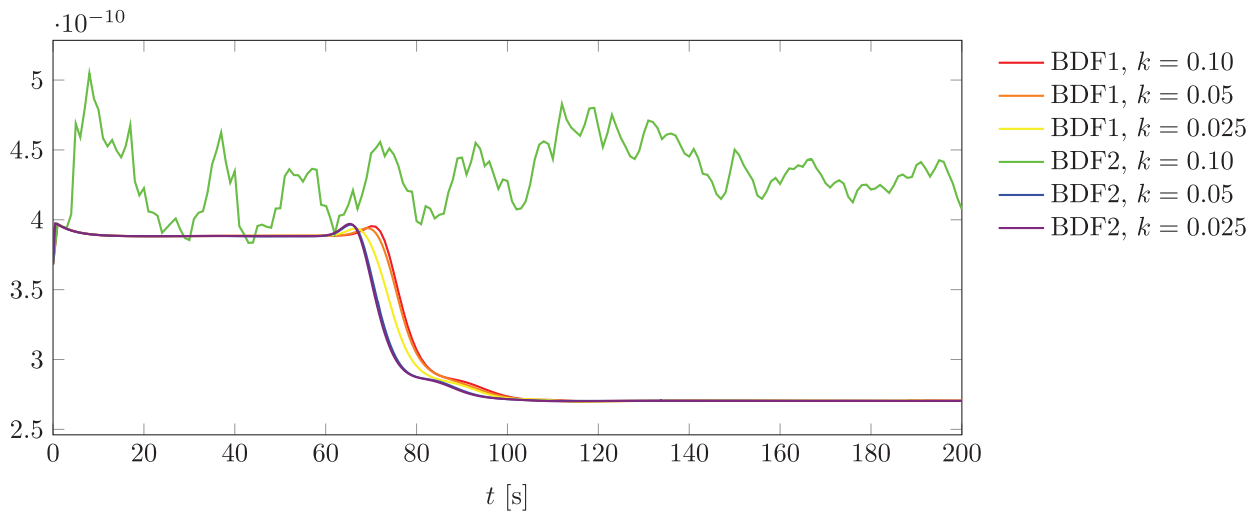


FIGURE 9. Temporal evolution of discrete energy dissipation $\nu\|\nabla\mathbf{u}_h^n\|_{0,2}^2$ for different time step sizes and schemes for $\delta\Phi = 7.0$ kV.

estimate results when BDF1 is used. In case of BDF2, however, \mathbf{F}_{K_*} does not satisfy the required assumptions. It remains an open question, whether this is the reason for the observed behaviour for $k = 0.1$.

Our choice of K_* also means that we de facto used \mathbf{F}_s since, according to Figure 7, we have $\max_{n=0,\dots,N}\|\nabla\Phi_h^n\|_{0,\infty} < K_*$ for $\delta\Phi = 7000$ V, and therefore, $\mathbf{F}_s(\theta_h^n, \Phi_h^n) = \mathbf{F}_{K_*}(\theta_h^n, \Phi_h^n)$ by construction.

Summing up, we have presented an application relevant scenario, for which the numerical potential indeed fulfills the required small data condition over a parameter range of physical interest. Further, we want to point out that if the sensitivity of the potential solution w.r.t. temperature is rather low for a given dielectric fluid (here $\gamma = \mathcal{O}(10^{-3})$), then the potential obtained by solving the TEHD equations only modestly deviates from the one obtained by setting $\epsilon = \epsilon(\theta_r) = \text{const}$. In case of constant ϵ , however, it is often possible to derive

analytical expressions for Φ if the considered geometry takes the form of typical condensators which are often considered when investigating DEP driven flow, *e.g.* spherical gaps [46] and infinitely long cylindrical gaps [45]. For such an analytical form of Φ , one can easily determine a parameter range, over which the small data condition (7.2) holds. Regarding the previously investigated scenario for instance, it was shown in [12], that the relative difference between Φ_h^n and the analytical solution $\bar{\Phi}$ for Gauss' law with constant ϵ in an infinitely long cylinder is only of order $\mathcal{O}(10^{-3})$ at each time instance, measured in $\|\cdot\|_{1,2}$ norm. This ideal potential $\bar{\Phi}$ fulfills (7.2) for $\delta\Phi < 8620$ V (BDF1) and $\delta\Phi < 4860$ V (BDF2), respectively.

8. CONCLUSION

In this paper, we proposed an H^1 -conformal FEM/BDF discretization for the instationary TEHD Boussinesq equations and showed well-posedness of the discrete equations. Moreover, we derived *a priori* error estimates in a general framework, that allows some freedom in the selection of the temporal discretization components. Based on this framework we defined a semi-implicit 1- and 2-step method and showed that the resulting schemes are first and second order accurate in time, respectively. In doing so, the main difficulty lied in the modeling of the cubic DEP term. Here, we proposed a modification of the original term by means of a cut-off operator. The theoretically obtained convergence rates for velocity, temperature and potential could be verified by numerical experiments in a 2D test case, whereas the pressure error converged faster than predicted. The experiments also demonstrated that a reduced convergence rate is obtained if the exact solutions lacks temporal regularity.

The presented error analysis relies on a small data condition that involves the maximal value of the electric field. The validness of this condition was shown for the presented test case and for a realistic scenario. However, the conducted experiments indicate that this might be not a necessary condition and further research has to be done to relax or even remove this condition by a more sophisticated analysis or a modification of the spatial discretization scheme. We further showed that the derived error estimates do also hold for the original DEP term, if the norm of the exact electric field is below a computable threshold.

APPENDIX A.

Lemma A.1 (Discrete Grönwall's inequality). *Let $k, B \geq 0$ and $(a_l)_l, (b_l)_l, (c_l)_l, (\gamma_l)_l \subset [0, \infty)$ such that*

$$a_n + k \sum_{l=0}^n b_l \leq k \sum_{l=0}^n \gamma_l a_l + k \sum_{l=0}^n c_l + B \quad \text{for } n \geq 0.$$

Suppose that $k\gamma_l < 1$ for all l and set $\sigma_l := (1 - k\gamma_l)^{-1}$. Then,

$$a_n + k \sum_{l=0}^n b_l \leq \exp\left(k \sum_{l=0}^n \sigma_l \gamma_l\right) \cdot \left(k \sum_{l=0}^n c_l + B\right) \quad \text{for } n \geq 0.$$

If $\sum_{l=0}^n \gamma_l a_l$ can be replaced by $\sum_{l=0}^{n-1} \gamma_l a_l$, then the restriction $k\gamma_l < 1$ is not necessary and σ_l can be set to 1.

Proof. See Lemma 5.1 and subsequent remark in [17]. □

Lemma A.2 (Temporal approximation). *Let difference operators be given by $\mathbf{a}^{(1)} = (0, 1)$, $\mathbf{a}^{(2)} = (0, 2, -1)$, $\mathbf{b}^{(1)} = (1, -1)$, $\mathbf{b}^{(2)} = (\frac{3}{2}, -2, \frac{1}{2})$. Let Z denote a Hilbert space, $z \in L^2(0, T; Z)$ with $z' \in L^1(0, T; Z)$, $z^n = z(t_n)$ for $n = 0, \dots, N$. Then*

(i) *If $t^\beta z' \in L^2(0, T; Z)$ for some $\beta \in [0, \frac{1}{2})$:*

$$k \sum_{n=1}^N \|z^n - J_{\mathbf{a}^{(1)}} z^n\|_Z^2 \lesssim k^{2(1-\beta)} \|t^\beta z'\|_{2;Z}^2$$

$$k \sum_{n=1}^N \|k^{-1} J_{\mathbf{b}(1)} z^n\|_Z^2 \lesssim k^{-2\beta} \|t^\beta z'\|_{2;Z}^2.$$

(ii) If $z'' \in L^1(0, T; Z)$, $t^\beta z'' \in L^2(0, T; Z)$ for some $\beta \in [0, \frac{3}{2})$:

$$k \sum_{n=2}^N \|z^n - J_{\mathbf{a}(2)} z^n\|_Z^2 \lesssim k^{2(2-\beta)} \|t^\beta z''\|_{2;Z}^2.$$

(iii) If $z'' \in L^1(0, T; Z)$, $t^\beta z'' \in L^2(0, T; Z)$ for some $\beta \in [0, \frac{3}{2})$:

$$k \sum_{n=1}^N \|\partial_t z^n - k^{-1} J_{\mathbf{b}(1)} z^n\|_Z^2 \lesssim k^{2(1-\beta)} \|t^\beta z''\|_{2;Z}^2.$$

(iv) If z'' , $z''' \in L^1(0, T; Z)$, $t^\beta z''' \in L^2(0, T; Z)$ for some $\beta \in [0, \frac{5}{2})$:

$$k \sum_{n=2}^N \|\partial_t z^n - k^{-1} J_{\mathbf{b}(2)} z^n\|_Z^2 \lesssim k^{2(2-\beta)} \|t^\beta z'''\|_{2;Z}^2.$$

(v) If $z'' \in L^1(0, T; Z)$, $t^\beta z'$, $t^\gamma z'' \in L^2(0, T; Z)$ for some $\beta \in [0, \frac{1}{2})$, $\gamma \in [0, \frac{3}{2})$:

$$k \sum_{n=2}^N \|k^{-1} J_{\mathbf{b}(2)} z^n\|_Z^2 \lesssim k^{-2\beta} \|t^\beta z'\|_{2;Z}^2 + k^{2(1-\gamma)} \|t^\gamma z''\|_{2;Z}^2.$$

Proof. Follows by application of Taylor expansion, see [12] for details. \square

Acknowledgements. We appreciate the valuable comments by Andreas Rupp. This work was supported by German Research Foundation (DFG), grant EG 100/20-1 and INST 35/1134-1 FUGG, bwHPC and Klaus Tschira Foundation (KTS).

REFERENCES

- [1] R. Aldbaissy, F. Hecht, G. Mansour and T. Sayah, A full discretisation of the time-dependent Boussinesq (buoyancy) model with nonlinear viscosity. *Calcolo* **55** (2018) 44.
- [2] K. Allali, A priori and a posteriori error estimates for Boussinesq equations. *Int. J. Numer. Anal. Model.* **2** (2005) 179–196.
- [3] M.V. Balashov and M.O. Golubev, About the Lipschitz property of the metric projection in the Hilbert space. *J. Math. Anal. App.* **394** (2012) 545–551.
- [4] J. Boland and W. Layton, An analysis of the finite element method for natural convection problems. *Numer. Methods Part. Differ. Equ.* **6** (1990) 115–126.
- [5] J. Boland and W. Layton, Error analysis for finite element methods for steady natural convection problems. *Numer. Funct. Anal. Optim.* **11** (1990) 449–483.
- [6] S. Brenner and L.R. Scott, The Mathematical Theory of Finite Element Methods. *Texts in Applied Mathematics*. Springer, New York, NY (2008).
- [7] B. Chandra and D.E. Smylie, A laboratory model of thermal convection under a central force field. *Geophys. Fluid Dyn.* **3** (1972) 211–224.
- [8] C. Egbers, W. Beyer, A. Bonhage, R. Hollerbach and P. Beltrame, The geoflow-experiment on ISS (part I): experimental preparation and design of laboratory testing hardware. *Adv. Space Res.* **32** (2003) 171–180.
- [9] E. Emmrich, Error of the two-step BDF for the incompressible Navier–Stokes problem. *ESAIM: M2AN* **38** (2004) 757–764.
- [10] B. Futterer, N. Dahley and C. Egbers, Thermal electro-hydrodynamic heat transfer augmentation in vertical annuli by the use of dielectrophoretic forces through A.C. electric field. *Int. J. Heat Mass Transfer* **93** (2016) 144–154.
- [11] S. Gawlok, P. Gerstner, S. Haupt, V. Heuveline, J. Kratzke, P. Lösel, K. Mang, M. Schmidtobreck, N. Schoch, N. Schween, J. Schwegler, C. Song and M. Wlotzka, HiFlow3 – technical report on release 2.0. *Prepr. Ser. Eng. Math. Comput. Lab* (2017). DOI: [10.11588/emc1pp.2017.06.42879](https://doi.org/10.11588/emc1pp.2017.06.42879).

- [12] P. Gerstner, *Analysis and numerical approximation of dielectrophoretic force driven flow problems*. Ph.D. thesis, Heidelberg University (2020).
- [13] V. Girault and P.A. Raviart, *Finite Element Approximation of the Navier–Stokes Equations*. Lecture Notes in Mathematics. Springer-Verlag (1979).
- [14] V. Girault and P.A. Raviart, *Finite Element Methods for Navier–Stokes Equations: Theory and Algorithms*. *Springer Series in Computational Mathematics*. Springer-Verlag (1986).
- [15] V. Girault, R.H. Nochetto and R. Scott, Stability of the finite element Stokes projection in $W^{1,\infty}$. *C. R. Math.* **338** (2004) 957–962.
- [16] J.G. Heywood and R. Rannacher, Finite element approximation of the nonstationary Navier–Stokes problem. I. Regularity of solutions and second-order error estimates for spatial discretization. *SIAM J. Numer. Anal.* **19** (1982) 275–311.
- [17] J.G. Heywood and R. Rannacher, Finite-element approximation of the nonstationary Navier–Stokes problem. Part IV: error analysis for second-order time discretization. *SIAM J. Numer. Anal.* **27** (1990) 353–384.
- [18] V. John, *Finite Element Methods for Incompressible Flow Problems*. Springer International Publishing (2016).
- [19] C. Kang and I. Mutabazi, Dielectrophoretic buoyancy and heat transfer in a dielectric liquid contained in a cylindrical annular cavity. *J. Appl. Phys.* **125** (2019) 184902.
- [20] C. Kang, A. Meyer, H.N. Yoshikawa and I. Mutabazi, Numerical simulation of circular Couette flow under a radial thermoelectric body force. *Phys. Fluids* **29** (2017) 114105.
- [21] C. Kang, A. Meyer, H.N. Yoshikawa and I. Mutabazi, Thermoelectric convection in a dielectric liquid inside a cylindrical annulus with a solid-body rotation. *Phys. Rev. Fluids* **4** (2019) 093502.
- [22] S.V. Malik, H.N. Yoshikawa, O. Crumeyrolle and I. Mutabazi, Thermo-electro-hydrodynamic instabilities in a dielectric liquid under microgravity. *Acta Astronaut.* **81** (2012) 563–569.
- [23] M. Meier, M. Jongmanns, A. Meyer, T. Seelig, C. Egbers and I. Mutabazi, Flow pattern and heat transfer in a cylindrical annulus under 1g and low-g conditions: experiments. *Microgravity Sci. Technol.* **30** (2018) 699–712.
- [24] A. Meyer, *Active control of heat transfer by an electric field*. Ph.D. thesis, Université du Havre (2017).
- [25] A. Meyer, M. Jongmanns, M. Meier, C. Egbers and I. Mutabazi, Thermal convection in a cylindrical annulus under a combined effect of the radial and vertical gravity. *C. R. Mécanique* **345** (2017) 11–20.
- [26] A. Meyer, O. Crumeyrolle, I. Mutabazi, M. Meier, M. Jongmanns, M.-C. Renoult, T. Seelig and C. Egbers, Flow patterns and heat transfer in a cylindrical annulus under 1g and low-g conditions: theory and simulation. *Microgravity Sci. Technol.* **30** (2018) 653–662.
- [27] A. Meyer, M. Meier, M. Jongmanns, T. Seelig, C. Egbers and I. Mutabazi, Effect of the initial conditions on the growth of thermoelectric instabilities during parabolic flights. *Microgravity Sci. Technol.* **31** (2019) 11.
- [28] I. Mutabazi, H.N. Yoshikawa, M.T. Fogaing, V. Travnikov, O. Crumeyrolle, B. Futterer and C. Egbers, Thermo-electrohydrodynamic convection under microgravity: a review. *Fluid Dyn. Res.* **48** (2016) 061413.
- [29] R. Oyarzúa and P. Zúñiga, Analysis of a conforming finite element method for the Boussinesq problem with temperature-dependent parameters. *J. Comput. Appl. Math.* **323** (2017) 71–94.
- [30] R. Oyarzúa, T. Qin and D. Schötzau, An exactly divergence-free finite element method for a generalized Boussinesq problem. *IMA J. Numer. Anal.* **34** (2013) 1104–1135.
- [31] C.E. Pérez, J.-M. Thomas, S. Blancher and R. Creff, The steady Navier–Stokes/energy system with temperature-dependent viscosity – Part 2: the discrete problem and numerical experiments. *Int. J. Numer. Methods Fluids* **56** (2008) 91–114.
- [32] Y. Saad, *Iterative Methods for Sparse Linear Systems*, 2nd edition. Society for Industrial and Applied Mathematics (2003).
- [33] P.W. Schröder and G. Lube, Stabilised dG-FEM for incompressible natural convection flows with boundary and moving interior layers on non-adapted meshes. *J. Comput. Phys.* **335** (2017) 760–779.
- [34] P.W. Schröder, C. Lehrenfeld, A. Linke and G. Lube, Towards computable flows and robust estimates for inf-sup stable FEM applied to the time-dependent incompressible Navier–Stokes equations. *SeMA J.* **75** (2018) 629–653.
- [35] T. Seelig, A. Meyer, P. Gerstner, M. Meier, M. Jongmanns, M. Baumann, V. Heuveline and C. Egbers, Dielectrophoretic force-driven convection in annular geometry under Earth’s gravity. *Int. J. Heat Mass Trans.* **139** (2019) 386–398.
- [36] M. Smiszek, O. Crumeyrolle, I. Mutabazi and C. Egbers, Numerical simulation of thermoconvective instabilities of a dielectric liquid in a cylindrical annulus, in 59th International Astronautical Congress Glasgow 29/09-3/10 (2008).
- [37] P.J. Stiles, Electro-thermal convection in dielectric liquids. *Chem. Phys. Lett.* **179** (1991) 311–315.
- [38] P.J. Stiles and M. Kagan, Stability of cylindrical Couette flow of a radially polarised dielectric liquid in a radial temperature gradient. *Phys. A Stat. Mech. App.* **197** (1993) 583–592.
- [39] M. Tabata and D. Tagami, Error estimates of finite element methods for nonstationary thermal convection problems with temperature-dependent coefficients. *Numer. Math.* **100** (2005) 351–372.
- [40] M. Takashima, Electrohydrodynamic instability in a dielectric fluid between two coaxial cylinders. *Q. J. Mech. Appl. Math.* **33** (1980) 93–103.
- [41] R. Temam, *Navier–Stokes Equations: Theory and Numerical Analysis*. AMS/Chelsea Publication (2001).
- [42] V. Travnikov, O. Crumeyrolle and I. Mutabazi, Numerical investigation of the heat transfer in cylindrical annulus with a dielectric fluid under microgravity. *Phys. Fluids* **27** (2015) 054103.
- [43] V. Travnikov, O. Crumeyrolle and I. Mutabazi, Influence of the thermo-electric coupling on the heat transfer in cylindrical annulus with a dielectric fluid under microgravity. *Acta Astronaut.* **129** (2016) 88–94.
- [44] V. Travnikov, F. Zaussinger, P. Haun and C. Egbers, Influence of the dielectrical heating on the convective flow in the radial force field. *Phys. Rev. E* **101** (2020) 053106.

- [45] H.N. Yoshikawa, O. Crumeyrolle and I. Mutabazi, Dielectrophoretic force-driven thermal convection in annular geometry. *Phys. Fluids* **25** (2013) 024106.
- [46] F. Zaussinger, P. Haun, M. Neben, T. Seelig, V. Travnikov, C. Egbers, H. Yoshikawa and I. Mutabazi, Dielectrically driven convection in spherical gap geometry. *Phys. Rev. Fluids* **3** (2018) 093501.



Please help to maintain this journal in open access!

This journal is currently published in open access under the Subscribe to Open model (S2O). We are thankful to our subscribers and supporters for making it possible to publish this journal in open access in the current year, free of charge for authors and readers.

Check with your library that it subscribes to the journal, or consider making a personal donation to the S2O programme by contacting subscribers@edpsciences.org.

More information, including a list of supporters and financial transparency reports, is available at <https://edpsciences.org/en/subscribe-to-open-s2o>.